UNIVERSIDADE DE SÃO PAULO

INSTITUTO DE QUÍMICA DE SÃO CARLOS

NATALIA GABRIELLY PEREIRA DOS SANTOS

Desenvolvimento de colunas tubulares abertas para aplicação em nano cromatografia líquida acoplada à espectrometria de massas em tandem

São Carlos

2023

NATALIA GABRIELLY PEREIRA DOS SANTOS

Desenvolvimento de colunas tubulares abertas para aplicação em nano cromatografia líquida acoplada à espectrometria de massas em tandem

Tese apresentada ao Instituto de Química de São Carlos da Universidade de São Paulo como parte dos requisitos para a obtenção do título de doutor em ciências.

Área de concentração: Química Orgânica e Analítica

Orientador: Prof. Dr. Fernando Mauro Lanças

São Carlos

2023

Assinatura:
Data:

Ficha Catalográfica elaborada pela Seção de Referência e Atendimento ao Usuário do SBI/IQSC

Santos, Natalia Gabrielly Pereira dos
Desenvolvimento de colunas tubulares abertas para aplicação em nano cromatografia líquida acoplada à espectrometria de massas em tandem / Natalia Gabrielly Pereira dos Santos. — São Carlos, 2023.
109 f.

Tese (Doutorado em Química Analítica e Inorgânica) — Instituto de Química de São Carlos / Universidade de São Paulo, 2023.

Orientador: Prof. Dr. Fernando Mauro Lanças

1. Cromatografia miniaturizada. 2. NanoLC. 3. Espectrometria de massas. 4. Colunas tubulares Abertas. 5. N-nitrosaminass. I. Título.

Sonia Alves - CRB: 4280/8

DEDICATÓRIA

Dedico esse trabalho aos meus pais e irmã, Reginaldo, Odete e Nicolly, por toda paciência e acolhimento que tiveram durante esse período.

AGRADECIMENTOS

Primeiramente, quero agradecer à Deus pela força, amparo e por me permitir concretizar mais uma etapa da minha vida.

Agradeço a todos os professores que passaram pela minha vida, e me permitiram ter o conhecimento que tenho hoje. E, em especial, ao meu orientador Dr. Fernando Mauro Lanças, que acompanhou toda minha trajetória desde a iniciação científica até o doutorado. Agradeço pelo companheirismo, orientação, dedicação e por ter confiado em mim desde o início.

Agradeço à minha família por sempre torcer por mim, e acreditar que posso enfrentar qualquer desafio.

Agradeço aos meus colegas do Laboratório de Cromatografia, Edvaldo por ter me orientado durante meus primeiros meses no laboratório; ao Arley pela parceria de trabalho; a Thaís e Alessandra pela amizade e companheirismo.

Agradeço aos técnicos do laboratório Guilherme e Elaine, pelo apoio e discussão durante meu período de doutorado.

Agradeço ao Instituto de Química da Universidade de São Paulo pela infraestrutura e apoio técnico.

E, agradeço a todos as agências de fomento, FAPESP (processo 2019/26263-4), CAPES e CNPQ, pelo financiamento da minha bolsa de doutorado, e pelo investimento financeiro para o desenvolvimento da pesquisa.

“A mente que se abre a uma nova ideia jamais voltará ao tamanho original”

Albert Einstein

RESUMO

O desenvolvimento dessa tese de doutorado foi constituído por alguns dos principais trabalhos escritos pela aluna durante o período de pós-graduação, os quais podem ser considerados como temas inovadores dentro da área de cromatografia, como por exemplo, a aplicação de colunas tubulares abertas em cromatografia líquida, e o acoplamento da técnica com espectrometria de massas com ionização por impacto de elétrons. Além disso, o último capítulo trás o desenvolvimento de uma metodologia analítica para análise de N-nitrosaminas em medicamentos da classe das sartanas, impureza com potencial carcinogênico à qual vem sendo pauta de discussão e controle no mercado farmacêutico. Portanto, este trabalho visou contribuir para o desenvolvimento de colunas tubulares abertas, do tipo - WCOT, para nanoLC-ESI-MS/MS. Em um primeiro momento, foi proposta uma metodologia para a preparação dessas colunas, adaptando o método proposto por Kurt Grob às condições experimentais do laboratório. Em seguida, foi feita uma triagem de fases estacionárias para o revestimento da coluna WCOT. As fases testadas foram: OV-73, OV-17, OV-210, OV-225 e OV-275, adquiridas da Ohio Valley. Para a avaliação das colunas, os padrões de atrazina, clomazona e metolacloro foram utilizados como padrões analíticos. A fase estacionária que apresentou os melhores resultados para nanoLC-ESI-MS/MS, dentre as avaliadas, foi a OV-210 (50% trifluoropropil 50% dimetil poli siloxano), que passou para a próxima etapa do trabalho: otimização da coluna WCOT. Nessa etapa de otimização, foram avaliados parâmetros como comprimento da coluna, diâmetro interno, massa de fase estacionária para revestimento da coluna, volume de injeção e, parâmetros cinéticos como velocidade linear ótima e avaliação performance-velocidade, pelos gráficos de Van Deemter e Poppe, respectivamente. Por último, a coluna WCOT otimizada foi acoplada à uma coluna *trapping* empacotada, à qual possibilitou melhores resultados de separação cromatográfica. O outro trabalho experimental consistiu no desenvolvimento de uma metodologia analítica para análise de N-nitrosaminas em medicamentos, no caso, em Losartana Potássica, amplamente consumido no tratamento de hipertensão. A metodologia consistiu na automatização do preparo de amostra do tipo MEPS (microextração por sorvente empacotado) em um sistema robótico controlado por arduino. O método analítico foi desenvolvido e validado em UHPLC-APCI-MS/MS, e apresentou bons resultados de linearidade, precisão intra-dias e inter-dias, dentre outras figuras de mérito. O que mais se destaca nessa metodologia é a capacidade de *high-throughput* do sistema robótico, o qual permite a preparação de seis amostras simultâneas, em menos de 20 minutos, o que é um grande avanço para o monitoramento dessas impurezas em análises de rotina.

ABSTRACT

The development of this doctoral thesis consisted of one of the main works written by the student during the postgraduate period, which can be considered as innovative themes within the field of chromatography, such as the application of open tubular columns in chromatography liquid, and the coupling of the technique with mass spectrometry with electron impact ionization. In addition, the last chapter brings the development of an analytical methodology for the analysis of N-nitrosamines in drugs from the sartan class, an impurity with carcinogenic potential which has been the subject of discussion and control in the pharmaceutical market. Therefore, this work aimed to contribute to the development of WCOT-type open tubular columns for nanoLC-ESI-MS/MS. At first, a methodology for the preparation of these columns was proposed, adapting the method proposed by Kurt Grob to the laboratory's experimental conditions. Then, a screening of stationary phases for coating the WCOT column was performed. The phases tested were: OV-73, OV-17, OV-210, OV-225 and OV-275, purchased from Ohio Valley. For column evaluation, atrazine, clomazone and metolachlor standards were used as analytical standards. The stationary phase that presented the best results for nanoLC-ESI-MS/MS, among those evaluated, was OV-210 (50% trifluoropropyl 50% dimethyl poly siloxane), which went on to the next stage of the work: WCOT column optimization. In this optimization step, parameters such as column length, internal diameter, mass of stationary phase for column coating, injection volume and kinetic parameters such as optimal linear velocity and performance-velocity evaluation, using Van Deemter and Poppe graphs, were evaluated. respectively. Finally, the optimized WCOT column was coupled to a packed trapping column, which enabled better chromatographic separation results. The other experimental work consisted in the development of an analytical methodology for the analysis of N-nitrosamines in medicines, in this case, in Losartan Potassium, widely consumed in the treatment of hypertension. The methodology consisted of automating MEPS-type sample preparation (packaged sorbent microextraction) in an arduino-controlled robotic system. The analytical method was developed and validated in UHPLC-APCI-MS/MS, and showed good results for linearity, intra-day and inter-day precision, among other figures of merit. What stands out most about this methodology is the high-throughput capacity of the robotic system, which allows the preparation of six simultaneous samples in less than 20 minutes, which is a great advance for the monitoring of these impurities in routine analyses.

SUMÁRIO

Capítulo 1.....10

1 INTRODUÇÃO.....11

2 REFERÊNCIAS BIBLIOGRÁFICAS.....14

3 OBJETIVOS.....18

3.1 Objetivos gerais.....18

3.2 Objetivos específicos.....18

Capítulo 2.....19

1 COLETÂNEA DE ARTIGOS CIENTÍFICOS.....20

Capítulo 3.....22

1 An overview of open tubular liquid chromatography with a focus on the coupling with mass spectrometry for the analysis of small molecules.....23

Capítulo 4.....37

1 Development of wall-coated open tubular column and their application to nano liquid chromatography coupled to tandem mass spectrometry.....38

Capítulo 5.....57

1 Current prospects on nano liquid chromatography coupled to eléctron ionization mass spectrometry (nanoLC-EI-MS).....58

Capítulo 6.....68

1 Electron ionization mass spectrometry: Quo vadis?.....69

Capítulo 7.....83

Microextraction by packed of N-nitrosamines from losartan tablets using a high-throughput robot platform followed by liquid chromatography-tandem mass spectrometry.....84

Capítulo 8.....101

1 CONSIDERAÇÕES FINAIS.....102

2 PERSPECTIVAS FUTURAS.....103

Capítulo 9.....104

1 PUBLICAÇÕES CIENTÍFICAS.....105

Capítulo 1

Introdução

1 INTRODUÇÃO

Uma das tendências modernas para o campo da cromatografia líquida (LC) é a miniaturização da técnica, visando atingir o mesmo patamar alcançado pela cromatografia gasosa capilar em termos de velocidade, eficiência e sensibilidade[1,2]. Além disso, a LC miniaturizada oferece várias vantagens que justificam o investimento nessa área, como a redução do consumo de amostras e solventes para fase móvel, aumento de eficiência (devido a redução do diâmetro interno das colunas), possibilidade de aplicação da programação de temperatura, e principalmente o acoplamento com técnicas de detecção como a espectrometria de massas[3]. Assim, vários esforços vêm sendo conduzidos ao longo dos tempos para redimensionar todo o sistema cromatográfico da LC convencional, bem como desenvolver colunas com diâmetro interno inferiores.

Considerando os aspectos históricos referentes a miniaturização da LC, pode-se citar as contribuições de Horvárth que é considerado um dos pioneiros na área[4]. Segundo seus estudos, colunas capilares empacotadas de pequeno diâmetro eram mais eficientes do que capilares não revestidos. Mais adiante, Tsuda e Novotny dedicaram esforços para reduzir o diâmetro interno de colunas para uma faixa de 50-200 µm empacotadas com partículas de ~30-10 µm[5,6]. Além dessas contribuições que dizem respeito à colunas ainda tivemos esforços para redimensionar o sistema de LC, o qual foi conduzido por Ishii. Em seu trabalho foi desenvolvido um sistema de LC de micro alta eficiência (MHPLC) compatível com colunas empacotadas[8] e tubulares abertas (OT), o qual permitiu o progresso da LC miniaturizada durante a década de 80.

A instrumentação para LC miniaturizada foi sendo cada vez mais aprimorada com o passar do tempo[9,10]. Atualmente temos equipamentos comerciais que entregam fluxos precisos e sem pulsos, de forma reprodutível, normalmente empregando bombas de pistão duplo. E, para fazer a injeção de amostra, é muito comum o emprego de *loop* externo no qual os analitos são focalizados na entrada da coluna, e posteriormente eluídos em uma banda estreita. Além disso, é possível controlar o volume a ser injetado e que seja compatível com a capacidade de carga da coluna, considerando seu diâmetro[11,12].

Dentro dessa área de instrumentação, uma das grandes preocupações é o alargamento de banda extra-coluna que pode comprometer a eficiência cromatográfica[13]. Portanto, as tubulações devem ser redimensionadas de acordo com o diâmetro interno da coluna, sendo considerado adequado tubulações com d.i. 125 e 250 µm para colunas micro e capilares, e tubos com d.i. ≤ 5 µm para colunas nano[2]. Com respeito aos detectores, normalmenteUV-Vis, o qual é o mais empregado, a célula de detecção precisa ser redimensionada para a escala de LC

miniaturizada, cerca de 2-50 nL, porém, de acordo com a Lei de Lambert-Beer, a redução do caminho óptico diminui a absorção dos analitos e, consequentemente, compromete a detectabilidade[9]. Portanto, alguns dos detectores que vem sendo empregado com LC miniaturizada é a fluorescência induzida por laser (LIF); detecção eletroquímica (ECD); diodo emissor de luz (LEDs), e principalmente, a espectrometria de massas[14,15].

Normalmente, quando falamos em acoplamento da LC miniaturizada com a espectrometria de massas, a *electrospray* (ESI) é o modo de ionização de maior compatibilidade, devido sua ampla faixa de massas e capacidade de analisar compostos de diversas classes[10,16]. No entanto, diversas pesquisas vêm sendo conduzidas para tentar acoplar a ionização por elétrons (EI) ao LC, destacando-se o grupo do professor Cappiello[17-19]. Como a LC miniaturizada emprega fluxos de fase móvel reduzido, a eliminação do solvente é facilitada, o que permitiria o acoplamento com a EI, assim sendo, faz-se necessário uma interface para receber o fluxo da fase móvel líquido proveniente da coluna e volatilizar os analitos, antes de entrarem na fonte-EI.

Esse tipo de ionização ocorre sob condições de alto vácuo, em que as moléculas dos analitos (na forma gasosa) são colididas com elétrons altamente energizados (70eV). A vantagem em se empregar EI com LC, é a possibilidade de analisar compostos que não são facilmente analisados por ESI, além do perfil de fragmentação que é altamente reprodutível, o que permite identificar compostos desconhecidos a partir da comparação entre o espectro da amostra com uma biblioteca de espectros (NIST)[20].

Como pode ser visto, o progresso da LC miniaturizada envolve todo um redimensionamento do sistema, bem como da coluna cromatográfica, a qual é apontada por Desmet como sendo o principal pilar dentro desse campo[3,21]. De forma generalizada, busca-se reduzir o diâmetro interno dessas colunas que aliado a redução do fluxo da fase móvel, há uma redução na diluição cromatográfica. Ou seja, quanto menor o volume de líquido dentro da coluna, menor a diluição da amostra, o que irá resultar numa redução da dispersão e ganho de sensibilidade. Outro aspecto que é levado em consideração é a redução do tamanho das partículas, quando se trata de colunas empacotadas. Outros tipos de colunas que podem ser empregadas em LC são as colunas monolíticas e as tubulares abertas, esta última pouco explorada ainda, e mais recentemente os chips microfluídicos, introduzidos na década de 90. A seguir será sumarizado as principais características de cada tipo de coluna:

I) Colunas empacotadas: normalmente são constituídas por partículas baseadas em sílica, as quais podem ser superficialmente porosas (SP, core-shell), em que temos um núcleo sólido revestido por uma fina camada porosa; as não porosas (NP), e as totalmente porosas (FP),

comumente mais utilizadas[3,22]. Devido à redução do tamanho dessas partículas, há um aumento significativo na eficiência cromatográfica, uma vez que o processo de transferência de massa entre a fase estacionária e móvel é facilitado. No entanto, essa redução de tamanho gera uma grande pressão no sistema cromatográfico, o que requer bombas que suportem altas pressões[13]. Justamente por essa razão que o desenvolvimento da LC miniaturizada foi concretizado com o redimensionamento do sistema, e aprimoramento de bombas para entrega de solventes.

II) Colunas monolíticas: são outra possibilidade de colunas preenchidas, porém nesse caso com um material poroso, constituídos por macroporos e mesoporos. Tal material oferece menor pressão ao sistema, e rápida transferência de massa, o que permite o uso de fluxo de fase móvel mais elevados e tempos de análise reduzidos[9]. Essa fase porosa é produzida *in-situ* na coluna, e pode ser de composição inorgânica ou orgânica. Os polímeros inorgânicos normalmente são baseados em sílica, e apresentam porosidade superior à 80%, logo, são altamente eficientes em separação de moléculas pequenas, aliado a uma baixa pressão. Contudo, uma de suas desvantagens é a adesão da fase à parede do tubo[3]. Por outro lado, os polímeros orgânicos são mais utilizados, devido sua facilidade de preparação e, normalmente são utilizados para análise de moléculas grandes. Sua principal limitação é a instabilidade frente a solventes orgânicos.

III) Colunas tubulares aberta: são caracterizadas por um tubo vazio de sílica fundida revestido por uma fina camada de fase estacionária, a qual pode ser de natureza porosa (PLOT – *porous layer open tubular column*), ou não-porosa (WCOT- *wall open tubular column*)[23,24]. Do ponto de vista teórico, são consideradas as colunas mais promissoras para LC miniaturizada, sendo consideradas mais eficientes que uma coluna empacotada, isso pois, não apresentam o efeito do termo A (dispersão longitudinal/ efeito de múltiplos caminhos da equação de Van Deemter) à qual as colunas empacotadas estão susceptíveis. Por essa razão, as colunas tubulares apresentam um menor alargamento de banda, o que garante um maior número de pratos teóricos. Além disso, apresentam baixa pressão, grande permeabilidade a fase móvel o que permite o emprego de fluxos de fase móvel mais elevados. Contudo, uma das suas grandes limitações é a capacidade de carga que é bem inferior à uma coluna empacotada[3]. Com relação a composição da fase estacionária, as colunas PLOT, normalmente mais estudadas para LC, são baseadas em polímeros de polidivinilbenzeno (DVB) e polimetacrilato (PMMA). Já as colunas WCOT são normalmente baseadas em polímeros de dimetil polisiloxano (DMPS).

IV) Chips microfluídicos: os sistemas baseados em chips são uma forma de aumentar a portabilidade em um único dispositivo entre as principais funções da LC: amostragem, transporte de amostras, separação e detecção[25,26]. Além dessa portabilidade, os chips ainda

podem oferecer maior confiabilidade, velocidade de análise, e redução de custos. Em termos de estrutura, os chips podem ter os mesmos formatos que as colunas convencionais: empacotado com partículas, a qual apresenta maior capacidade de carga e reprodutibilidade; do tipo monolíticas e tubulares abertas, estas últimas com maior resistência ao fluxo da fase móvel, porém com menores capacidades de carga, o que dificulta a detecção de analitos em baixas concentrações[2,27].

Em suma, o aprimoramento da LC miniaturizada está voltado principalmente para o desenvolvimento de colunas, e para a construção de dispositivos mais portáteis como os chips. Porém, algumas colunas já são mais robustas que outras, à exemplo as empacotadas que são mais conceituadas do que as colunas monolíticas e tubulares abertas. Considerando que teoricamente as colunas tubulares abertas podem ser uma boa opção para LC miniaturizada, ainda se faz necessário diversos estudos na área, visando superar as limitações desse tipo de coluna, para que futuramente possa ser empregado em laboratórios de análise de rotina.

2 REFERÊNCIAS BIBLIOGRÁFICAS

[1]GOLAY, M. J. E. Vapor phase chromatography and the telegrapher's equation. **Analytical Chemistry**,Washington, v. 29, n. 6, p. 928–932, Jun. 1957.

[2]VARGAS MEDINA, D. A.; SOARES MACIEL, E. V.; LÚCIA DE TOFFOLI, A.; LANÇAS, F. M. Miniaturization of liquid chromatography coupled to mass spectrometry. 2. Achievements on modern instrumentation for miniaturized liquid chromatography coupled to mass spectrometry. **TrAC Trends in Analytical Chemistry**, Amsterdam, v.128, p. 2-17, Jul. 2020.

[3]MEJÍA-CARMONA, K.; SOARES DA SILVA BURATO, J.; BORSATTO, J. V. B.; DE TOFFOLI, A. L.; LANÇAS, F. M. Miniaturization of liquid chromatography coupled to mass spectrometry. **TrAC Trends in Analytical Chemistry**, Amsterdam, v. 122, p. 2-15, Jan. 2020.

[4]HORVATH, C. G.; PREISS, B. A.; LIPSKY, S. R. Fast liquid chromatography. Investigation of operating parameters and the separation of nucleotides on pellicular ion exchangers. **Analytical Chemistry**, Washington, v. 39, n. 12, p. 1422–1428, Out. 1967.

[5]TSUDA, T.; NOVOTNY, M. Packed microcapillary columns in high performance liquid chromatography. **Analytical Chemistry**, Washington, v. 50, n. 2, p. 271–275, Fev. 1978a.

[6]TSUDA, T.; NOVOTNY, M. Band-broadening phenomena in microcapillary tubes under the conditions of liquid chromatography. **Analytical Chemistry**, Washington, v. 50, n. 4, p. 632–634, Abr. 1978b.

[7]HIBI, K.; ISHII, D.; FUJISHIMA, I.; TAKEUCHI, T.; NAKANISHI, T. Studies of open

tubular micro capillary liquid chromatography. 1. The development of open tubular micro capillary liquid chromatography. **Journal of High Resolution Chromatography**, Hoboken, v. 1, n. 1, p. 21–27, Jul. 1978.

[8]ISHII, D.; ASAI, K.; HIBI, K.; JONOKUCHI, T.; NAGAYA, M. A study of micro-high-performance liquid chromatography: I. Development of technique for miniaturization of high-performance liquid chromatography. **Journal of Chromatography A,** Amsterdam, v. 144, n. 2, p. 157–168, Dez. 1977.

[9]LYNCH, K. B.; CHEN, A.; LIU, S. Miniaturized high-performance liquid chromatography instrumentation. **Talanta**, Amsterdam, v.177, p. 94-103, Jan. 2018.

[10]VASCONCELOS SOARES MACIEL, E.; DE TOFFOLI, A. L.; SOBIESKI, E.; DOMINGUES NAZÁRIO, C. E.; LANÇAS, F. M. Miniaturized liquid chromatography focusing on analytical columns and mass spectrometry: a review. **Analytica Chimica Acta**, Amsterdam, v. 1103, p. 11–31, Mar. 2020.

[11]BLUE, L. E.; FRANKLIN, E. G.; GODINHO, J. M.; GRINIAS, J. P.; GRINIAS, K. M.; LUNN, D. B.; MOORE, S. M. Recent advances in capillary ultrahigh pressure liquid chromatography. **Journal of Chromatography A**, Amsterdam, v. 1523, p. 17–39, Nov. 2017.

[12]NAZARIO, C. E. D.; SILVA, M. R.; FRANCO, M. S.; LANÇAS, F. M. Evolution in miniaturized column liquid chromatography instrumentation and applications: an overview. **Journal of Chromatography A**, Amsterdam, v. 1421, p. 18 -37, Nov. 2015.

[13]NAZARIO, C. E. D.; FUMES, B. H.; SILVA, M. R.; LANÇAS, F. M. Miniaturized column liquid chromatography. *In*: HUSSAIN, C. M. (ed.). **Nanomaterials in chromatography**: current trends in chromatographic research technology and techniques. Amsterdam: Elsevier, 2018. p. 359–385.

[14]HEUS, F.; GIERA, M.; DE KLOE, G. E.; VAN IPEREN, D.; BUIJS, J.; NAHAR, T. T.; SMIT, A. B.; LINGEMAN, H.; DE ESCH, I. J. P.; NIESSEN, W. M. A.; IRTH, H.; KOOL, J. Development of a microfluidic confocal fluorescence detection system for the hyphenation of nano-LC to on-line biochemical assays. **Analytical and Bioanalytical Chemistry**, London, v. 398, n. 7–8, p. 3023–3032, Dez. 2010.

[15]KALAY, H.; AMBROSINI, M.; CHIODO, F.; VAN KOOYK, Y.; GARCÍA-VALLEJO, J. J. Enhanced glycan nanoprofiling by weak anion exchange preparative chromatography, mild acid desialylation, and nanoliquid chromatography-mass spectrometry with nanofluorescence detection. **Electrophoresis**, Hoboken, v. 34, n. 16, p. 2350–2356, Ago. 2013.

[16]CHETWYND, A. J.; DAVID, A. A review of nanoscale LC-ESI for metabolomics and its potential to enhance the metabolome coverage. **Talanta**, Amsterdam, v. 182, p. 380–390, Jan. 2018.

[17]CAPPIELLO, A.; FAMIGLINI, G.; PIERINI, E.; PALMA, P.; TRUFELLI, H. Advanced liquid chromatography-mass spectrometry interface based on electron ionization. **Analytical Chemistry**, Amsterdam, v. 79, n. 14, p. 5364–5372, Jun. 2007.

[18]CAPPIELLO, A.; FAMIGLINI, G.; PALMA, P.; PIERINI, E.; TERMOPOLI, V.; TRUFELLI, H. Direct-EI in LC-MS: towards a universal detector for small-molecule applications. **Mass Spectrometry Reviews**, Hoboken, v. 30, n. 6, p. 1242–1255, Nov. 2011.

[19]TERMOPOLI, V.; FAMIGLINI, G.; PALMA, P.; PIERGIOVANNI, M.; ROCIO-BAUTISTA, P.; OTTAVIANI, M. F.; CAPPIELLO, A.; SAEED, M.; PERRY, S. Evaluation of a liquid electron ionization liquid chromatography–mass spectrometry interface. **Journal of Chromatography A**, Amsterdam, v. 1591, p. 120–130, Apr. 2019.

[20]PALMA, P.; FAMIGLINI, G.; TRUFELLI, H.; PIERINI, E.; TERMOPOLI, V.; CAPPIELLO, A. Electron ionization in LC-MS: recent developments and applications of the direct-EI LC-MS interface. **Analytical and Bioanalytical Chemistry**, Washington, v. 399, n. 8, p. 2683–2693, Mar. 2011.

[21]DESMET, G.; EELTINK, S. Fundamentals for LC Miniaturization. **Analytical Chemistry**, Amsterdam, v. 85, n. 2, p. 543–556, Jan. 2013.

[22]UNGER, K. K.; LIAPIS, A. I. Adsorbents and columns in analytical high-performance liquid chromatography: a perspective with regard to development and understanding. **Journal of Separation Science**, Hoboken, v. 35, n. 10–11, p. 1201–1212, Jun. 2012.

[23]LAM, S. C.; SANZ RODRIGUEZ, E.; HADDAD, P. R.; PAULL, B. Recent advances in open tubular capillary liquid chromatography. **Analyst**, London, v. 144, n. 11, p. 3464–3482, Dez. 2019.

[24]ZHU, M.; ZHANG, L.; CHU, Z.; WANG, S.; CHEN, K.; ZHANG, W.; LIU, F. Preparation and evaluation of open-tubular capillary columns modified with metal-organic framework incorporated polymeric porous layer for liquid chromatography. **Talanta**, Amsterdam, v. 184, p. 29–34, Jul. 2018.

[25]HAGHIGHI, F.; TALEBPOUR, Z.; NEZHAD, A. S. Towards fully integrated liquid chromatography on a chip: evolution and evaluation. **TrAC - Trends in Analytical Chemistry**, Amsterdam, v. 105, p. 302–337, Aug. 2018.

[26]YUAN, X.; OLESCHUK, R. D. Advances in microchip liquid chromatography. **Analytical Chemistry**, Amsterdam, v. 90, n. 1, p. 283–301, Nov. 2018.

[27]TSUNODA, M. On-Chip liquid chromatography. **Encyclopedia**, Basel, v. 2, n. 1, p. 617–624, Mar. 2022.

3 OBJETIVOS

3.1 Objetivos gerais

O presente projeto tem por finalidade realizar o preparo, otimização e aplicações analíticas de colunas tubulares aberta do tipo WCOT, em sistema de nano cromatografia acoplada a espectrometria de massas em tandem (nanoLC-ESI-MS/MS).

3.2 Objetivos específicos

Para alcançar os objetivos gerais mencionados, os objetivos específicos serão:

- Elaborar um procedimento para o preparo de colunas tubulares abertas do tipo WCOT, considerando as condições já descritas na literatura e adaptando-as às condições experimentais do laboratório de pesquisa onde o presente trabalho é desenvolvido.
- Avaliar diversos materiais empregados como fase estacionária para a preparação das colunas WCOT, visando eleger a melhor fase (com desempenho adequado) para prosseguir nas etapas de otimização da coluna.
- Preparar a coluna WCOT com a fase estacionária de melhor desempenho e otimizá-la para o sistema de nanoLC-ESI-MS/MS. Os parâmetros a serem otimizados são: comprimento do tubo, diâmetro interno, massa de fase estacionária e volume de injeção.
- Estudar o efeito do acoplamento da coluna WCOT otimizada acoplada à uma coluna empacotada com partículas, em modo de extração, para avaliar o efeito sobre a separação cromatográfica.

Capítulo 2

Coletânea de artigos científicos

1 COLETÂNEA DE ARTIGOS CIENTÍFICOS

A área de química analítica pode ser subdividida em três partes: preparo de amostra, separação cromatográfica e detecção, as quais foram devidamente estudadas nesse projeto de Doutorado direto. Primeiramente, o projeto maior foi voltado para o desenvolvimento de colunas tubulares abertas, do tipo WCOT, para separação cromatográfica por nano cromatografia líquida acoplada a espectrometria de massas. Dentro desse arranjo, fora feito estudos utilizando *electrospray* como fonte de ionização, contudo, o que gostaríamos de esperar no futuro da cromatografia moderna, é a aplicação de colunas WCOT em sistemas de nanoLC-EI-MS/MS. Assim sendo, diversos artigos científicos foram publicados em periódicos de alto fator de impacto, no qual, foram abordadas as principais interfaces utilizadas para fazer o acoplamento entre a LC com a ionização por elétrons (EI), suas limitações a serem superadas, e também as vantagens desse acoplamento.

Por último, foi desenvolvido um método miniaturizado e automatizado de preparo de amostra para análise de N-nitrosaminas em matriz de medicamentos (comprimidos), mais especificamente em losartana, a qual é amplamente utilizada por pacientes hipertensos. Tal método foi otimizado por planejamento experimental, e depois validado segundo as normativas da RDC n°166/2017 da ANVISA e ICH Q2(R2). Portanto, essa tese foi estruturada na forma de coletânea de artigos científicos, visando demonstrar a abrangência da formação científica do pesquisador de Doutorado dentro da área de química analítica.

A seguir será feito um breve resumo de cada artigo que compõe a tese, e no Capítulo 9, há a citação de todos os artigos escritos pela aluna.

1. An overview of open tubular liquid chromatography with a focus on the coupling with mass spectrometry for the analysis of small molecules. *Journal of Chromatography A*.

Esse artigo de revisão visa apresentar uma visão teórica de como as colunas tubulares abertas podem ser um grande exemplo de coluna de alta performance para cromatografia líquida miniaturizada. Contudo, estudos teóricos predizem que para alcançarmos eficiência de uma OTLC como já temos em cromatografia gasosa, é necessário preparar colunas com diâmetro interno na faixa de 2 µm, o que talvez ainda possa ser um grande desafio a comunidade científica.

Assim sendo, o artigo vem trazer uma visão geral dos dois tipos de colunas tubulares abertas disponíveis: as colunas do tipo *wall coated open tubular column* (WCOT) revestidas

por um filme líquido polimérico em sua parede e, a *porous layer open tubular column* (PLOT) revestidas por um filme polímerico poroso.

Também é apresentada a possibilidade de acoplamento entre as colunas OT com a cromatografia líquida e espectrometria de massas. Em se tratando de MS, a fonte de ionização mais comum nesse tipo de cromatografia é a *electrospray* (ESI), porém, diversas pesquisas vêm tentando aplicar a nanoLC com impacto de elétrons (EI), e usando colunas OT.

2. Development of Wall-Coated Open Tubular Columns and Their Application to Nano Liquid Chromatography Coupled to Tandem Mass Spectrometry. *Molecules*.

Em sequência, é apresentado um artigo de pesquisa no qual é desenvolvido colunas tubulares abertas do tipo WCOT para aplicação em cromatografia líquida acoplada a espectrometria de massas em tandem com ionização por *electrospray* (ESI). A princípio foi descrita uma metodologia para preparo de colunas, que constituí uma adaptação ao método proposto por Grob, o idealista de colunas tubulares abertas para cromatografia gasosa.

Adiante, foi feita uma otimização dessas colunas, no qual alguns parâmetros que pudessem afetar a eficiência dessas colunas foram avaliados, sendo eles: comprimento do tubo, diâmetro interno da coluna, massa de fase estacionária líquida que irá impactar na espessura do filme e, volume de injeção. Algumas outras avaliações também foram conduzidas, de caráter mais teórico, como a avaliação da velocidade linear da coluna, e a relação performance/velocidade (Gráfico de Poppe).

Por último foi feito o acoplamento da coluna WCOT com uma coluna trapping empacotada, para avaliar se há um aumento na eficiência de separação do método.

3. Current prospects on nano liquid chromatography couplet to eléctron ionization mass spectrometry (nanoLC-EI-MS). *Journal of Liquid Chromatography & Related Technologies.*

Esse artigo de revisão vem trazer uma visão sobre o acoplamento da cromatografia líquida a ionização de elétrons (EI), comumente aplicada somente em cromatografia gasosa. Ainda enfrentamos dificuldades para fazer esse acoplamento, uma vez que o EI trata-se de uma ionização sob condições de vácuo, portanto, o eluato da coluna analítica deve entrar na câmara

de ionização na forma gasosa, o que já é inviabilizado pela cromatografia líquida, em que o eluato é líquido.

Assim, as pesquisas dentro dessa área, dando destaque principalmente ao grupo do professor Cappiello/Itália, visam desenvolver interfaces capazes de possibilitar o acoplamento entre a LC e EI, ou seja, tais dispositivos tem por função conveter o eluato da LC líquido em uma forma gasosa, antes de adentrarem a câmara de ionização em condições à vácuo. Nesse artigo em específico são apresentadas as interfaces mais novas: direct-EI, liquid eléctron ionization inteface (LEI) e a Cold-EI.

4. Electron ionization mass spectrometry: Quo vadis? *Electrophoresis*.

Este artigo de revisão é apenas uma complementação do artigo anterior no que diz respeito ao acoplamento entre a cromatografia líquida e a ionização por elétrons (EI). Contudo, tal artigo acaba trazendo uma visão mais aprofundada e sistemática sobre todas as interfaces já desenvolvidas para fazer o acoplamento LC-EI.

5. Microextraction by packed sorbent of N-nitrosamines from Losartan tablets using a high-throughput robot platform followed by liquid chromatography -tandem mass spectrometry. *Journal of Separation Science*.

Esse artigo de pesquisa foge do tema proposto para a tese, contudo, surgiu de uma necessidade de controle de N-nitrosaminas em medicamentos. Desde 2018, foram reportados tais impurezas cancerígenas em medicamentos aplicados para hipertensão (principalmente da classe das sartanas), que levou a vários recalls no mercado mundial. Portanto, o objetivo aqui foi propor uma metodologia de preparo de amostra baseado em MEPS (microextração em fase sólida) automatizado em um robô experimental desenvolvido no próprio laboratório de pesquisa. Assim, foi feita toda a otimização experiemental, desde a escolha do melhor sorvente, e das condições de extração: ciclos de extração, ciclos de dessorção, dentre outros parâmetros.

Após toda a otimização do preparo de amostra, fora desenvolvido um método analítico por cromatografia líquida acoplada a espectrometria de massas em tandem com ionização química a pressão atmosférica (UHPLC-APCI-MS/MS), no qual foram avaliadas as principais figuras de mérito analítico (LOD, LOQ, linearidade, precisão, exatidão, fator de enriquecimento, etc).

Capítulo 3

Artigo publicado no *Journal of Chromatography A* (2021)

Journal of Chromatography A 1641 (2021) 461989

Contents lists available at ScienceDirect

Journal of Chromatography A

journal homepage: www.elsevier.com/locate/chroma

An overview of open tubular liquid chromatography with a focus on the coupling with mass spectrometry for the analysis of small molecules

Deyber Arley Vargas Medina, Natalia Gabrielly Pereira dos Santos, Juliana Soares da Silva Burato, João Victor Basolli Borsatto, Fernando Mauro Lanças*

University of São Paulo, São Carlos, Institute of Chemistry of São Carlos, SP, Brazil

ARTICLE INFO

Article history:
Received 16 October 2020
Revised 29 January 2021
Accepted 9 February 2021
Available online 12 February 2021

Keywords:
nano-liquid chromatography
open tubular column
open tubular liquid chromatography
mass spectrometry
nano-electrospray ionization
electron ionization

ABSTRACT

Open tubular liquid chromatography (OT-LC) can provide superior chromatographic performance and more favorable mass spectrometry (MS) detection conditions. These features could provide enhanced sensitivity when coupled with electrospray ionization sources (ESI-) and lead to unprecedented detection capabilities if interfaced with a highly structural informative electron ionization (EI) source. In the past, the exploitation of OT columns in liquid chromatography evolved slowly. However, the recent instrumental developments in capillary/nanoLC-MS created new opportunities in developing and applying OT-LC-MS. Currently, the analytical advantages of OT-LC-MS are mainly exploited in the fields of proteomics and biosciences analysis.

Nevertheless, under the right conditions, OT-LC-MS can also offer superior chromatographic performance and enhanced sensitivity in analyzing small molecules. This review will provide an overview of the latest developments in OT-LC-MS, focusing on the wide variety of employed separation mechanisms, innovative stationary phases, emerging column fabrication technologies, and new OT formats. In the same way, the OT-LC's opportunities and shortcomings coupled to both ESI and EI will be discussed, highlighting the complementary character of those two ionization modes to expand the LC's detection boundaries in the performance of targeted and untargeted studies.

1. Introduction

The remarkable instrumental advances of the last two decades make the capillary and nano liquid chromatography coupled to mass spectrometry (Capillary/nano-LC-MS) the primary analytical technique of interest in many scientific areas [1–3]. Capillary/nano-LC can provide not only enhanced sensitivity when coupled with the traditional electrospray ionization sources (ESI-MS) [2] but also unprecedented detection capabilities derived from its emerging coupling with the electron ionization mode (EI-MS) [4]. Up to date, capillary/nano LC-MS interfacing has been mainly based on exploiting filled (monolithic and particle-packed) columns. The study of open tubular (OT) columns in this field has remained somewhat neglected in the last 30 years.

Although the OT analytical columns have only recently been reintroduced into liquid chromatography (LC), after a long time without novelties in this niche, recent studies have demonstrated their practical applicability in proteomics, metabolomics, and other areas in which quantities of samples are quite reduced [5]. New research and important innovation and developments in OT-LC-MS have being done in the last years. New stationary phases, with diversified retention and separation mechanisms, are being explored, while alternative column formats and microfabrication techniques have brought new insight into the OT-LC potentialities.

Although we think of packed columns as synonymous with LC nowadays, it was different in the '60s, '70s, and '80s. At that time, substantial efforts were made to develop OT-LC systems capable of providing competitive performance, predicted by the theoretical considerations. Although early promising results were obtained [6], the OT-LC systems' evolution was mainly hindered by the difficulties to prepare columns with an optimal inner diameter (2-10 µm) for LC applications. Also, the lack of instrumentation to handle the very low flow rates, and to detect with minimal band broad-

* Corresponding author. Tel: +(55) 16 3373 9983; Fax: +(55) 16 3373 9984. E-mail address: (F. M. Lanças)
E-mail address: flancas@iqsc.usp.br (F.M. Lanças).

https://doi.org/10.1016/j.chroma.2021.461989
0021-9673/

ening contribution, retarded the progress of the OT-LC systems. Nowadays, the recent advances in miniaturized LC instrumentation have made the reborn of the OT-LC investigation, mainly thanks to the Karger research group, who have produced new land-marking studies on this technology [7].

Although in the light of the current stationary phases that classification can be questioned, OT-LC columns have been historically categorized into two main groups: WCOT (Wall Coated Open Tubular) and PLOT (Porous Layer Open Tubular). Between those, PLOT has been more exploited in LC applications due to their bigger sample capacity derived from the porous layer employed as the stationary phase. Hence, PLOT columns were reintroduced recently by Karger et al. [8,9], who prepared a 10 µm i.d. PLOT columns recovering the capillary inner wall with a porous poly(styrene-divinylbenzene) (PS-DVB) film, showing their applicability on mono and multidimensional separations. That study exposed new opportunities for the PLOT columns coupled with modern instrumentation. After that, other studies started to be published using PLOT columns, which became the main kind of columns exploited in OT-LC [10–12]. On the other hand, although WCOT columns are almost the only column-type used in current GC, in LC, those have received less attention once its stationary phase, conformed by a thin non-porous film, provides low sample capacity [13]. Nevertheless, new and interesting insights in the exploitation of very narrow WCOT columns in LC applications had been recently introduced by the Liu research group [14–17] and presented in the next sections. Other types of OT columns, such as the support-coated open tubular columns (SCOT) [18], also were described in the past, but hitherto they practically were forgotten.

The more frequent use of PLOT in LC and WCOT in GC has confused some current nomenclature. Usually, the term OT has been used as synonymous with PLOT in LC while with WCOT in GC. Most modern publications do not differ between these types of OT columns in their titles and keywords; so that searching for a specific kind of OT column could be challenging.

Although recently mainly used in proteomic analysis, OT columns present some unique characteristics in the LC-MS analysis of small molecules. From the chromatographic point of view, OT columns can provide superior column efficiency, higher overall peak capacity, and higher column permeability [12,13,19]. Guthrie and Jorgenson published one of the landmark works that showed the potentials of OT-columns in 1983 [20]. On that paper, the theory and fabrication of reversed-phase capillary OT columns for liquid chromatography is described and discussed. Additionally, the advantages and limitations were also explored. The authors showed the superior efficiency obtained on smaller inner diameter columns of capillary dimensions as a major advantage and the required miniaturization on detection system as the main limitation at that time. In the last decades, new detection cells and MS interfaces were developed to better fit the capillary and nanoscale flow rates, reducing the detection limitations that were present in the past. The factor that causes the improvement of efficiency on OT-columns is the use of the stationary phase in thin-film formats generates columns with a void in the capillary center, which drastically reduces the multipath dispersion factor (A-term, van Deemter equation). Consequently, more significant chromatographic efficiencies can be obtained [21]. At same efficiency values, OT columns have separation impedance 100-times lower than the packed ones. As a consequence, OT columns can theoretically provide separation 100-times faster or afford enhanced resolution for the same time of analysis [22].

Fig. 1a represents the increment in the ratio between the reduced linear velocity and the reduced plat height. As the A-term value, which is related to the multipath dispersion, is reduced, the separation performance improves [23]. Moreover, for the A-term value of zero, near to that obtained from OT columns, the optimal efficiency is found to be faster than for particle-packed and monolithic columns (with higher A-term values).

That improved performance of OT columns also was confirmed by Desmet and coworkers, who developed a metric that allows a better comparison of OT and packed columns [24]. This metric, called kinetic performance factor (KPF), is a dimensionless metric that shows a trade-off between separation, analysis time, and pressure. The KPF approach projects that both PLOT and WCOT columns would reach higher performance in a shorter time than obtained with the filled columns and even the modern pillar array columns (PACs), as displayed in Fig. 1b. The main factor that makes OT columns performed better than packed columns for LC is the filling material's absence. This allows a very low column pressure drop and a much better column permeability, increasing the value on the maximum kinetic performance factor [25]. Based on those considerations, it is also possible to conclude that WCOT columns, in theory, would perform better than PLOT columns.

On the other hand, the capillary inner diameter also affects the column performance; the smaller the tube's inner diameter (i.d.), the higher the chromatographic efficiency. Knox and Gilbert [21], based on the Taylor equation [26], early demonstrated that the plate height is directly proportional to the capillary inner diameter. The plot presented in Fig. 1c shows this difference in performance and was obtained from data calculated for OT columns from 10 to 100 µm i.d., 25 cm length, and a linear velocity of the mobile phase of 1 cm/s. A significant advantage of the smaller diameters is that it allows the columns to be operated at significantly reduced linear velocity, resulting in better separations [27].

Likewise, thicker films provide a more significant area for the analyte interaction and reduce the diffusion rate between phases, leading to a reduction in column performance (Fig. 1d) [28]. Nevertheless, it is essential to highlight that those considerations are dependent on stationary phase-type and its chemistry. For example, Poppe and coworkers [29] studied the effect of the film thickness and column i.d. on different stationary phases (liquid-liquid and siloxanes), concluding that both presented differences in separation performance and column loadability.

On the other hand, when coupled with mass spectrometry (MS), the OT columns can offer significant advantages such as i) The OT column's very low optimal flow rates (<100 nL/min) are more appropriate than those used for packed columns obtaining enhanced sensitivity using nanoESI sources. ii) Reduced backpressures and their capability to offer diversified chemical interactions with adequate retention, even operating under up to 100 % of organic solvent, makes the OT columns more suitable for the capillary/nano-LC coupling with EI sources. iii) OT columns can be connected directly from the injection port to the ionization source, avoiding additional connections and mitigating the extra-column band broadening contributions.

In this review, we provide an overview of the OT-LC-MS state of the art and its prospects in the analysis of small organic compounds (MW <1000 Da). New and emergent technologies in the OT column fabrication and innovative stationary phase development are summarized, establishing a clear differentiation between PLOT and WCOT OT-columns and highlighting the differences and similarities in their stationary phase synthesis. We underline the main instrumental advancements, opportunities, and shortcomings of the OT-LC coupling to mass spectrometry, highlighting the EI complementary character to the ESI ionization mode. Finally, lists of the publications describing the application of OT-LC-MS to small molecules' analysis are presented. For each paper summarized in those lists, analytes, the type of separation, stationary phase, column dimension, and detection system are also described and commented on.

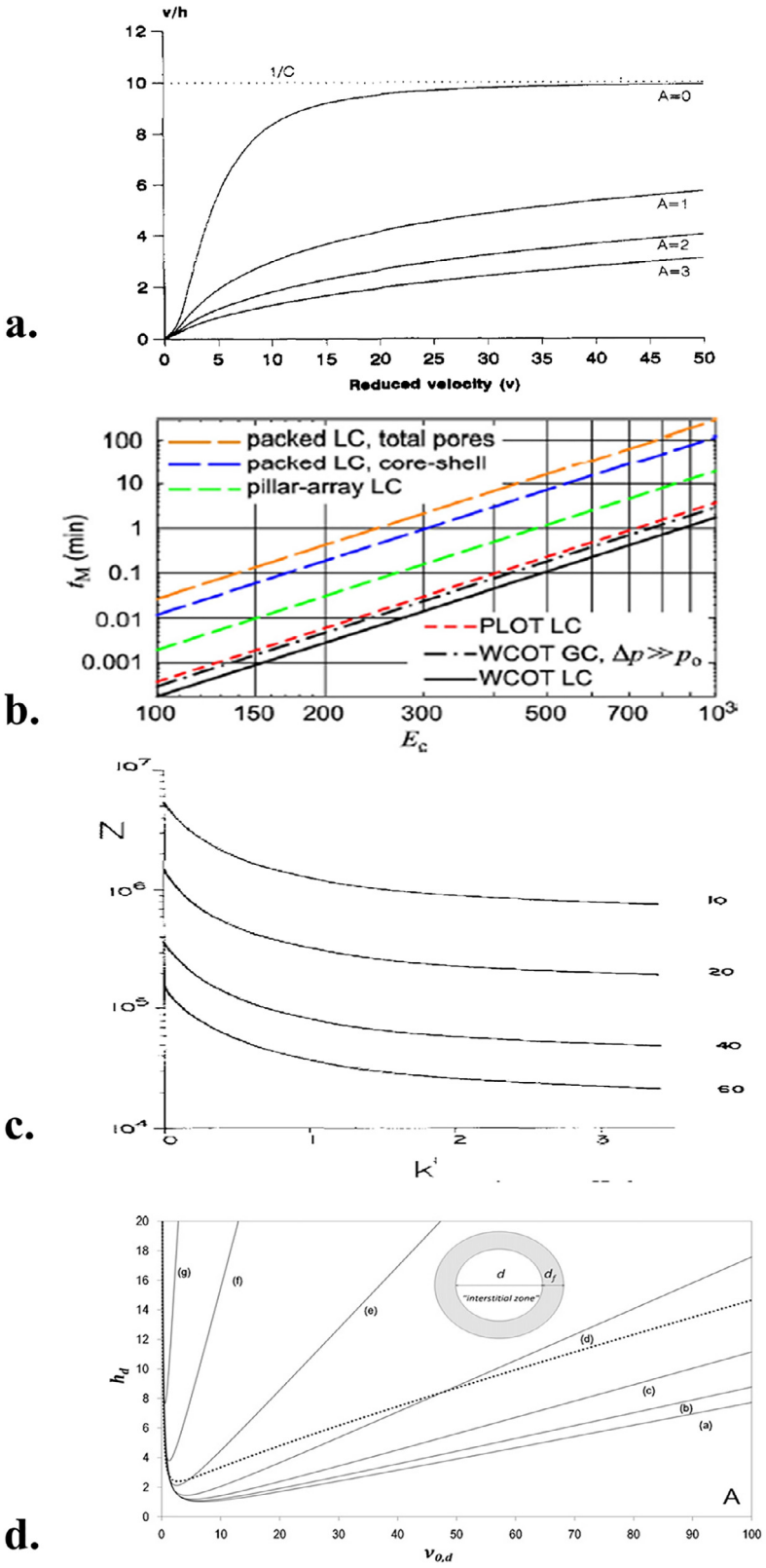

Fig. 1. Evaluation of important metrics of capillary columns in different columns configuration. **a**) Representation of υ/h in function of υ for coluns with values of A of 0, 1, 2, and 3. Reprinted with permission of [23]; **b**) Void time (tM) vs. efficiency (Ec), at maximum kinetic performance factor (ec,max). Reprinted with permission of [24]; **c**) Efficiency (N) in the function of the retention factor for OT columns of different i.d. Reprinted with permission of [21]; **d**) Reduced plate in function to the reduced linear velocity of varying film thickness ratios (ı = df/i.d.). (a) 0.001, (b) 0.05, (c) 0.125, (d) 0.25, (e) 0.5, (f) 1.0, and (g) 2.0. Reprinted with permission of [23].

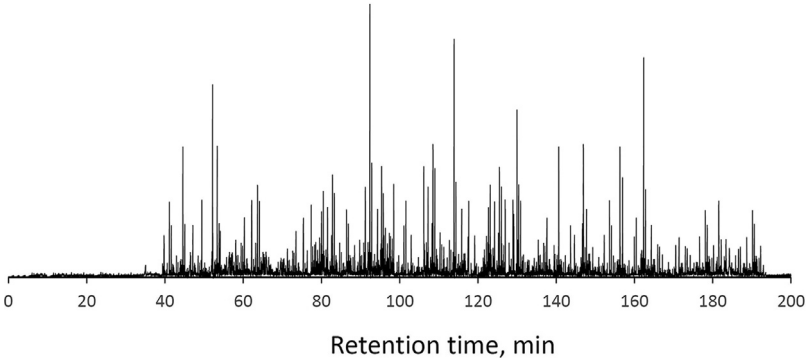

Fig. 2. Chromatogram for separating pepsin/trypsin digested E. coli lysate using a i.d. of 2 μm i.d x 160-cm-long OT column (70% OTMS), reported by Liu and coworkers [14].

2. New OT-LC columns and their role in the analysis of small molecules

Nowadays, although the application in the proteomics field and the reverse (RP) mode of elution are predominant, the use of OT columns for the separation of small molecules has also started to get researchers' attention in recent years. In the last decades, a wide diversity of OT columns using innovative materials as stationary phases have been assessed in the separation of diverse classes of organic compounds, not only via RP [30] but also involving hydrophilic interaction chromatography (HILIC) [31], chiral chromatography [32], and micellar chromatography [33], among other separation mechanisms.

The development of stationary phases based on nanoparticles (NPs), micelles [31], metal-organic frameworks (MOFs) [34], allotropic carbon materials [35], and molecular recognition functionalities, such as cyclodextrin [32], and imprinted polymers (MIP) [36], enriched the scientific activity in OT-LC development and application [37,38].

Moreover, OT columns also have the advantage of not requiring frits, so that this type of column allows the exploration of alternative column formats. These formats include multiple parallel channels columns prepared in photonic crystal fibers (FS-PCFs) [30] and the on-chip LC devices obtained via modern microfabrication technologies [39,40], as will be explained in the following sections.

2.1. Wall coated open tubular columns (WCOT)

WCOTs are characterized by the use of a non-porous thin film (usually 0.2 - 0.5 µm) as a stationary phase [41]. The most common WCOT stationary phases are based on high molecular weight, low volatility, and high viscosity polydimethylsiloxane polymers (PDMS) [42]. The substitution of the functional groups present in the pending siloxane groups leads to several types of phases with different polarities. The typical groups substituting the methyl ones from the PDMS include phenyl, cyano, and vinyl groups [43,44], polyethylene glycols (PEGs) - such as Carbowax-20M, superox and innovax – and other groups as GeO_2-PDMS, TiO_2-PDMS, polypyrrole, and 3-mercaptopropyltrimethoxylanosilica [13].

The preparation of WCOT columns can be performed by a dynamic [41] or static procedure [45]. Although the dynamic procedures are faster and more straightforward, those lead to smaller phase ratios and inaccurate control of the film's thickness. Hence, static procedures have more spread used [13,22]. Briefly, the procedure involves the following steps: i) the capillary pre-treatment, under acidic or alkaline conditions, ii) the capillary washing, iii) dehydrating the capillary in an oven, iv) the persylation via the application of a silanizing agent to the tube wall (disilazanes, disiloxanes, and chlorosilanes), and v) immobilization of the stationary phase by crosslinking with the aid of radical generators agents, such as peroxides (t-butyl peroxide (TBP), benzoyl peroxide (BP), dicumyl peroxide (DCP) and 2,4-dichlorobenzoyl peroxide (DCBP) [46]) or azo compounds (azo-t-butane (ATB) and azo-t-octane (ATO)) [47].

WCOTs were firstly proposed by Golay in 1957 [48] and nowadays are the most widely used type of column in GC. Likewise, WCOTs were the first OT separation media explored in LC [13]. One of the pioneer studies in this arena was published by Hibi et al. [49]. In 1979 they reported developing a column in polytetrafluoroethylene (PTFE) tubes of 15 cm length and 0.5 mm internal diameter having the walls coated with SE-30 as a stationary phase. These columns resulted in high-efficiency separations of polynuclear aromatic hydrocarbons (PAHs) [50,51]. Although with promissory results, the use of WCOT in LC was mainly limited by the low sample capacity of those columns, resultant from the small contact surface between the analyte and the stationary phase [13], and the difficulties to prepare columns with diameters less than 5.0 µm [49], required for actually efficient separations.

In recent years, with new developments in capillary/nanoLC, the interest in using WCOT in LC has come to resurge, and new developments allow to overcome the low analyte loadability problem traditionally attributed to WCOT columns. For example, recently the Liu research group hypothesizes and demonstrated that the low loadability problem can be overcome by using thin but dense non-porous coatings in columns with i.d. of 1-2 μm [14]. According to the authors, under those conditions, the stationary-phase loadability starts matching the mobile-phase loadability. Hence, these researchers prepared and assessed the performance of columns of 2 μm i.d, in different lengths, coated with octadecyltrimethoxysilane (OTMS). Through this approach, they demonstrated not only good retention and reproducibility in the separation of amino acids but also a high peak capacity (~2000 within 3 h) for one dimension LC separations, at a moderately-high elution pressure ($<$ 1000 psi), as illustrated by the chromatogram obtained during the analysis of pepsin/trypsin digested E. coli lysate (Fig. 2).

Although the reports on this subject are still scarce, very narrow WCOT columns have great potential in the rapid LC separation of organic compounds. For example, Mejía-Carmona and coworkers [13] recommended using HPAs and alkylbenzenes as probes to assess WCOT columns' efficiency. Similarly, Göhlin et al. early described the separation of anthracene derivatives using columns of 6 m length and 5-15 µm internal diameter, coated with polyorganosiloxanes stationary phases, showing high-efficiency separations with more than 10^6 theoretical plates [46]. In another study, a WCOT-LC separation of some of these analytes was also evaluated using 12-55 µm i.d.columns coated with PS-255 (methyl, 0.5-1.5% vinyl silicone gum) and SE-54 (methyl, 5% phenyl, 1% vinyl silicone gum) stationary phases. In this case,

efficient chromatographic separations were completed in less than 70 seconds [47].

Another great application was reported by Marchioni and coworkers [52], who reported using a WCOT column (11 cm length and 530 µm i.d.) coated with ionic liquids. The column was successfully used as the first dimension in a multidimensional in-tube solid-phase micro-extraction (in-tube SPME)-LC-MS setup employed to endocannabinoids determination in plasma samples.

Also, recently Yang et al. [53] — although with application in proteomics, out of the scope of the present review — proposed the coupling of WCOT columns to nanoESI-MS. In their study, the authors established that due to the advantageous low mobile phase flow rates (100 – 200 pL/min), WCOT-LC-MS could provide advantageous sensitivity and had the potential to become one of the primary analytical separation techniques of modern times.

The examples above demonstrate WCOT columns' potential and stimulate new contributions in this area. However, it is still necessary to overcome some limitations in the manufacturing process, since smaller internal diameters (around 5 µm or less) tend to be more challenging, and are susceptible to clogging when coating with stationary phases based on polydimethylsiloxanes, which are highly slimy. Besides, the descriptions in the literature of the manufacturing of modern very narrow WCOTs frequently are not informative enough to allow replication of the process.

The work in this area requires an investigation of the molecular probes that are suitable with the selectivity of the column's stationary phase, and with the MS (e.g. electrospray ionization), so that no analyte coelutions occur and, therefore, achieve a good performance chromatographic separation. We should expect new contributions within this scope, aimed at the study of small molecules, which will expand the applicability of WCOT columns beyond the analysis in proteomics.

2.2. Porous layer open tubular columns (PLOT)

PLOT columns have better compatibility with LC than WCOT. The stationary phase's porous nature provides a more significant interaction with the analytes, increasing the retention factors [38]. As previously mentioned, PLOT columns were reintroduced for LC applications in the past decade by Luo et al. [8]. They prepared and assessed PLOT columns coated with PS-DVB stationary phase with internal diameters equal to or less than 10 μm in the protein separation. Lately, other research groups, such as those led by Lundanes, and Brett, have introduced new PLOT stationary phases, demonstrating their application of PLOT-LC into different niches, such as food and environmental samples.

Due to the great diversity of stationary phases that can be used, there is no general procedure that can be used for the synthesis of PLOT columns for LC. Nevertheless, the preparation of PLOT columns is mainly characterized by the initial acid or basic pretreatment of the capillary tube, which conduced to the generation of a porous structure in the inner wall. After that, signaling and polymerization stages are performed to grant the formation of strong chemical bonds that ensures the stable immobilization of the stationary phase, preventing column bleeding [54].

The porous material that constitutes the stationary phase of a PLOT column can have an organic character, such as those based on polystyrene, or inorganic character, as in silica-based ones. It can also be developed from new materials, such as hybrid phases with organic and inorganic character [11].

For polymeric stationary phase generation, the previously treated support substrate is filled with a polymeric mixture. The ends are sealed, and the supply of heat or light causes the polymerization reaction. Such processes are called thermal initiation and photoinitiation, and both provide stationary phases covalently anchored to the capillary wall [55,56]. For example, the Lundanes research group developed a sample preparation/separation platform with PLOT columns [57]. A solid-phase extraction column was developed by joining 126 PLOT columns of 8 μm internal diameter (a PCF) and internally coated with poly (styrene-co-octadecene-co-divinylbenzene) (PS-OD-DVB). Moreover, the separation column was 10 μm in internal diameter and 2 m long, and its stationary phase was poly (styrene-co-divinylbenzene) (PS-DVB). This system allowed quick loading of the sample and the possibility of analyzing small analytes, such as sulfonamides [57].

Silica-based stationary phases are usually obtained by i) generation of porous silica structures, via capillary etching or by deposition of a porous silica layer promoted by a silica precursor, such as tetraethoxysilane, followed by ii) functionalization of the silica layer with an alkyl modified silica precursor, which allows the incorporation of carbon-riched moieties ables to provide retention via hydrophobic interactions. For example, Foster et al., aiming to improve PLOT columns' load capacity, developed a stationary phase where C-18 was anchored to silica. The capillary column was evaluated through its usability, permeability, and chromatographic efficiency in reverse phase mode. The data were compared to a commercially available monolithic and particulate C-18 capillary column. High theoretical numbers of plates were generated in a test mixture separation made up of small molecules. Two reverse-phase applications demonstrated the applicability of this new type of column [58].

Likewise, Rodriguez et al. also developed PLOT columns internally coated with C-18 functionalized with silica in 126 channels of 4.2 µm in i.d. PCF. Together, these channels became a single PLOT column that provided a great capacity to preconcentrate sample loading [30]. Also, recently Hara et al. separated amino acids through a PLOT column with an internal diameter of 5 μm, with a C-18 stationary phase obtained from tetramethoxysilane/methyltrimethoxysilane (TMOS/MTMS) hybrid layers with methyl groups inserted. This stationary phase has a hydrophobic character, allowing thinner porous layers to be sufficient to achieve a retention factor similar to C-18 PLOT columns synthesized using only TMOS. Columns with stationary phases of various thicknesses were developed. The number of plates for the longest capillary columns ranged from N = 282000 to N = 379000 for the most retained compound [59].

In addition to C-8 and C-18, some allotropic forms of carbon have come to be used recently as hydrophobic interaction sources. One of the most frequent practical problem in the use of OT columns is the low retention of the analytes on these columns due to the small amount of stationary phase. Hence, the use of carbon allotropes, such as graphene, could be a good alternative to the obtention of more hydrophobic stationary phases, compensating to some extent the low interaction analytes/stationary phase. For example, Qu et al. developed PLOT columns with stationary phases containing graphene oxide (GO) and graphene(G). PLOT columns with GO as a stationary phase were developed through the immobilization of graphene oxide nanosheets immobilized on the capillary wall using 3-aminopropyl diethoxymethylsilane as a coupling agent. Moreover, the graphene-coated column was manufactured by reduction with GO modified with hydrazine. Both columns were tested for separation of PAHs; the PLOT column with GO phase presented better performance and shows more potential for the separation of different analytes [60]. Likewise, Kubo et al. also developed new work in this direction by producing a PLOT column coated internally with C60-fullerene through a covalent bond using an active photo/thermal agent. These columns also demonstrated a suitable capability to separate small molecules like PAHs [35].

PLOT columns have been a target for new columns development by several research groups. Most of the research on this topic aims to develop new stationary phases that enable alternative interaction mechanisms to expand their applicability scope. Hence,

other materials such as MOFs have come to be tested as OT stationary phases. For example, Zhu et al. developed a 25 µm id PLOT column with a stationary phase in which vancomycin-modified organic metal particles were incorporated directly into the zwitterionic polymer coating synthesized by the copolymerization of [2-(methacryloyloxy) ethyl dimethyl - (3- sulfopropyl) ammonium hydroxide and N, N'-methylenebisacrylamide. The incorporation of the particles into the zwitterionic polymer coating improved the column's stationary phase's selectivity. The column was applied to analyze trypsin digestion of bovine serum albumin, revealing the potential for separation of biological samples and demonstrating good repeatability [31].

Open tubular columns can also be used in sophisticated systems capable of analyzing tiny volumes. For example, Li et al. developed a high-performance pico-HPLC system, which can directly pipette femtoliters of a sample using a separation column tip driven by an electroosmotic pump. Enantiomers of amino acids were successfully analyzed [61].

In conclusion, the miniaturized diameter of PLOT columns allows the analysis of tiny samples, and the diversity of stationary phases allows the separation of complex mixtures [56]. Another highlight of these columns is the ease of coupling with the MS detection technique, demonstrating the full potential of PLOT columns in miniaturized LC.

2.3. Microfabricated OT columns

An exciting alternative to overcome the difficulties of preparing OT columns in capillary format is the use of the LC-Chip microfabrication technologies. OTs are the most easily manufacturable chromatographic medium in a chip format, once an open channel is already the first stage of all LC-Chip devices [62]. From the first on-chip LC system, involving an open channel (6 µm x 15 cm), reported by Manz et al. [63], the fabrication and use of OT columns in a chip format, involving both bare substrates and functionalized porous reverse phases or immobilization of nanoparticles [64,65], has been demonstrated in recent years [66]. For example, Shimizu et al. [67] developed an LC chip containing an open nanofluidic channel (2.3 µm-wide by 350 nm-deep) employing a bare fused silica surface with silanol and siloxane groups as the stationary phase. That device demonstrated a separation efficiency of 150000 plates per m (170 plates per 1.1 mm) in the normal phase separation of Sudan I and Sudan Orange G pigments. Likewise, Benvenuto and coworkers [68] developed an on-chip OT-LC system containing a 10 cm long by a rectangular cross-section of 100 µm $\times$ 20 µm microcolumn functionalized with C-8-tetraethoxysilane (C-8-TEOS). Although chromatographic performance parameters were not reported, the authors demonstrated the OT-LC device's feasibility of achieving acetic acid's suitable retention. This small molecule is hardly retained in the RP mode. Smirnova and coworkers [39] prepared an on-chip OT column functionalized with C-18 as a stationary phase. That device was tested in the RP separation of fluorescein and sulforhodamine and different amino acid mixtures, demonstrating, for example, a 300000 plates/m theoretical plate number for sulforhodamine B and 320000 plates/m for serine.

On the other hand, microfabricated OT columns suffer the same drawbacks as the OT columns in capillary format, and its major limitation is the low sample load capacity [69]. In addition to the incorporation of porous layers to increase the sample capacity, other alternatives, such as the fabrication of PAC media — also reported in the literature as collocated monolithic support structures (COMOSS) [70] — are nowadays demonstrating excellent results.

PACs consist of an ordered microchannels base of equal size and shape, resulting in a fully reproducible structure. These shapes can be semicircular, rectangular, trapezoidal, quadratic, elliptical, and diamond, and are made using photolithography and DRIE techniques [71]. At the moment, the elongated hexagonal shape has provided the best chromatographic efficiency [72–74]. The pillar array columns have a specific design so that the distribution of the flow follows a binary division in the inlet and outlet channels [70]. This type of architecture allows the mobile phase to travel all channels evenly. As for the stationary phase, the channels can be coated with layers of porous or non-porous materials (the same applied on PLOT and WCOT columns). The first option provides better load capacity [71]. In terms of advantages and limitations, pillar array columns are found between packed columns and open tubular. These types of columns can generate the same performance as open tubular columns (considered the best chromatographic column format), but with the advantage of having greater load capacity [75].

To the best of our knowledge, PACs have been mainly exploited in the field of proteomics, more specifically, of tryptic peptides [76,77]. Their performance in the separation of small organic compounds has yet to be studied [78]. We considerer that new interesting works in this regard could appear in the literature in the coming years

3. Coupling OT-LC with mass spectrometry for the analysis of small molecules

Although the capillary/nanoLC's improved chromatographic performance was early established, the prospects for increasing LC speed and resolving power via column downscaling were sharply limited by the feasibility of detecting with minimal volumes [79–81]. Knox and Gilbert [21] stated that, according to the eluting band volume in a capillary/nano-column, the detection volume's contribution to the extra-column peak variance should be $\leq$ 1nL. Hence, from the beginning, mass spectrometry was one of the first choices under consideration for detection at a reduced LC scale [82,83]. Moreover, early was also perceived that OT columns could minimize the extra-column effects by introducing the column exit into the MS ionization source. With these columns, the contribution of the detection to peak variance can be considered null.

Mass spectrometry is a highly sensitive technique, which allows for both universal and selective detection. Undoubtedly, the leading modern analytical advantage of the capillary/nanoLC is its improved sensitivity, derived from the excellent compatibility between the nano/micro flow rate and the nano-mass spectrometry detection. Nowadays, capillary/nanoLC-MS provides exceptional detection capabilities in untargeted and targeted analysis, one of the most powerful analytical tools of the current separation sciences [84].

3.1. OT-LC-MS primordia: coupling with Electron Ionization MS (EI-MS)

The first attempts to interface OT columns with MS — and capillary/nanoLC in general — were previous to the apparition of the modern ESI sources and were performed through EI interfaces, as summarized in Table 1.

To the best of our knowledge, the first OT-LC-MS coupling was reported by Ishii and coworkers [85], who in 1979 described the direct insertion of an OT-LC effluent into the injection port of a GC-MS system. N,N-diethylaniline, N-ethylaniline e N-methylaniline were employed as model compounds, separated in a 47 µm i.d. x 608 cm glass capillary column coated with β,β'-oxydipropionitrile (BOP) and detected via EI-MS by chemical ionization (CI). Chromatograms obtained by both scan and selected ion monitoring acquisition were very similar to those recorded by UV detection in terms of band broadening and intensity, demonstrating the OT-LC-MS coupling feasibility for the first time.

Table 1
Summarized applications of OT-LC to the analysis of small molecules, using EI-MS detection.

Analytes	OT column	Elution mode	Detection	Ref
Toluene, naphthalene, perylene, nitropyrene, cholesterol, adenine, adenosine, epinephrine, acridine, isoleucine, and trifluralin,	10-μm-i.d. x 100 cm untreated fused-silica		CI-MS EI-MS	[93]
Trifluralin Metabolites	10-μm-i.d. x 150 cm OV-17-V WCOT	RP	CI-MS	[95]
Toluene, diuron, Nicotinamide, caffeine, phenacetin, diazepam, aldrin, Ascorbic acid,	8-μm-i.d. x 150 cm untreated fused-silica		EI-MS	[91]
Naphthalene, acridine, propazine, trietazine, Metrlbuzln, Methyl parathion, Pmrathlon, ethyl, Morphos)lflwalln	15 μm-i.d. x 150 cm C-18 PLOT 10-μm-i.d. x 150 cm OV-17-V WCOT	RP	CI-MS EI-MS	[94]
Toluene, aniline,	5 μm-i.d. x 181 cm, 10-i.d. x 203 cm and 25-i.d. x 682 cm untreated fused-silica		CI-MS	[92]
Benzene, Naphthalene, pyrene, anthracene, squalene, undecane, benzene sulfonic acid, ionol, and triphenylphosphine tungsten pentacarbonyl,	32 μm -i.d. x 181 cm Apiezon L. WCOT	RP	CI-MS	[89]
N,N-diethylaniline; N-ethylaniline; N-rnethylaniline.	47 µm I.D. X 608 cm BOP WCOT	RP	EI-MS	[85]

In the middle of the '80s, more than 15 different approaches for capillary/nanoLC and EI-MS coupling had been described [86,87]. Among those, the capillary inlet interface (CII) and direct liquid introduction (DLI) were the most extensively explored [88]. CII was the first and a more straightforward approach and was based on the direct introduction of the column end at the ionization sources so that no contribution to the peak variance due to the detection was expected. On the other hand, DLI incorporated additional vaporization techniques to speed-up the vaporization of the column eluent.

Due to its simplicity, the CII was especially suitable for the coupling of OT columns. Nevertheless, its applicability was limited to very volatile molecules (MW <250), such as stated by Tijssen and coworkers [89]. For compounds with higher molecular mass, this interface provided chromatographic noise bands with irregular shapes and significant fluctuation in the ionization source pressure. Also, Niessen and Pope explored the OT-LC and EI-MS hyphenation via the CII [88,90–92]. Those researchers incorporated an external heater to the interface, so that heat transference was improved, avoiding the solvent's freezing at the end or in the capillary tube (Fig. 3a). Detection and identification of over 50 compounds in the EI mode were studied. In this case, analytes with a high boiling point, polarity, or thermal lability also produced broad and irregular peak shapes. Even for some polar compounds, such as ascorbic acid, Theophylline, hydrochloride, phenylalanine, and glucose, no spectrum was recorded, and in some cases, those compounds blocked the capillary tube [88,91].

The irregular peak shapes and fluctuations in the ionization source's pressure revealed that an additional fast vaporization mechanism should be incorporated for effective OT-LC-EI-MS detection of compounds with higher molecular weights. Hence, Tijssen et al. proposed a DLI interface, promoting the formation of a liquid jet via incorporation of a tapered column end tip with a 2.5 µm i.d outlet orifice (Fig. 3b) [89]. In this way, symmetrical peaks and suitable CI spectra were recorded for squalene (MW = 422), undecane benzene sulphonic acid (MW=312), sucrose (MW=422), Lubad J (MW=424), and some thermally unstable compounds as triphenylphosphine tungsten pentacarbonyl (MW=584), among many others. A similar approach was proposed by Wit et al. [93,94], who explored the synergic effect of the use of tapering end columns and tip heating. A thermostated copper tip was incorporated at the end of a tapered OT column (1.5µm outlet orifice) of a 1m x 10 µm-i.d. column. By heating, at 300°C, significant improvement in the peak shape of naphthalene (bp 218°C) and acridine (bp 350°C) were obtained. This interface allowed the acquisition in both EI and CI modes [94], and its suitability for non-target analysis was demonstrated in the analysis of trifluralin and its metabolites by OT-LC-EI-MS in the negative CI mode [95].

Likewise, Niessen and Poppe also developed an alternative DLI interface used in combination with CI in the study of peak broadening effects for 5 and 10 µm i.d. OT columns [92]. In this case, for liquid jet formation, an interface with a miniaturized diaphragm was developed (Fig. 3c). Forming a liquid jet in the kinetically near to optimal operation of OT-LC flow-rates (1.0 and 600 nL/min) could require diaphragms smaller than 1 µm, i.d. [96]. Such diaphragms could be challenging to fabricate and susceptible to clogging. Therefore, diaphragms of about 4.0 µm, i.d., were used, requiring applying a make-up flow to guarantee the jet formation. The nature of the make-up liquid, in turn, allowed to control of the CI conditions. For volatile solutes, such as toluene and aniline, detection limits (S/N=3) ranged from 1-10 pg. Nevertheless, according to the authors, limits of detection (LOD) at least l000-fold lower must be reached to make the proposed OT-LC-EI-MS reliable in analyzing complex samples.

Although promising, the coupling of capillary/nano-LC with EI-MS was almost entirely relegated by the ESI-MS interfaces' introduction at the end of the '80s. Just a few research groups continued working in the hyphenation of LC with EI-MS [97–102]. Even so, their efforts lead to the development of modern, efficient interfaces, based on i) the electron ionization LC-MS with supersonic molecular beams [103]; ii) the direct LC-EI-MS coupling [97,104,105]; and iii) the interfacing with nebulization/spraying systems [106–108], including the modern Liquid Electron Ionization (LEI) source [106,107]. However, the capillary/nano-LC coupling with EI-MS is still not competitive with nanoESI-MS detection.

Nevertheless, thanks to the informative structural advantages and the untargeted identification capabilities [109] derived from the rich and highly reproducible fragmentation patterns of the EI-MS detection, substantial scientific efforts [4,110–113] continue being made to achieve the efficient coupling of capillary/nanoLC with EI-MS. In this regard, OT columns can offer remarkable advantages once OT-LC optimal linear velocity occurs at very low flow-rates (< 100 nL/min) so that the mobile phase effect over the EI process is drastically minimized. Besides, OT-LC operation backpressures are more compatible with the vacuum operation conditions of the EI sources. The diversified chemical interactions offered by the diversity of OT columns stationary phases can provide suitable retention and resolution with a water-free mobile phase that is more volatile and more compatible with the EI conditions. So, we consider that

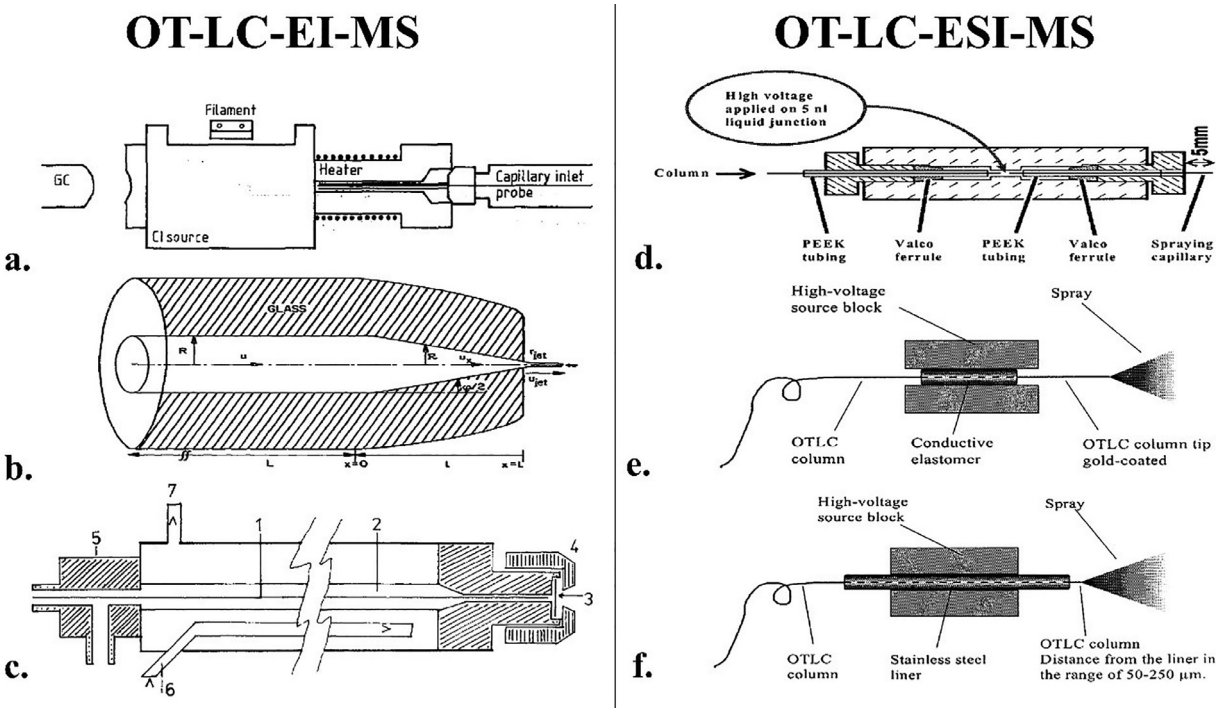

Fig. 3. First attempts to couple OT-LC with MS. **a-c)** interfacing with EI-MS; **d-f)** Coupling of OT-LC to ESI-MS; **a)** Schematic diagram of the capillary-inlet interface probe with external [91]; **b)** Schematic representation of the liquid jet forming tip at the column exit [89]; **c)** Schematic diagram of the laboratory-built DLI probe (10 mm OD). 1, Fused-silica open-tubular column; 2, make-up liquid; 3, 4-pm nickel diaphragm enclosed between two PFTE spacers; 4, stainless steel nut; 5, modified Swagelock l/16 in. T-piece; 6, cooling water in; 7, cooling water out. Reprinted with permission of [92]; **d)** Standard Micromass dynamic nanospray interface; **e)** Gold-coated column interface; **f)** Stainless steel liner interface [121].

the exploitation of modern technology in the efficient coupling of OT-LC with EI-MS is still missing. Essential reports describing these developments' potential applicability could appear in the coming years, bringing new insights into the small molecules' LC-Ms analysis.

3.2. Modern OT-LC-MS: coupling with Electrospray Ionization MS (ESI-MS)

Although other atmospheric pressure ionization (API) sources, such as matrix-assisted laser desorption ionization (MALDI) [114], atmospheric pressure chemical ionization (APCI) [115], have been used in the hyphenation of capillary/nano-LC with MS, undoubtedly, ESI is currently the primary ionization mode used in the coupling of LC and MS at the miniaturized scale.

Capillary/nanoLC-ESI-MS provides enhanced chromatographic resolution and improved sensitivity and detection capabilities derived from those techniques' outstanding compatibility at the miniaturized scale [84]. Once, miniaturization of the ESI-MS also had evidenced much higher sensitivity [116]. At micro/nanoflow rates, the Taylor cone droplets are small enough to yield a more efficient ionization process [117], with less ion suppression and matrix effects. As a result, the nanoESI efficiency is less susceptible to matrix composition and salt contamination, providing more uniform analytical responses [118–120].

Although at the moment, the hyphenation of LC and ESI-MS at miniaturized scale has been mainly based on the use of packed columns, OT columns offer the advantage of allowing the direct coupling from the injection port to the nanoESI emitter, without additional tubes or connectors. As a result, the extra column band broadening contributions can be significantly minimized.

The first attempts to interface OT-LC with nanoESI-MS were performed by Hulthe et al. at the end of the '90s [121]. Employing a modified Micromass dynamic nanospray probe, the authors assessed the detection of fatty acids in the negative ionization mode coupling 5 and 20 µm i.d WCOT columns with three different types of nanospray interfaces: i) the standard dynamic nanospray interface (SDNS), ii) the gold-coated column end interface and iii) the stainless steel liner interface.

The coupling via i) SDNS (Fig. 3d) was set by interfacing the columns with the fused-silica spray emitter through a 0.25-mm-bore Valco stainless steel 1/16-inch junction. High voltage for Taylor cone formation was supplied through the stainless junction. However, this interface was not suitable for the proposed application, since the 5nL volume of the junction was too large for the OT operation flow rates, causing excessive band broadening. Besides, the spray obtained with this approach was very unstable and irreproducible.

The ii) Gold-Coated Column End Interface successfully addressed dead volume problems generated by connecting the column to a separate spraying tip. In this case, the end of the column was sharpened symmetrically, and covered with a layer of gold (0.5 µm thick), sputtered onto the last 4 cm of the column (Fig. 3e). High voltage was supplied through conductive elastomer so that the Taylor cone was formed directly at the end of the column. Stable sprays were quickly established, even at flow rates down of 5 nL/min. This interface provided high sensitivity and outstanding separation efficiency, without post-column band broadening. Nevertheless, the sputtered gold layer showed a short lifetime, leading to instability and then malfunctioning in a few days. This interface was unsuitable for routine analysis.

The iii) Stainless Steel Liner interface provided longer-time signal stability than the gold-coated tip, with similar sensitivity and separation efficiency, but more easily and cheaply. The column end was drawn through a stainless steel tubing piece, to which the high voltage was directly applied (Fig. 3f). No treatment (coating, tapered, nor sharpened) at the column end was necessary. While maintaining the polyimide coating, a stable Taylor cone was estab-

Table 2
Summarized applications of OT-LC to the analysis of small molecules, classified employing ESI-MS detection.

Analytes	OT column	Elution mode	MS	Ref
Ofloxacin, caffeine, atrazine, and diuron	Multi-lumen capillary 126 parallel channels of 4.2 μm-i.d x 60 cm C-18 PLOT	RP	QTOF	[30]
Sulfonamides	10 μm-i.d x 60 - 200 cm PS-DVB PLOT	RP	QqQ	[57]
Hydroxylated cholesterol (OHC) isomers	10 μm-i.d. x 300 cm C-18 PLOT	RP	Orbitrap	[125]
Ketoprofen racemate	30 μm-i.d. x 60 cm Enantioselective MIP-PLOT	RP	QqQ	[36]
Fatty acids: lauric (C12:0), myristic (C14:0), palmitic (C16:0), and stearic (C18:0)	20-μm-i.d. x 225 cm PS 264 WCOT 5-μm-i.d. x 80 cm PS 255, WCOT	RP	QqQ	[121]

lished at the column tip's flat surface. This was the most appealing configuration for OT-LC-ESI-MS interfacing.

Nowadays, most of the LC-MS manufacturers offer nano-ESI sources, which works very well and with minimal post-column band broadening contribution. Being mainly coupled to ESI-MS, the OT-LC-MS's excellent performance has been currently exploited in the trace bioanalysis of complex proteomic samples, glycans, nucleic acids, and cells [7,19,37,122–124]. On the other hand, although OT-LC also promises high resolution in the fast separation of small molecules (<1000 Da) [28], its use in this type of application — although nowadays there is no practical reason for it — is still quite limited, as can be inferred from the reduced number of reported applications (Table 2).

A recent and relevant application of OT-LC-ESI-MS to the analysis of small molecules was reported by Kulsing et al. [36]. They prepared porous layers of molecularly imprinted polymers (MIP-PLOT) in an open tubular capillary column format for use in chiral separations. The enantioselective capillaries obtained were coupled to an LC/MSD-SL ion trap mass spectrometer through an Agilent Technologies G1607A orthogonal electrospray interface and evaluated in the separations of ketoprofen racemate, showing suitable resolution and sound sensitivity. Afterward, Vehus and coworkers [125] featured an attoLC-ESI-MS system by coupling a monolithic trap column (50 µm × 40 mm poly(styrene-co-octadecyl-co-divinylbenzene) to a 10 μm i.d, fused silica OT-LC separation column functionalized with C18-groups. The system was successfully employed for separating a wide range of molecules, including small metabolites (Fig. 4.a).

Combined with a Q-Exactive Orbitrap MS equipped with a nanospray ESI source [126], this setup was used in a targeted metabolomics study of sub-μg amounts exosomes derived from breast cancer-related hydroxylated cholesterol. The authors found similar sample capacity and superior sensitivity and chromatographic performance compared with packed columns based on capillary/nanoLC approaches. Another exciting result of this study was that, while reducing scale up to the attoLC-ESI-MS yields sensitivity improvements of up to 100-fold for small molecules such as sulfonamides, and significant sensitivity gains for peptides as well, no sensitivity improvement was observed for the analysis of intact proteins.

In another recent study, Ribeiro da Silva et al. [57] developed an *in-tube* SPME-OT-LC-ESI-MS/MS method. A extraction/preconcentration PLOT column, prepared into a multi-lumen capillary (MLC, 126 channels of 8 µm i.d., coated with poly(styrene-co-octadecene-co-divinylbenzene)), was coupled to a 10 µm × 2 m poly(styrene-co-divinylbenzene) OT column and a triple quadrupole mass spectrometer equipped with a nanospray FlexTM ion source (Thermo Scientific) (Fig. 4.b). That setup was employed to analyze sulfonamides in surface water samples, demonstrating competitive fast loading and suitable refocusing on the OT analytical column compared to monolithic/particle-packed in-tube SPME columns.

Rodriguez et al. [30] also functionalized an MLC (126 channels of 4.2 μm i.d) with C18 to produce multi-channel PLOT columns, assessing its performance as an on-capillary preconcentration column, a separation column, and ESI emitter (Fig. 4.c). The direct coupling of the PLOT-MLC with the QTOF via a capillary electrosprayer facilitated the simultaneous use of the modified MLC as a pre-concentrator, separator column, and electrospray emitter, avoiding the use of additional connectors and/or capillaries between the injector and MS inlet.

4. Additional applications of the OT-LC to the analysis of small molecules

Although a little out of the scope of this review, it is relevant to highlight that, thanks to the modern developments in capillary/nanoLC instrumentation, the feasibility of the OT-LC in the analysis of small molecules also has been demonstrated in recent years employing spectrophotometric detectors, such as ultraviolet (UV), diode array detectors (DAD), fluorescence (FL), and laser-induced fluorescence (FLI). Some selected applications are summarized in Table 3.

For example, Zhang and coworkers [127] prepared a PLOT column for microcell membrane chromatography (m-CMC) by physical adsorption of rabbit red blood cell (rRBC) membranes onto the inner of the capillary. This system was used in the study of the dynamic binding capacity (DBC) of verapamil. The mCMC column with the PLOT capillary demonstrated comparable cellular membrane capacity to traditional CMC methods, but with significantly lower consumption of costly biological reagents, such as membrane cells. In another interesting example, Quirino by et al. [33] introduced an environmentally friendly OT-LC approach based on nanosized micellar pseudo phases. Exploiting the molecular organization of typical long-chain ionic surfactants to form micelles at the solid surface-liquid interface and the differential solubilization/distribution of solutes between interfacial and solution micelles under different concentration pH and ionic strength, the authors demonstrated the retention/separation of various types of molecules, such as PHAs, drugs, pesticides, antioxidants, and peptides. Zhu and coworkers also developed an interesting approach by incorporating MOFs particles modified with vancomycin directly into the zwitterionic polymer coating of an OT column. This separation media demonstrated good separation/resolution power for neutral, acidic, and basic compounds, mainly through hydrophilic interactions, π-π interactions, and the coordination between unsaturated Zn^{2+} and analytes. Although all those examples (Table 3) do not correspond to the coupling of OT columns with mass spectrometry, all of them help illustrate the OT columns' potential to

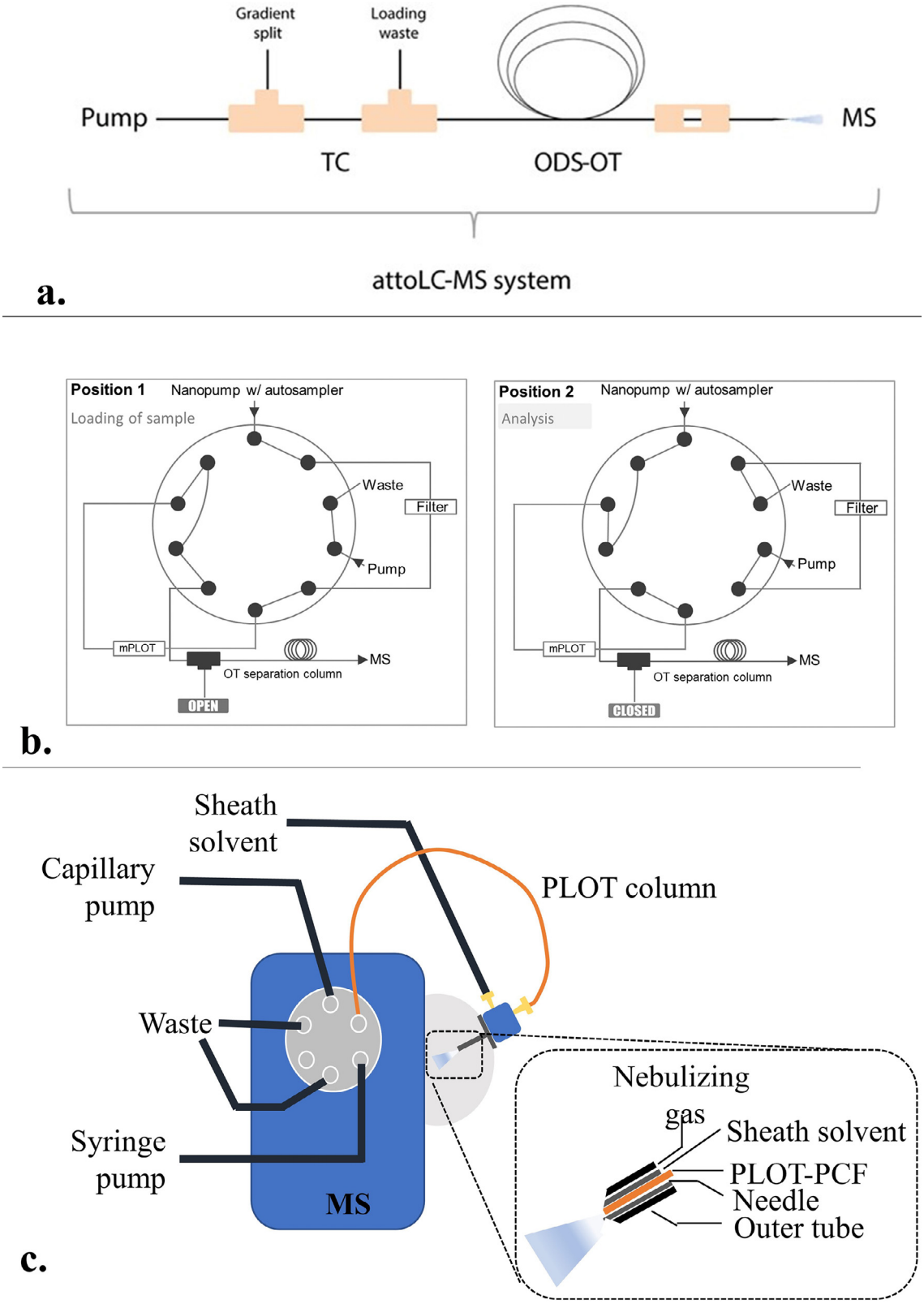

Fig. 4. Some modern examples of the coupling of OT-LC with ESI-MS detection. **a)** AttoLC-ESI-MS system developed by Vehus et al. [125]; **b)** mPLOT based *in-tube* SPME-OT-LC-ESI-MS/MS system developed by Ribeiro da Silva et al. [57]; **c)** OT-LC-ESI-MS system developed by Rodriguez et al. [30], featuring a multi-channel porous layer open tubular (PLOT) column as pre-concentrator, separator, and ESI emitter.

Table 3
Summarized applications of OT-LC to the analysis of small molecules, employing spectrophotometric detectors.

Analytes	OT column	Elution mode	detection	Ref.
Amino acids	2-μm-i.d. x 2.7 cm C18 PLOT	RP	LIF	[17]
Toluene, nucleosides, bases, amides, chlorophenols, and benzoic acids	150 µm-i.d x 150 cm PEGDA PLOT	HILIC	UV	[128]
Coumarin compounds (C440, C460 and C480)	5-μm-i.d. x 40 and 130 cm TMOS/MTMS PLOT	RP	FL	[59]
Toluene, DMF, formamide, and thiourea, aromatic and phenols	25-μm-i.d. x 100 IRMOF-3@vancomyin-pMSA PLOT	HILIC	UV	[129]
Aromatic hydrocarbons, anionic, cationic, and amphiphilic drugs, pesticides, peptides	25-200 μm-i.d. x 60-120 cm Surfactant micelles (CTAB and SDS)	Micellar LC	UV	[33]
Amino acid enantiomers	75 μm-i.d. x 15 cm β-cyclodextrin	HILIC	UV	[32]
Amino acid enantiomers	900 nm-i.d x 54.5 cmm poly(MQD-co-HEMA-co-EDMA) PLOT		LIF	[61]
Coumarins C440, C460, and C480	5 μm-i.d. x 250 cm C-18 PLOT	RP	FL	[54]
Flavonoids, toluene, N,N-dimethylformamide, formamide, and thiourea	25 μm-i.d. x 60 cm pMSA PLOT	HILIC	UV	[31]
Biphenyl, naphthalene; 4,2-methyl naphthalene; acenaphthene	75 μm-i.d. x 50 cm C-18 PLOT	RP	DAD	[130]
Verapamil	75 μm-i.d. x 35 cm Physical adsorbed rabbit red blood cell (rRBC) PLOT	CMC	UV	[127]
Phenanthrene, triphenylene, and benz[a]pyrene	25 μm-i.d. x 30 cm C_{60}-fullerene	RP	UV	[35]
Six alquilbenzenes and 32 Pesticides	15 μm-i.d. x 300 cm C-8 PLOT	RP	UV	[58]
Triphenylphosphine oxides	Multi-lumen capillary 30, 54 and 168 parallel channels of 3.8 – 5.5 μm-i.d x 20 cm C_6F_{13}	RP	UV	[131]
Naphthalene, biphenyl, fluorene, phenanthrene, anthracene, Fluoranthene	5, 10 and 50-μm-i.d. x 120-190 cm C-18 PLOT	RP	UV	[83]

provide diversified interaction and retention mechanisms to separate diverse organic small molecules.

6. Conclusion

Although Ishii and coworkers early introduced OT-LC, this technique's evolution had been slow, primarily due to very low flow rates and restrictions imposed by the instrumental requirements, to guarantee no excessive band broadening. Modern developments in capillary/nanoLC and nanoESI-MS have created new possibilities for OT columns in the analysis of bio- and small molecules with unpreceded detection capabilities. OT-LC provides fast separations, with kinetic efficiencies of at least ten times more theoretical plates than those observed for packed columns [28]. The multipath dispersion band broadening contribution is practically eliminated while retaining the open capillary structure, providing high permeability and high resolution at very narrow inner diameters.

Although the separation of small molecules employing innovative sorbent materials as stationary phases in diverse separation modes is being expectantly explored, PLOT (mainly based on PS-DVD polymers) and WCOT (mainly based on PDMS and PEG polymers) columns continue to predominate, together with reversed-phase based materials. Most recent research focused on OT-LC involves PLOT columns once they are more compatible with LC instrumentation. The presence of the porous layer provides a higher sample capacity, which increases the analytes retention factor. WCOT-LC was widely explored in the '70s and '80s, with outstanding promissory results, such as the separation of anthracene derivatives with more than 10^6 theoretical plates [50] or the separation of 25 compounds in just 70 seconds [51]. Nowadays, new investments are being made in this area, using WCOT columns with an internal diameter of 2 µm [16,53], aiming their future coupling with EI- and ESI-MS.

The use of multi-lumen capillaries and microfabrication technologies are providing alternatives to increase the OTs sample capacity. In µPAC columns, the microfabricated channels with the same size and shape guarantees more reproducibility; each channel functions as an OT column and a particle present in the packed columns. For this reason, pillar array columns have similar efficiency to an OT, with the sample capacity of a packed column.

OT-LC coupled to mass spectrometry — although underdeveloped compared to miniaturized packed columns - demonstrates enhanced sensitivity and outstanding detection capabilities. OT columns offer attractive advantages for their hyphenation to MS once they work with a very low optimum flow rate (<100 nL/min). OT-LC-ESI-MS had gained considerable acceptance in the separation of proteomic and similar complex mixtures. Although widely explored until the end of the '80s, OT-LC-EI-MS remained after that relegated as a function of the ESI-MS invention. OT columns promise considerable advances in nanoLC-MS, especially in the analysis of biomolecules. However, new advances need to be made to analyze small molecules.

Declaration of Competing Interest

The authors declare that they have no known competing financial interests or personal relationships that could have appeared to influence the work reported in this paper.

CRediT authorship contribution statement

Deyber Arley Vargas Medina: Writing - original draft, Writing - review & editing. **Natalia Gabrielly Pereira dos Santos:** Writ-

ing - original draft, Writing - review & editing. **Juliana Soares da Silva Burato:** Writing - original draft, Writing - review & editing. **João Victor Basolli Borsatto:** Writing - original draft, Writing - review & editing. **Fernando Mauro Lanças:** Conceptualization, Writing - review & editing, Funding acquisition, Writing - original draft.

Acknowledgments

The authors are grateful to the Coordenação de Aperfeiçoamento de Pessoal de Nível Superior—Brasil (CAPES)—Finance Code 001; to FAPESP (Grants 2019/22724-7 2017/02147-0, 2019/26263-4, 2015/15462-5, 2014/03765-0 and 2014/07347-9); and to CNPq (307293/2014-9 and 308843/2019-3) for the financial support provided for this research and to our laboratory.

References

[1] K.B. Lynch, A. Chen, S. Liu, Miniaturized high-performance liquid chromatography instrumentation, Talanta 177 (2018) 94–103, doi:10.1016/j.talanta.2017.09.016.
[2] E. Vasconcelos Soares Maciel, A.L. de Toffoli, E. Sobieski, C.E. Domingues Nazário, F.M. Lanças, Miniaturized liquid chromatography focusing on analytical columns and mass spectrometry: A review, Anal. Chim. Acta. 1103 (2020) 11–31, doi:10.1016/j.aca.2019.12.064.
[3] M.V. Novotny, Development of capillary liquid chromatography: A personal perspective, J. Chromatogr. A. 1523 (2017) 3–16, doi:10.1016/j.chroma.2017.06.042.
[4] G. Famiglini, P. Palma, V. Termopoli, A. Cappiello, S. Tsizin, B. Seemann, T. Alon, A.B. Fialkov, A. Amirav, Electron Ionization LC-MS: What Is It and Why Use It? Compr. Anal. Chem. 79 (2018) 1–28, doi:10.1016/bs.coac.2017.06.008.
[5] F. Rigano, P.Q. Tranchida, P. Dugo, L. Mondello, High-performance liquid chromatography combined with electron ionization mass spectrometry: A review, TrAC Trends Anal. Chem. 118 (2019) 112–122, doi:10.1016/j.trac.2019.05.032.
[6] T. Tsuda, K. Hibi, T. Nakanishi, T. Takeuchi, D. Ishii, Studies of open-tubular micro-capillary liquid chromatography. II. Chemically bonded octadecylsilane stationary phase, J. Chromatogr. A. 158 (1968) 227–232, doi:10.1016/S0021-9673(00)89969-0.
[7] G. Yue, Q. Luo, J. Zhang, S.L. Wu, B.L. Karger, Ultratrace LC/MS proteomic analysis using 10-μm-i.d. porous layer open tubular poly(styrene-divinylbenzene) capillary columns, Anal. Chem. 79 (2007) 938–946, doi:10.1021/ac061411m.
[8] Q. Luo, G. Yue, G.A. Valaskovic, Y. Gu, S. Wu, B.L. Karger, On-Line 1D and 2D Porous Layer Open Tubular/LC-ESI-MS Using 10-μm-i.d. Poly(styrene−divinylbenzene) Columns for Ultrasensitive Proteomic Analysis, Anal. Chem. 79 (2007) 6174–6181, doi:10.1021/ac070583w.
[9] Q. Luo, T. Rejtar, S.L. Wu, B.L. Karger, Hydrophilic interaction 10 μm I.D. porous layer open tubular columns for ultratrace glycan analysis by liquid chromatography-mass spectrometry, J. Chromatogr. A. 1216 (2009) 1223–1231, doi:10.1016/j.chroma.2008.09.105.
[10] W.J. Cheong, F. Ali, Y.S. Kim, J.W. Lee, Comprehensive overview of recent preparation and application trends of various open tubular capillary columns in separation science, J. Chromatogr. A. 1308 (2013) 1–24, doi:10.1016/j.chroma.2013.07.107.
[11] D.A. Collins, E.P. Nesterenko, B. Paull, Porous layer open tubular columns in capillary liquid chromatography, Analyst 139 (2014) 1292–1302, doi:10.1039/c3an01869e.
[12] S.C. Lam, E. Sanz Rodriguez, P.R. Haddad, B. Paull, Recent advances in open tubular capillary liquid chromatography, Analyst (2019), doi:10.1039/c9an00329k.
[13] K. Mejía-Carmona, J. Soares da Silva Burato, J.V.B. Borsatto, A.L. de Toffoli, F.M. Lanças, Miniaturization of liquid chromatography coupled to mass spectrometry: 1. Current trends on miniaturized LC columns, TrAC - Trends Anal. Chem. 122 (2020) 115735, doi:10.1016/j.trac.2019.115735.
[14] Y. Yang, S. Liu, Non-porous thin dense layer coating: Key to achieving ultrahigh peak capacities using narrow open tubular columns, Talanta Open 1 (2020) 100003, doi:10.1016/j.talo.2020.100003.
[15] H. Chen, Y. Yang, Z. Qiao, P. Xiang, J. Ren, Y. Meng, K. Zhang, J.Juan Lu, S. Liu, A narrow open tubular column for high efficiency liquid chromatographic separation, Analyst 143 (2018) 2008–2011, doi:10.1039/c7an02065a.
[16] Y. Yang, H. Chen, M.A. Beckner, P. Xiang, J.J. Lu, C. Cao, S. Liu, Narrow, Open, Tubular Column for Ultrahigh-Efficiency Liquid-Chromatographic Separation under Elution Pressure of Less than 50 bar, Anal. Chem. 90 (2018) 10676–10680, doi:10.1021/acs.analchem.8b02634.
[17] P. Xiang, Y. Yang, Z. Zhao, M. Chen, S. Liu, Ultrafast gradient separation with narrow open tubular liquid chromatography, Anal. Chem. 91 (2019) 10738–10743, doi:10.1021/acs.analchem.9b02190.
[18] J. Chauhan, A. Darbre, Determination of amino acids by means of glass capillary gas-liquid chromatography with temperature-programmed electron-capture detection, J. Chromatogr. A. 236 (1982) 151–156, doi:10.1016/S0021-9673(00)82508-X.
[19] S.R. Wilson, C. Olsen, E. Lundanes, Nano liquid chromatography columns, Analyst 144 (2019) 7090–7104, doi:10.1039/c9an01473j.
[20] J.W. Jorgenson, E.J. Guthrie, Liquid chromatography in open-tubular columns. Theory of column optimization with limited pressure and analysis time, and fabrication of chemically bonded reversed-phase columns on etched borosilicate glass capillaries, J. Chromatogr. A. 255 (1983) 335–348, doi:10.1016/S0021-9673(01)88293-5.
[21] J.H. Knox, M.T. Gilbert, Kinetic optimization of straight open-tubular liquid chromatography, J. Chromatogr. A. 186 (1979) 405–418, doi:10.1016/S0021-9673(00)95263-4.
[22] R. Swart, J.C. Kraak, H. Poppe, Recent progress in open tubular liquid chromatography, TrAC - Trends Anal. Chem. 16 (1997) 332–342, doi:10.1016/S0165-9936(97)00036-8.
[23] A.L. Crego, J.C. Diez-Masa, M.V Dabrio ', Preparation of Open Tubular Columns for High-Performance Liquid Chromatography Reversed-Phase, Anal. Chem. 65 (1993) 1615–1621, doi:10.1021/ac00059a022.
[24] L.M. Blumberg, G. Desmet, Kinetic performance factor – A measurable metric of separation-time-pressure tradeoff in liquid and gas chromatography, J. Chromatogr. A. 1567 (2018) 26–36, doi:10.1016/j.chroma.2018.06.048.
[25] G. Guiochon, Conventional Packed Columns vs. Packed or Open Tubular Microcolumns in Liquid Chromatography, Anal. Chem. 53 (1981) 1318–1325, doi:10.1021/ac00232a006.
[26] G. Taylor, P.R.S.L. A, Dispersion of soluble matter in solvent flowing slowly through a tube, Proc. R. Soc. London. Ser. A. Math. Phys. Sci. 219 (1953) 186–203, doi:10.1098/rspa.1953.0139.
[27] P. Kucera, G. Guiochon, Use of open-tubular columns in liquid chromatography, J. Chromatogr. A. 283 (1984) 1–20, doi:10.1016/S0021-9673(00)96238-1.
[28] T.J. Causon, R.A. Shellie, E.F. Hilder, G. Desmet, S. Eeltink, Kinetic optimisation of open-tubular liquid-chromatography capillaries coated with thick porous layers for increased loadability, J. Chromatogr. A. 1218 (2011) 8388–8393, doi:10.1016/j.chroma.2011.09.047.
[29] P.P.H. Tock, P.P.E. Duijsters, J.C. Kraak, H. Poppe, Theoretical optimization of open-tubular columns for liquid chromatography with respect to mass loadability, J. Chromatogr. A. 506 (1990) 185–200, doi:10.1016/S0021-9673(01)91577-8.
[30] E.S. Rodriguez, S.C. Lam, P.R. Haddad, B. Paull, Reversed-Phase Functionalised Multi-lumen Capillary as Combined Concentrator, Separation Column, and ESI Emitter in Capillary-LC–MS, Chromatographia 82 (2019) 197–209, doi:10.1007/s10337-018-3629-7.
[31] L. Peng, M. Zhu, L. Zhang, H. Liu, W. Zhang, Preparation and evaluation of 3 m open tubular capillary columns with a zwitterionic polymeric porous layer for liquid chromatography, J. Sep. Sci. 39 (2016) 3736–3744, doi:10.1002/jssc.201600535.
[32] C. Aydoğan, Chiral separation and determination of amino acid enantiomers in fruit juice by open-tubular nano liquid chromatography, Chirality 30 (2018) 1144–1149, doi:10.1002/chir.23006.
[33] J.P. Quirino, F.M. Tarongoy, Liquid chromatography with micelles in open-tube capillaries, Green Chem 20 (2018) 2486–2493, doi:10.1039/c8gc00409a.
[34] Q. Liu, N. Sun, C. hui Deng, Recent advances in metal-organic frameworks for separation and enrichment in proteomics analysis, TrAC - Trends Anal. Chem. 110 (2019) 66–80, doi:10.1016/j.trac.2018.10.033.
[35] T. Kubo, Y. Murakami, Y. Tominaga, T. Naito, K. Sueyoshi, M. Yan, K. Otsuka, Development of a C60-fullerene bonded open-tubular capillary using a photo/thermal active agent for liquid chromatographic separations by π-π interactions, J. Chromatogr. A. 1323 (2014) 174–178, doi:10.1016/j.chroma.2013.10.097.
[36] C. Kulsing, R. Knob, M. Macka, P. Junor, R.I. Boysen, M.T.W. Hearn, Molecular imprinted polymeric porous layers in open tubular capillaries for chiral separations, J. Chromatogr. A. 1354 (2014) 85–91, doi:10.1016/j.chroma.2014.05.065.
[37] M.A. Ahmed, B.M.B. Felisilda, J.P. Quirino, Recent advancements in open-tubular liquid chromatography and capillary electrochromatography during 2014–2018, Anal. Chim. Acta. 1088 (2019) 20–34, doi:10.1016/j.aca.2019.08.016.
[38] S.C. Lam, E. Sanz Rodriguez, P.R. Haddad, B. Paull, Recent advances in open tubular capillary liquid chromatography, Analyst 144 (2019) 3464–3482, doi:10.1039/C9AN00329K.
[39] A. Smirnova, H. Shimizu, K. Mawatari, T. Kitamori, Reversed-phase chromatography in extended-nano space for the separation of amino acids, J. Chromatogr. A. 1418 (2015) 224–227, doi:10.1016/j.chroma.2015.09.022.
[40] E. Méry, S. Alekseev, F. Portet-Koltalo, C. Morin, D. Barbier, V. Zaitsev, P.L. Desbène, Porous silicon based microdevice for reversed phase liquid chromatography, Phys. Status Solidi Curr. Top. Solid State Phys. 6 (2009) 1777–1781, doi:10.1002/pssc.200881098.
[41] R. Scott, Open-Tubular Columns, Encycl. Chromatogr. Third Ed. (Print Version), CRC Press, 2009, doi:10.1201/NOE1420084597.ch318.
[42] M.W. Ogden, H.M. McNair, Characterization of fused-silica capillary tubing by contact angle measurements, J. Chromatogr. A. 354 (1986) 7–18, doi:10.1016/S0021-9673(01)87006-0.
[43] J. de Zeeuw, J. Luong, Developments in stationary phase technology for gas chromatography, TrAC - Trends Anal. Chem. 21 (2002) 594–607, doi:10.1016/S0165-9936(02)00809-9.
[44] G. Desmet, D. Cabooter, K. Broeckhoven, Graphical Data Representation Methods To Assess the Quality of LC Columns, Anal. Chem. 87 (2015) 8593–8602, doi:10.1021/ac504473p.

[45] J. Bouche, M. Verzele, A Static Coating Procedure for Glass Capillary Columns, J. Chromatogr. Sci. 6 (1968) 501–505, doi:10.1093/chromsci/6.10.501.
[46] D.T. Harvey, The Essence of Chromatography (Poole, Colin F.), J. Chem. Educ. 80 (2003) 883, doi:10.1021/ed080p883.1.
[47] B.E. Richter, J.C. Kuei, N.J. Park, S.J. Crowley, J.S. Bradshaw, M.L. Lee, Azo compounds for free radical crosslinking of polysiloxane stationary phases, J. High Resolut. Chromatogr. 6 (1983) 371–374, doi:10.1002/jhrc.1240060705.
[48] L.S. Ettre, M.J.E. Golay and the invention of open-tubular (capillary) columns, J. High Resolut. Chromatogr. 10 (1987) 221–230, doi:10.1002/jhrc.1240100503.
[49] K. Hibi, D. Ishii, I. Fujishima, T. Takeuchi, T. Nakanishi, Studies of open tubular micro capillary liquid chromatography. 1. The development of open tubular micro capillary liquid chromatography, J. High Resolut. Chromatogr. 1 (1978) 21–27, doi:10.1002/jhrc.1240010106.
[50] K. Göhlin, M. Larsson, Study of polyorganosiloxanes (native and solvent swollen) for the preparation of narrow (5-15 μm I.D.) and long (1-6m) open tubular columns in reversed-phase liquid chromatography, J. Chromatogr. A. 645 (1993) 41–56, doi:10.1016/0021-9673(93)80616-G.
[51] S. Folestad, M. Larsson, Swollen polysiloxanes as stationary phases in reversed-phase open-tubular column liquid chromatography, J. Chromatogr. A. 394 (1987) 455–464, doi:10.1016/S0021-9673(01)83812-7.
[52] C. Marchioni, I.D. de Souza, V.R. Acquaro, J.A. de Souza Crippa, V. Tumas, M.E.C. Queiroz, Recent advances in LC-MS/MS methods to determine endocannabinoids in biological samples: Application in neurodegenerative diseases, Anal. Chim. Acta. 1044 (2018) 12–28, doi:10.1016/j.aca.2018.06.016.
[53] Y. Yang, P. Xiang, H. Chen, Z. Zhao, Z. Zhu, S. Liu, On-column and gradient focusing-induced high-resolution separation in narrow open tubular liquid chromatography and a simple and economic approach for pico-gradient separation, Anal. Chim. Acta. 1072 (2019) 95–101, doi:10.1016/j.aca.2019.04.008.
[54] T. Hara, S. Futagami, S. Eeltink, W. De Malsche, G.V. Baron, G. Desmet, Very High Efficiency Porous Silica Layer Open-Tubular Capillary Columns Produced via in-Column Sol-Gel Processing, Anal. Chem. 88 (2016) 10158–10166, doi:10.1021/acs.analchem.6b02713.
[55] G. Desmet, M. Callewaert, H. Ottevaere, W. De Malsche, Merging open-tubular and packed bed liquid chromatography, Anal. Chem. 87 (2015) 7382–7388, doi:10.1021/acs.analchem.5b01579.
[56] J.S. da S. Burato, F.M. Lanças, Colunas tubulares abertas recobertas internamente com uma camada porosa (PLOT) em cromatografia líquida miniaturizada, Sci. Chromatogr. 10 (2018) 150–173, doi:10.5935/sc.2018.010.
[57] M.R. da Silva, O.K. Brandtzaeg, T. Vehus, F.M. Lanças, S.R. Wilson, E. Lundanes, An automated and self-cleaning nano liquid chromatography mass spectrometry platform featuring an open tubular multi-hole crystal fiber solid phase extraction column and an open tubular separation column, J. Chromatogr. A. 1518 (2017) 104–110, doi:10.1016/j.chroma.2017.08.071.
[58] S. Forster, H. Kolmar, S. Altmaier, Performance evaluation of thick film open tubular silica capillary by reversed phase liquid chromatography, J. Chromatogr. A. 1283 (2013) 110–115, doi:10.1016/j.chroma.2013.01.107.
[59] T. Hara, Y. Izumi, M. Nakao, K. Hata, G.V. Baron, T. Bamba, G. Desmet, Silica-based hybrid porous layers to enhance the retention and efficiency of open tubular capillary columns with a 5 μm inner diameter, J. Chromatogr. A. 1580 (2018) 63–71, doi:10.1016/j.chroma.2018.10.023.
[60] Q. Qu, Y. Shen, C. Gu, Z. Gu, Q. Gu, C. Wang, X. Hu, Capillary column coated with graphene oxide as stationary phase for gas chromatography, Anal. Chim. Acta. 757 (2012) 83–87, doi:10.1016/j.aca.2012.10.032.
[61] R. Li, Y. Shao, Y. Yu, X. Wang, G. Guo, Pico-HPLC system integrating an equal inner diameter femtopipette into a 900 nm I.D. porous layer open tubular column, Chem. Commun. 53 (2017) 4104–4107, doi:10.1039/c7cc00799j.
[62] D.A. Vargas Medina, E.V.S. Maciel, F.M. Lanças, Miniaturization of liquid chromatography coupled to mass spectrometry. 3. Achievements on chip-based LC–MS devices, TrAC Trends Anal. Chem. 131 (2020) 116003, doi:10.1016/j.trac.2020.116003.
[63] A. Manz, Y. Miyahara, J. Miura, Y. Watanabe, H. Miyagi, K. Sato, Design of an open-tubular column liquid chromatograph using silicon chip technology, Sensors Actuators B Chem 1 (1990) 249–255, doi:10.1016/0925-4005(90)80210-Q.
[64] X. Yang, G. Jenkins, J. Franzke, A. Manz, Shear-driven pumping and Fourier transform detection for on chip circular chromatography applications, Lab Chip 5 (2005) 764–771, doi:10.1039/b502121a.
[65] H.F. Li, H. Zeng, Z. Chen, J.M. Lin, Chip-based enantioselective open-tubular capillary electrochromatography using bovine serum albumin-gold nanoparticle conjugates as the stationary phase, Electrophoresis 30 (2009) 1022–1029, doi:10.1002/elps.200800359.
[66] F. Haghighi, Z. Talebpour, A.S. Nezhad, Towards fully integrated liquid chromatography on a chip: Evolution and evaluation, TrAC Trends Anal. Chem. 105 (2018) 302–337, doi:10.1016/j.trac.2018.05.002.
[67] H. Shimizu, K. Mawatari, T. Kitamori, Femtoliter-scale separation and sensitive detection of nonfluorescent samples in an extended-nano fluidic device, Analyst 139 (2014) 2154–2157, doi:10.1039/c3an02353b.
[68] A. Benvenuto, V. Guarnieri, L. Lorenzelli, C. Collini, M. Decarli, A. Adami, C. Potrich, L. Lunelli, R. Canteri, C. Pederzolli, Fabrication of a MEMS-based separation module for liquid chromatography, Sensors Actuators, B Chem 130 (2008) 181–186, doi:10.1016/j.snb.2007.07.111.
[69] H. Poppe, Some reflections on speed and efficiency of modern chromatographic methods, J. Chromatogr. A. 778 (1997) 3–21, doi:10.1016/S0021-9673(97)00376-2.
[70] B. He, N. Tait, F. Regnier, Fabrication of Nanocolumns for Liquid Chromatography, Anal. Chem. 70 (1998) 3790–3797, doi:10.1021/ac980028h.
[71] X. Yuan, R.D. Oleschuk, Advances in microchip liquid chromatography, Anal. Chem. 90 (2018) 283–301, doi:10.1021/acs.analchem.7b04329.
[72] B.E. Slentz, N.A. Penner, F. Regnier, Geometric effects of collocated monolithic support structures on separation performance in microfabricated systems, J. Sep. Sci. 25 (2002) 1011–1018, doi:10.1002/1615-9314(20021101)25:15/17⟨1011::AID-JSSC1011⟩3.0.CO;2-N.
[73] S. Jung, A. Höltzel, S. Ehlert, J.A. Mora, K. Kraiczek, M. Dittmann, G.P. Rozing, U. Tallarek, Impact of conduit geometry on the performance of typical particulate microchip packings, Anal. Chem. 81 (2009) 10193–10200, doi:10.1021/ac902069x.
[74] J.H. Knox, Band dispersion in chromatography - A universal expression for the contribution from the mobile zone, J. Chromatogr. A. 960 (2002) 7–18, doi:10.1016/S0021-9673(02)00240-6.
[75] G. Desmet, M. Callewaert, H. Ottevaere, W. De Malsche, Merging open-tubular and Packed bed liquid chromatography, Anal. Chem. 87 (2015) 7382–7388, doi:10.1021/acs.analchem.5b01579.
[76] G. Tóth, T. Panić-Janković, G. Mitulović, Pillar array columns for peptide separations in nanoscale reversed-phase chromatography, J. Chromatogr. A. 1603 (2019) 426–432, doi:10.1016/j.chroma.2019.06.067.
[77] J.O. De Beeck, J. Pauwels, N. Van Landuyt, P. Jacobs, W. De Malsche, G. Desmet, A. Argentini, A. Staes, L. Martens, F. Impens, K. Gevaert, A well-ordered nanoflow LC-MS/MS approach for proteome profiling using 200 cm long micro pillar array columns, BioRxiv (2018), doi:10.1101/472134.
[78] M. Baca, G. Desmet, H. Ottevaere, W. De Malsche, Achieving a Peak Capacity of 1800 Using an 8 m Long Pillar Array Column, Anal. Chem. 91 (2019) 10932–10936, doi:10.1021/acs.analchem.9b02236.
[79] J.C. Giddings, Comparison of the Theoretical Limit of Separating Ability in Gas and Liquid Chromatography, Anal. Chem. 36 (1964) 1890–1892, doi:10.1021/ac60216a005.
[80] C.G. Horvath, B.A. Preiss, S.R. Lipsky, Fast Liquid Chromatography: An Investigation of Operating Parameters and the Separation of Nucleotides on Pellicular Ion Exchangers, Anal. Chem. 39 (1967) 1422–1428, doi:10.1021/ac60256a003.
[81] J.H. Knox, M. Saleem, Kinetic conditions for optimum speed and resolution in column chromatography, J. Chromatogr. Sci. 7 (1969) 614–622, doi:10.1093/chromsci/7.10.614.
[82] E. Kenndler, E.R. Schmid, Chapter 10 Combination of Liquid Chromatography and Mass Spectrometry, in: Instrum. High-Performance Liq. Chromatogr., 1978, pp. 163–177, doi:10.1016/S0301-4770(08)60485-6.
[83] A.L. Crego, J.C. Díez-Masa, M.V. Dabrio, Preparation of Open Tubular Columns for Reversed-Phase High-Performance Liquid Chromatography, Anal. Chem. 65 (1993) 1615–1621, doi:10.1021/ac00059a022.
[84] D.A. Vargas Medina, E.V. Soares Maciel, A. Lúcia de Toffoli, F.M. Lanças, Miniaturization of liquid chromatography coupled to mass spectrometry. 2. Achievements on modern instrumentation for miniaturized liquid chromatography coupled to mass spectrometry, TrAC Trends Anal. Chem. (2020) 115910, doi:10.1016/j.trac.2020.115910.
[85] D. Ishii, T. Tsuda, K. Hibi, T. Takeuchi, T. Nakanishi, Study of open-tubular micro-capillary liquid chromatography, J. High Resolut. Chromatogr. 2 (1979) 371–377, doi:10.1002/jhrc.1240020621.
[86] A.P. Bruins, Developments in interfacing microbore high-performance liquid chromatography with mass spectrometry (a review), J. Chromatogr. A. 323 (1985) 99–111, doi:10.1016/S0021-9673(01)90374-7.
[87] J. Henion, Chapter 8 Micro LC/MS Coupling, J. Chromatogr. Libr. 28 (1984) 260–300 Microcolumn High-Performance Liq. Chromatogr., doi:10.1016/S0301-4770(08)60699-5.
[88] W.M.A. Niessen, H. Poppe, Problems in interfacing open-tubular liquid chromatography and mass spectrometry, J. Chromatogr. A. 394 (1987) 21–34, doi:10.1016/S0021-9673(01)94157-3.
[89] R. Tijssen, J.P.A. Bleumer, A.L.C. Smit, M.E. van Kreveld, Microcapillary liquid chromatography in open tubular columns with diameters of 10–50 μm, J. Chromatogr. A. 218 (1981) 137–165, doi:10.1016/S0021-9673(00)82052-X.
[90] W.M.A. Niessen, H.P.M. van Vliet, H. Poppe, Studies on external peak broadening in open-tubular liquid chromatography systems using the exponentially modified Gaussian model, Chromatographia 20 (1985) 357–363, doi:10.1007/BF02269062.
[91] W.M.A. Niessen, H. Poppe, Open-tubular liquid chromatography—mass spectrometry with a capillary-inlet interface, J. Chromatogr. A. 385 (1987) 1–15, doi:10.1016/S0021-9673(01)94616-3.
[92] W.M.A. Niessen, H. Poppe, Open-tubular liquid chromatography-mass spectrometry using direct liquid introduction, J. Chromatogr. A. 323 (1985) 37–46, doi:10.1016/S0021-9673(01)90369-3.
[93] J.S.M. De Wit, K.B. Tomer, J.W. Jorgenson, Characterization of the direct-probe open-tubular liquid chromatography-mass spectrometry interface parameters, J. Chromatogr. A. 462 (1989) 365–375, doi:10.1016/S0021-9673(00)91363-3.
[94] J.S.M. de Wit, C.E. Parker, K.B. Tomer, J.W. Jorgenson, Direct Coupling of Open-Tubular Liquid Chromatography with Mass Spectrometry, Anal. Chem. 59 (1987) 2400–2404, doi:10.1021/ac00146a017.
[95] J.S.M. De Wit, C.E. Parker, K.B. Tomer, J.W. Jorgenson, Separation and identification of trifluralin metabolites by open-tubular liquid chromatography/negative chemical ionization mass spectrometry, Biol. Mass Spectrom. 17 (1988) 47–53, doi:10.1002/bms.1200170110.
[96] P.J. Arpino, P. Krien, S. Vajta, G. Devant, Optimization of the instrumental parameters of a combined liquid chromatograph-mass spectrometer, coupled by an interface for direct liquid introduction, J. Chromatogr. A. 203 (1981) 117–130, doi:10.1016/S0021-9673(00)80286-1.

[97] F. Rigano, A. Albergamo, D. Sciarrone, M. Beccaria, G. Purcaro, L. Mondello, Nano Liquid Chromatography Directly Coupled to Electron Ionization Mass Spectrometry for Free Fatty Acid Elucidation in Mussel, Anal. Chem. 88 (2016) 4021–4028, doi:10.1021/acs.analchem.6b00328.
[98] Y.N. Yao, L. Wu, D. Di, Z.C. Yuan, B. Hu, Vibrating tip spray ionization mass spectrometry for direct sample analysis, J. Mass Spectrom. 54 (2019) 772–779, doi:10.1002/jms.4429.
[99] J.V. Abonamah, B.A. Eckenrode, M. Moini, On-site detection of fentanyl and its derivatives by field portable nano-liquid chromatography-electron Ionization-mass spectrometry (nLC-EI-MS), Forensic Chem 16 (2019) 100180, doi:10.1016/j.forc.2019.100180.
[100] F. Rigano, M. Russo, A. Arigò, P. Dugo, L. Mondello, Combining linear retention index and electron ionization mass spectrometry for a reliable identification in nano liquid chromatography, J. Chromatogr. A. 1610 (2020), doi:10.1016/j.chroma.2019.460581.
[101] V. Vrkoslav, B. Rumlová, T. Strmeň, P. Nekvasilová, M. Šulc, J. Cvačka, Applicability of low-flow atmospheric pressure chemical ionization and photoionization mass spectrometry with a microfabricated nebulizer for neutral lipids, Rapid Commun. Mass Spectrom. 32 (2018) 639–648, doi:10.1002/rcm.8086.
[102] N. Riboni, L. Magrini, F. Bianchi, M. Careri, A. Cappiello, Sol-gel coated ion sources for liquid chromatography-direct electron ionization mass spectrometry, Anal. Chim. Acta. 978 (2017) 35–41, doi:10.1016/j.aca.2017.04.026.
[103] B. Seemann, T. Alon, S. Tsizin, A.B. Fialkov, A. Amirav, Electron ionization LC-MS with supersonic molecular beams - The new concept, benefits and applications, J. Mass Spectrom. 50 (2015) 1252–1263, doi:10.1002/jms.3695.
[104] A. Cappiello, G. Famiglini, P. Palma, E. Pierini, V. Termopoli, H. Trufelli, Direct-EI in LC-MS: Towards a universal detector for small-molecule applications, Mass Spectrom. Rev. 30 (2011) 1242–1255, doi:10.1002/mas.20329.
[105] C. Flender, C. Wolf, P. Leonhard, M. Karas, Nano-liquid chromatography-direct electron ionization mass spectrometry: Improving performance by a new ion source adapter, J. Mass Spectrom. 46 (2011) 1004–1010, doi:10.1002/jms.1981.
[106] V. Termopoli, G. Famiglini, P. Palma, M. Piergiovanni, P. Rocio-Bautista, M.F. Ottaviani, A. Cappiello, M. Saeed, S. Perry, Evaluation of a liquid electron ionization liquid chromatography–mass spectrometry interface, J. Chromatogr. A. 1591 (2019) 120–130, doi:10.1016/j.chroma.2019.01.034.
[107] V. Termopoli, G. Famiglini, P. Palma, M. Piergiovanni, A. Cappiello, Atmospheric pressure vaporization mechanism for coupling a liquid phase with electron ionization mass spectrometry, Anal. Chem. 89 (2017) 2049–2056, doi:10.1021/acs.analchem.6b04646.
[108] F. Bianchi, N. Riboni, V. Termopoli, L. Mendez, I. Medina, L. Ilag, A. Cappiello, M. Careri, MS-Based Analytical Techniques: Advances in Spray-Based Methods and EI-LC-MS Applications, J. Anal. Methods Chem. 2018 (2018), doi:10.1155/2018/1308167.
[109] P. Palma, G. Famiglini, H. Trufelli, E. Pierini, V. Termopoli, A. Cappiello, Electron ionization in LC-MS: recent developments and applications of the direct-EI LC-MS interface, Anal. Bioanal. Chem. 399 (2011) 2683–2693, doi:10.1007/s00216-010-4637-0.
[110] A. Cappiello, The Benefits of a Liquid-Electron Ionization Liquid Chromatography – Mass Spectrometry Interface, LCGC 32 (2019) 330–331.
[111] F. Rigano, P.Q. Tranchida, P. Dugo, L. Mondello, High-performance liquid chromatography combined with electron ionization mass spectrometry: A review, TrAC - Trends Anal. Chem. 118 (2019) 112–122, doi:10.1016/j.trac.2019.05.032.
[112] G. Famiglini, P. Palma, V. Termopoli, A. Cappiello, S. Tsizin, B. Seemann, T. Alon, A.B. Fialkov, A. Amirav, Electron Ionization LC-MS, in: Compr, Anal. Chem. (2018) 1–28, doi:10.1016/bs.coac.2017.06.008.
[113] P. Palma, E. Pierini, A. Cappiello, LC-MS Interfaces, in: Anal. Sep. Sci., Wiley-VCH Verlag GmbH & Co. KGaA, Weinheim, Germany, 2015: pp. 87–110. doi:10.1002/9783527678129.assep005.
[114] K. Wiangnon, R. Cramer, Advances in MALDI and Laser-Induced Soft Ionization Mass Spectrometry, Springer International Publishing, Cham, 2016, doi:10.1007/978-3-319-04819-2.
[115] I. Marchi, S. Rudaz, J.L. Veuthey, Atmospheric pressure photoionization for coupling liquid-chromatography to mass spectrometry: A review, Talanta 78 (2009) 1–18, doi:10.1016/j.talanta.2008.11.031.
[116] M.S. Wilm, M. Mann, Electrospray and Taylor-Cone theory, Dole's beam of macromolecules at last? Int. J. Mass Spectrom. Ion Process. 136 (1994) 167–180, doi:10.1016/0168-1176(94)04024-9.
[117] C.E. Domingues Nazario, B.H. Fumes, M.R. da Silva, F.M. Lanças, Miniaturized Column Liquid Chromatography, Nanomater. Chromatogr. (2018) 359–385, doi:10.1016/B978-0-12-812792-6.00013-3.
[118] M. Karas, U. Bahr, T. Dülcks, Nano-electrospray ionization mass spectrometry: addressing analytical problems beyond routine, Fresenius. J. Anal. Chem. 366 (2000) 669–676, doi:10.1007/s002160051561.
[119] A. Schmidt, M. Karas, T. Dülcks, Effect of different solution flow rates on analyte ion signals in nano-ESI MS, or: when does ESI turn into nano-ESI? J. Am. Soc. Mass Spectrom. 14 (2003) 492–500, doi:10.1016/S1044-0305(03)00128-4.
[120] A.B. Kanu, B.S. Kumar, H.H. Hill, Evaluation of micro- versus nano-electrospray ionization for ambient pressure ion mobility spectrometry, Int. J. Ion Mobil. Spectrom. 15 (2012) 9–20, doi:10.1007/s12127-011-0075-8.
[121] G. Hulthe, M.A. Petersson, E. Fogelqvist, Coupling of open tubular liquid chromatography to electrospray mass spectrometry with a nanospray interface, Anal. Chem. 71 (1999) 2915–2921, doi:10.1021/ac981352f.
[122] H.K. Hustoft, T. Vehus, O.K. Brandtzaeg, S. Krauss, T. Greibrokk, S.R. Wilson, E. Lundanes, Open tubular lab-on-column/mass spectrometry for targeted proteomics of nanogram sample amounts, PLoS One 9 (2014) 1–10, doi:10.1371/journal.pone.0106881.
[123] L. Liu, K. Yang, X. Zhu, Y. Liang, Y. Chen, F. Fang, Q. Zhao, L. Zhang, Y. Zhang, Aptamer-immobilized open tubular capillary column to capture circulating tumor cells for proteome analysis, Talanta 175 (2017) 189–193, doi:10.1016/j.talanta.2017.07.041.
[124] R.-N. Li, Y.-N. Wang, M.-H. Peng, X.-Y. Wang, G.-S. Guo, Preparation and Application of Porous Layer Open Tubular Capillary Columns with Narrow Bore in Liquid Chromatography, Chinese J. Anal. Chem. 45 (2017) 1865–1873, doi:10.1016/S1872-2040(17)61057-0.
[125] T. Vehus, H. Roberg-Larsen, J. Waaler, S. Aslaksen, S. Krauss, S.R. Wilson, E. Lundanes, Versatile, sensitive liquid chromatography mass spectrometry-Implementation of 10 μm OT columns suitable for small molecules, peptides and proteins, Sci. Rep. 6 (2016) 1–10, doi:10.1038/srep37507.
[126] M. Rogeberg, T. Vehus, L. Grutle, T. Greibrokk, S.R. Wilson, E. Lundanes, Separation optimization of long porous-layer open-tubular columns for nano-LC-MS of limited proteomic samples, J. Sep. Sci. 36 (2013) 2838–2847, doi:10.1002/jssc.201300499.
[127] F. Zhang, X. Zhao, B. Xu, S. Cheng, C. Tang, H. Duan, X. Xiao, W. Du, L. Xu, Preparation and characterization of micro-cell membrane chromatographic column with silica-based porous layer open tubular capillary as cellular membrane carrier, Anal. Bioanal. Chem. 408 (2016) 2441–2448, doi:10.1007/s00216-016-9339-9.
[128] Feng Yue Chang, Yang Yunfang, Huang Zihui, Liu Si, Wang Zhihua, Peng Kunmiao, Chen Yan, Ma Yingzhuang, Chen Bo, The fabrication of poly (polyethylene glycol diacrylate) monolithic porous layer open tubular (mono-PLOT) columns and applications in hydrophilic interaction chromatography and capillary gas chromatography for small molecules, Electrophoresis 40 (2019) 521–529, doi:10.1002/elps.201800410.
[129] Manman Zhu, Lingyi Zhang, Zhanying Chu, Shulei Wang, Kai Chen, Weibing Zhang, Fan Liu, Preparation and evaluation of open-tubular capillary columns modified with metal-organic framework incorporated polymeric porous layer for liquid chromatography, Talanta 184 (2018) 29–34, doi:10.1016/j.talanta.2018.02.010.
[130] Qishu Qu, Yuanyuan Liu, Wenjun Shi, Chao Yan, Xiaoqing Tang, Tunable thick porous silica coating fabricated by multilayer-by-multilayer bonding of silica nanoparticles for open-tubular capillary chromatographic separation, J. Chromatogr. A. 1399 (2015) 25–31, doi:10.1016/j.chroma.2015.04.037.
[131] Adam Daley, Ramin Wright, Richard Oleschuk, Parallel, fluorous open-tubular chromatography using microstructured fibers, Anal. Chim. Acta 690 (2011) 253–262, doi:10.1016/j.aca.2011.02.007.

Capítulo 4

Artigo publicado no *Molecules*, 2023.

molecules

MDPI

Article

Development of Wall-Coated Open Tubular Columns and Their Application to Nano Liquid Chromatography Coupled to Tandem Mass Spectrometry

Natalia G. P. Santos, Deyber A. V. Medina and Fernando M. Lanças *

São Carlos Institute of Chemistry, University of São Paulo, São Carlos 13566-590, Brazil
* Correspondence: flancas@iqsc.usp.br

Abstract: This work presents a study on the application of wall open tubular column (WCOT) in liquid chromatography coupled with tandem mass spectrometry. Each process step reports the column preparation method in detail, subdivided into column pretreatment, silanization, stationary phase coating, and immobilization. Then, an evaluation of the parameters that can affect the efficiency of these columns was made. Atrazine, clomazone, and metolachlor were used as probes during this step. Factors such as stationary phase composition, length, internal diameter, stationary phase mass employed, and injection volume were investigated. In addition, with the help of Knox and Poppe graphs, the columns' performance was evaluated to determine the optimal flow rate and the speed-efficiency relationship, respectively. Based on the results, the best configurations for the WCOT column application to the LC system were defined: length—8 m; inner diameter—25 µm; mass of OV-210—2.5% *m*/*v*; and, injection volume—100 nL. Finally, the optimized WCOT column developed in this work was coupled with a commercially-packed trapping column in the nano liquid chromatography system (nanoLC). In this configuration, more significant results were obtained regarding separation resolution, with Rs = 5.9 achieved for the most retained pair of analytes (clomazone and metolachlor).

Keywords: column development; open tubular columns; nano liquid chromatography; mass spectrometry; wall coated open tubular column (WCOT)

Citation: Santos, N.G.P.; Medina, D.A.V.; Lanças, F.M. Development of Wall-Coated Open Tubular Columns and Their Application to Nano Liquid Chromatography Coupled to Tandem Mass Spectrometry. *Molecules* **2023**, *28*, 5103. https://doi.org/10.3390/molecules28135103

Academic Editor: Paraskevas D. Tzanavaras

Received: 6 June 2023
Revised: 21 June 2023
Accepted: 26 June 2023
Published: 29 June 2023

1. Introduction

Modern liquid chromatography is increasingly moving towards the miniaturization of the technique. This procedure involves investments in resizing the analytical instrumentation to work at micro-LC, capillary-LC, and nano-LC scales. Furthermore, analytical columns have received significant attention aiming at reducing the particle's size and internal diameter [1]. Therefore, emphasis on the miniaturization of the LC technique started and is directly linked to conventional columns packed with particles by just decreasing the column's internal diameter. However, other columns, such as monolithic and open tubular (OT), received much less attention despite also being helpful in producing high-quality miniaturized LC columns.

Nota introduced open tubular columns in liquid chromatography in 1970 [2]. Such columns contain a thin layer of stationary phase that covers the inner wall of the capillary tube, leaving its interior empty or "open". This layer can be of porous or non-porous composition, therefore called a porous layer open tubular column (PLOT) and wall-coated open tubular column (WCOT), respectively [3]. Golay applied these columns in gas chromatography in 1957 [4], which quickly replaced the packed columns, as they presented better separation efficiency under pressure and similar analysis time. Therefore, OT columns in gas chromatography are already well established; however, the scenario for OT-LC is not the same. Unfortunately, studies of these columns applied to liquid chromatography were mainly restricted to the period between the '1970s' and '1990s' [5–10], in which there was

no suitable instrumentation and miniaturized detectors adequate for OT-LC progress. Consequently, without adequate instrumentation, OT-LC columns lost scientific investments, and packed columns began to gain attention until they reached their current efficiency.

During the early OT-LC period, the design, properties, and performance of these columns were compared to packed columns. According to Hibi [11], the application of OT columns with an internal diameter commonly used in gas chromatography (0.25–0.50 mm i.d.) would cause a drastic reduction in the number of theoretical plates (N) since the diffusion coefficients of the analytes in liquid phases is up to 100 times smaller than in gaseous phases [12]. Consequently, for OT-LC to have an efficiency similar to OT-GC, the internal diameter of these columns must be much smaller. According to studies by Knox and Gilbert, the i.d. in LC should be less than 10 µm [13,14], ideally around 2 µm [15]. This restriction makes producing capillary columns with optimal performance extremely difficult. Recently, Liu's group [16] reported the development of an OT column with 2.7 cm of effective length and 2 µm i.d., coated with an octadecylsilane film for separating six amino acids by LC-UV-Vis. However, the chromatographic separation obtained still presents a noisy baseline, demonstrating that we still need improvement to obtain high-quality robust OT-LC columns with 2 µm i.d.

The main general advantage of OT columns is excluding the A term from the Van Deemter equation, which accounts for almost half of the band broadening in packed columns. They also have high permeability, leading to lower system pressure and giving the possibility of increasing column length. The main limitation related to these columns is their low sample capacity, considering that the thin stationary phase layer has a small surface area to interact with the analytes. For that reason, limited sample concentrations must be introduced into the column in order to avoid clogging and other undesirable effects [1], requiring a drastic reduction in the dimensions of the sample introduction system ("injector").

Although OT-LC columns of the PLOT kind have been consistently more explored in the last two decades, particularly in the proteomic analysis, WCOT columns have not received the same attention. Further studies in OT-WCOT-LC are still required to establish a column preparation methodology capable of producing robust columns with smaller internal diameters. Besides, limitations such as load capacity, column clogging, and/or the chromatographic system still need to be overcome. Therefore, this work aims to contribute to a systematic study of OT-LC columns. Here, we developed WCOT-type columns for application in nano-LC coupled to tandem mass spectrometry fitted with electrospray ionization. Columns were coated with liquid stationary phases based on polysiloxane phases commonly applied only in open tubular gas chromatography. Afterward, a systematic study of parameters that can affect the efficiency of this type of column was carried out, including the stationary phase composition, column length, internal diameter, mass of stationary phase, and injection volume. Furthermore, a study coupling WCOT columns with packed trapping columns was also evaluated, aiming to understand several aspects that may contribute to the better performance of these columns in liquid chromatography.

2. Results and Discussion

2.1. Preparation of WCOT Columns

To achieve reproducible results in obtaining robust WCOT columns, the development process is quite laborious. The fused silica capillary should be well treated (physically and chemically) before coating with the stationary phase film. Such processes (pretreatment and silanization) are necessary to ensure separation efficiency and column inertia. Therefore, we need the formation of a homogeneous film and the reduction of secondary adsorption effects of silanol groups, respectively. Separation efficiency and column inertia are concepts related to the film's formation on the column's inner surface. That is, the better the column is covered with this liquid film, the less residual silanols will be exposed, and the column inertia will be guaranteed.

To perform a good column coating, the concept of wettability must be considered, which is the ability of a liquid to maintain contact with a solid surface [17]. A homogeneous film is formed on the wall if the surface has high wettability. However, if the surface has low wettability, the liquid tends to agglutinate on the tube wall, and the separation efficiency and inertia will be compromised, generating chromatographic peaks with greater width at the base and with a tail (Figure 1A). One way to promote the silica surface's wettability is through its treatment with a silanizing agent that contains functional groups similar to those of the liquid stationary phase. In this work, all the columns were silanized with the same agent HMDS (hexamethyldisilazane), which is one of the agents that guarantees more inertia for the columns [18].

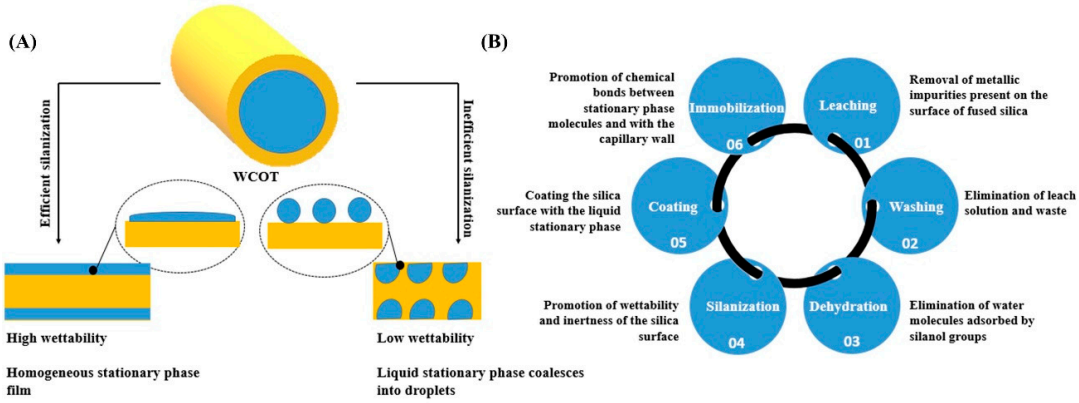

Figure 1. (**A**) The difference in the silica surface's coating with the liquid stationary phase depends on the wettability profile; (**B**) summary of the steps involved in developing WCOT columns and their respective functions.

Figure 1B presents a systematization of all the steps in preparing WCOT columns and their functions. Briefly, the pretreatment steps remove any traces of metals and/or dirt that may be present in the fused silica capillary. Next, as discussed, the silanization will promote the capillary wall's wettability to receive the stationary phase film. Furthermore, finally, the formed film will be immobilized on the column wall using a radical primer. This immobilization involves chemical bonds between the stationary phase film and the tube wall and chemical bonds between film molecules.

2.2. Screening of Stationary Phases

This work chose five liquid stationary phases to prepare WCOT columns. The choice of phases was guided by the McReynolds constants commonly applied in gas chromatography. Such constants give an idea of the polarity of the stationary phase [19,20]. Table 1 presents the respective McReynolds constants for each chosen phase.

Table 1. Chemical composition and McReynolds constants of the stationary phases tested in the coating of WCOT columns.

n°	Composition	Stationary Phase	McReynolds Constants
1	5% phenyl 95% DMPS	OV-73	334
2	50% phenyl 50% DMPS	OV-17	884
3	50% trifluoropropyl 50% DMPS	OV-210	1520
4	25% cyano 25% phenyl 50% DMPS	OV-225	1867
5	100% cyanopropyl DMPS	OV-275	3652

DMPS: dimethylpolysiloxane

Figure 2 presents a radar plot constructed with chromatographic resolution (Rs) data between clomazone and metolachlor analytes. Furthermore, the total ion chromatograms

(TIC) and the respective MRM transitions for each analyte (atrazine, clomazone, and metolachlor) obtained for each stationary phase tested in the work were presented. Finally, selecting the best stationary phase for developing WCOT-LC columns was conducted, considering the Rs and the evaluation of the chromatograms.

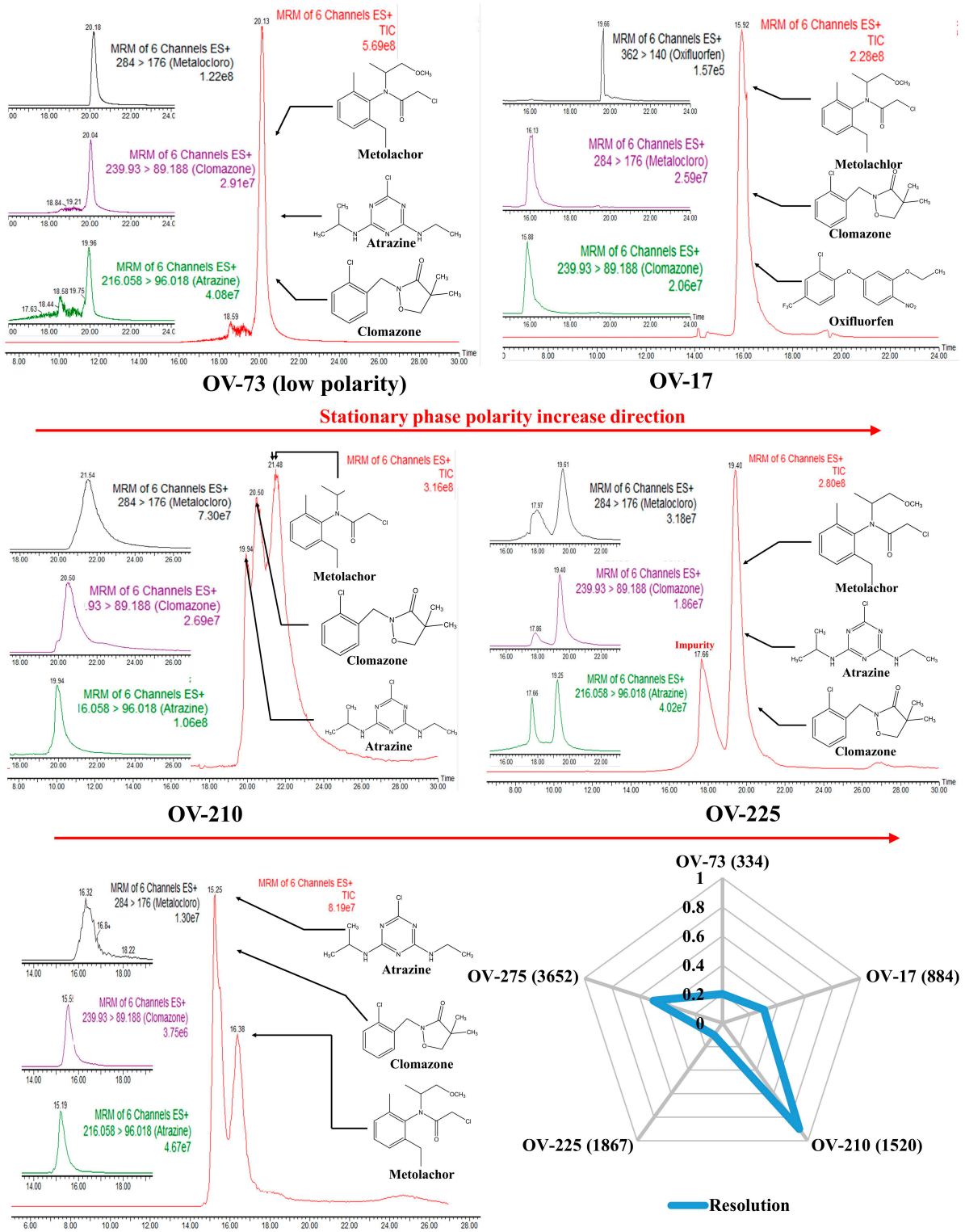

Figure 2. Radar charts and chromatograms obtained for WCOT columns coated with OV-73, OV-17, OV-210, OV-225, and OV-275 stationary phases.

The OV-73 column (5% phenyl 95% dimethyl polysiloxane) constitutes a stationary phase of low polarity with a low selectivity due to the presence of mostly methyl groups. This phase is widely used in gas chromatography, but it did not present enough separation for the analytes tested to justify proceeding with OV-73 in liquid chromatography. Similarly, the OV-17 column (50% phenyl, 50% dimethyl polysiloxane), of medium polarity, also did not show chromatographic separation, with the analytes coeluting in one large band. Atrazine did not result in an excellent chromatographic probe for evaluating this column. Therefore, it was changed to oxyfluorfen. Although we could identify each analyte separately from their MRM transitions by mass spectrometry, the same would not happen if another type of detector were used, such as UV-Vis or fluorescence, once their retention times were too close.

The OV-210 column (50% trifluoro propyl 50% dimethyl polysiloxane) of medium polarity was the one that presented the best results, among the evaluated columns, to separate the analytical probes selected. Therefore, this phase was selected to proceed with our work on the WCOT-LC columns preparation. As we can see in Figure 3, the selected analytes are separated into three peaks. Despite not being a separation with individual peaks, as would be desired, this was the best column among the evaluated phases. Furthermore, although the MRM transitions have relatively broad peaks, we should consider that this is an experimental column, and it still needed to go through the evaluation stage of the parameters affecting its performance.

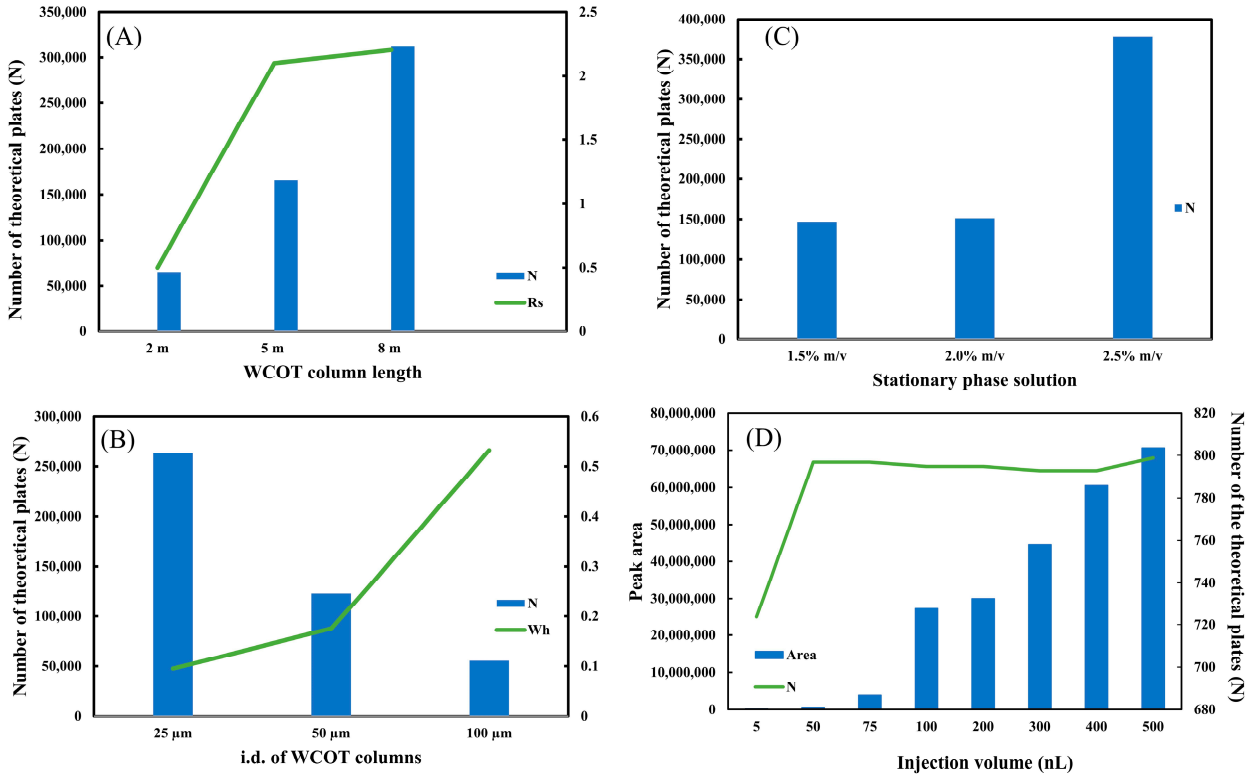

Figure 3. Optimization of WCOT columns. (**A**) Graph of length; (**B**) graph of stationary phase solution; (**C**) graph of inner diameter; (**D**) graph of injection volume. All graphics were constructed with clomazone standard data (500 µg L^{-1}).

The OV-225 column (25% phenyl, 25% cyano, 50% dimethyl polysiloxane) of medium polarity also did not present a chromatographic separation, in addition to observing some "unknown peaks" in the baseline of the chromatogram, which can even be confused with an analyte, but probably corresponds to some impurity in the stationary phase. Precisely for this reason, we disregarded the OV-225 column.

Finally, the higher polarity OV-275 column (100% cyanopropylsiloxane) was tested. The stationary phases with cyano content can operate in reversed-phase and normal-phase chromatography, but the best results are obtained in the last-mentioned way. In Figure 3, we have the OV-275 column being applied in reverse phase chromatography, demonstrating a partial separation since there was a coelution of atrazine with clomazone and separation only of metolachlor. Unfortunately, normal phase chromatography is not a favorable mode for electrospray mass spectrometry since, in this mode, non-polar mobile phases—usually hexane—are commonly used, which are not ionizable. Consequently, there is instability of the MS signal, resulting in low-reproducibility chromatograms. Some attempts were made in our laboratory in this direction, but no successful results were obtained. Therefore, the OV-275 column was also not further considered.

In general, Figure 2 demonstrates that increasing the polarity of the stationary phase increases its selectivity and the separation capacity. Additionally, in reversed-phase liquid chromatography, it is not recommended to use columns of low polarity such as OV-73, as they have much lower selectivity, provoking coelution of the analytes. However, in our experimental conditions it is not appropriate to use high polarity columns such as OV-275, as they are more suitable for normal phase chromatography. Therefore, the best stationary phase composition for WCOT-LC among the investigated in this work is medium polarity phases (OV-17, OV-210, and OV-225), with the best result obtained for OV-210, which was chosen to continue the work.

2.3. Evaluating Parameters That Affect WCOT Columns

The WCOT columns, now with the OV-210 stationary phase, were evaluated to investigate the influence of some parameters on the efficiency of the column. The first variable was the column length. Three lengths (2 m, 5 m, and 8 m) were investigated. In gas chromatography, where WCOT columns are most used, columns of 30 m in length are found, but this length is not yet very suitable in liquid chromatography. Considering that the molecular diffusion of analytes in a liquid medium is slower than in a gaseous medium, too-long columns would result in very long analysis times [21]. Ishii published some work employing octadecylsilane (ODS) coated WCOT columns to separate polycyclic aromatic hydrocarbons. These columns had a length of around 20.8 m [5] and 22.0 m [10]. They required about 90 and 120 min to complete the chromatographic analysis, even using a higher mobile phase flow rate than the one reported in this work.

Figure 3A shows the plot of N and Rs (between clomazone and metolachlor) as a function of length. It is observed that the increase in length leads to an increase in column efficiency, expressed in N. Furthermore, there is a significant gain in separation resolution starting from L = 2 m to L = 5 m. Comparing the Rs for the 5 m and 8 m columns, it is concluded that the separation capacity is practically the same. Therefore, we chose L = 5 m as the most suitable length for WCOT columns. Although L = 8 m has an excellent efficiency (N), its separation capacity (Rs) is similar to L = 5 m. In addition, the greater the column length, the greater the difficulty in experimentally preparing WCOT columns, ensuring homogeneous stationary phase films throughout the column, and increasing the chances of clogging in the column itself or analytical instrumentation. The chromatographic separation data can be consulted in Figure S1, and the numerical Rs and N data in Tables S2 and S3, respectively, in the Supplementary Materials.

The second parameter evaluated was the internal diameter. Similar to the length, three levels of i.d. (25 µm, 50 µm, and 100 µm) were also tested. Figure 3B shows the graph of N and Wh as a function of internal diameter. As predicted by the miniaturization theory in liquid chromatography [1], the smaller the internal diameter, the greater the column efficiency (N). Therefore, the graph demonstrates a fall of N from i.d. 25 µm to i.d. 100 µm. Another interesting piece of data is the width at half height of the peak (Wh). As the diameter increases, the Wh increases significantly, demonstrating an enlargement of the chromatographic band. This band expansion can be consulted in Figure S2. Therefore,

the best internal diameter investigated in this work is 25 µm, as we guarantee maximum efficiency (N) with the lowest band widening (Wh).

Then, the stationary phase solution used to coat the WCOT column was evaluated. Three conditions were tested: 1.5%, 2.0%, and 2.5% m/v of stationary phase solution. The mass amount of the liquid phase employed will directly impact the thickness of the film generated within the column. The thinner the film generated, the more stable it is, but the lower the load capacity of the column, causing possible overloading problems. On the other hand, the thicker the film generated, the less stable it is, but the greater is its loading capacity. Figure 3C plots N versus stationary phase solution. It is observed that the efficiency of a 1.5% and 2.0% m/v column is very similar. However, when it increases to 2.5% m/v (=50 mg of stationary phase), there is a significant increase in N. For WCOT columns, the 2.5% m/v solution was chosen. Unfortunately, we still cannot estimate the thickness of the film generated in the column under the experimental conditions employed. Usually, PLOT columns that have a porous film on their inner wall can be analyzed by scanning electron microscopy (SEM), being able to estimate the generated film. However, WCOT columns have a liquid film on their wall, which is not visible by SEM, making it more difficult to determine the film thickness. Therefore, for future research within the WCOT-LC theme, it would be interesting to seek a characterization technique for these films.

The injection volume was also studied at this stage. As previously described, columns with thin films have a lower load capacity and a greater possibility of overloading. Therefore, a potential source of column loading is the sample injection volume. Figure 3D shows the plot of N and peak area as a function of injection volume.

The data suggest that injection between 100–500 nL provides a similar efficiency (N), with the peak area value proportional to the injection volume. However, the efficiency is lower under low injection volumes (5 to 75 nL). Furthermore, very low volumes may be outside the commercially available chromatograph's accuracy limit, compromising data reproducibility. Therefore, the optimal working range for the WCOT-LC columns produced is 100–500 nL. Nevertheless, to preserve the column and avoid clogging due to the low load capacity of these columns, the most ideal would be to work with 100 nL.

2.4. Performance Evaluation: Knox and Poppe Graphics

One of the main graphs used to evaluate the performance of a column is the H/u_o graph, also known as the Van Deemter curve [22]. This graph allows us to conclude the best linear velocity (u_o) for a given column that provides the maximum efficiency (H). In the graph, this best condition is found on the lowest slope of the curve. However, the Van Deemter curve is commonly employed to analyze LC-packed columns. Therefore, the Knox curve should be used to better analyze WCOT-type capillary columns in micro and nanoLC scales. The graph is very similar to Van Deemter's, with the difference of applying reduced parameters (h/v), which are dimensionless. The form of interpretation is also the same. In Figure 4A, the experimental data of the reduced height of a theoretical plate (h) was plotted as a function of the reduced linear velocity (v). Additionally, in Figure 5A, we can compare the experimental and theoretical curves. The experimental data follow the same trend as the theoretical curve. However, the experimental data do not have a maximum h (as observed in the theoretical curve). This occurs because this region of the graph represents the A term, which characterizes the diffusion of analytes due to multiple paths in a packed column. As open tubular columns have a "hollow interior", they do not suffer this effect (A term = 0), and therefore, there is no such region in the experimental data. Therefore, from the Knox plot, we can conclude that the best v range is between 50–100, which experimentally corresponds to a mobile phase flow rate between 100–175 nL min^{-1}.

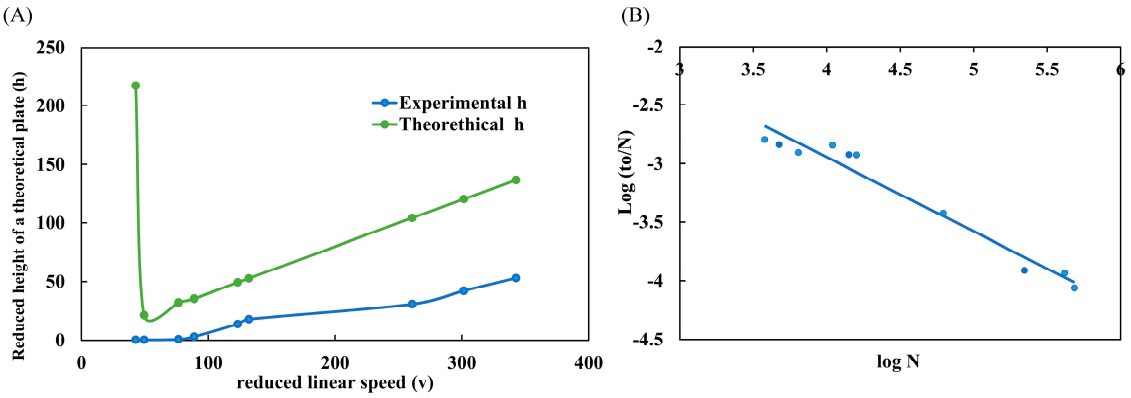

Figure 4. Performance evaluation of WCOT columns. (**A**) Knox plot (h/v) comparing experimental and theoretical curves; (**B**) Poppe plot (log to/N × log N) demonstrating the speed-efficiency relationship. Both graphs were constructed with the standard clomazone data (500 μg L^{-1}).

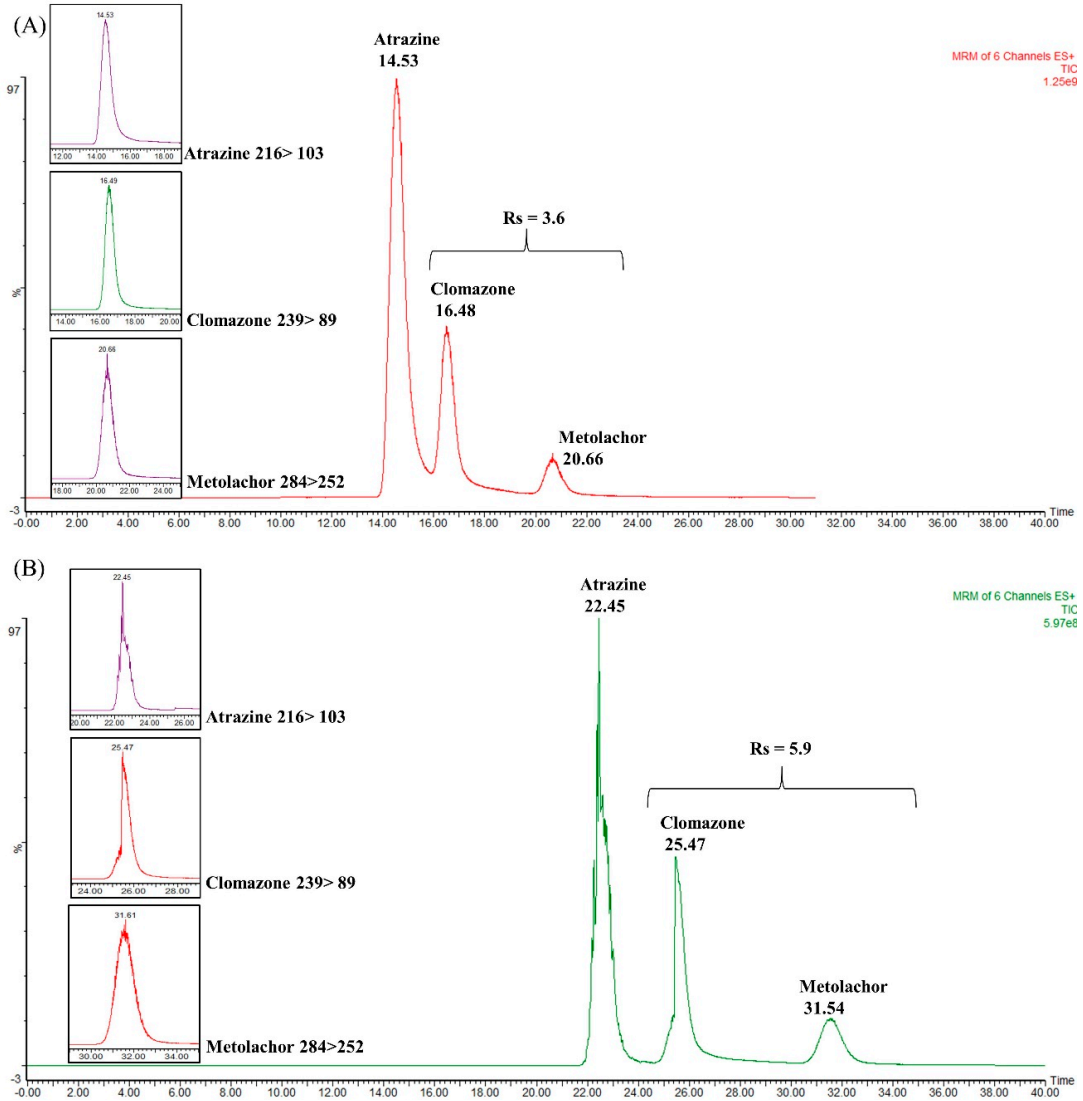

Figure 5. Total ion chromatograms (TIC) obtained in the coupling between WCOT column and packed trapping column to separate the atrazine, clomazone, and metolachlor mixture. (**A**) TIC obtained for commercial trapping column (2 cm × 180 μm i.d. × 5 μm), with Rs = 3.6; (**B**) TIC obtained by coupling the commercial trapping column and a WCOT (5 m × 25 μm i.d. × 2.5% *m*/*v* OV-210) with Rs = 5.9.

Poppe's graph was also plotted with the same data as Knox's graph. Poppe brings a good idea about the speed-efficiency relationship [23,24]. In Figure 4B, we plot log to/N as a function of log N. From the graph, we understand that we need slower analyses (greater log N) to obtain maximum efficiency (greater log to/N). On the other hand, to obtain faster analyses (lower log to/N), the column efficiency is sacrificed (lower log N). This conclusion was visualized throughout all work with WCOT columns. If we used fast gradients, the chromatographic peaks were narrower (high efficiency) but with low separation (practically coeluted). Moreover, if we used slower gradients, there would be an enlargement of the chromatographic peaks (loss of efficiency) but with separation.

Poppe's graph satisfactorily demonstrates the speed-efficiency relationship of columns and corroborates the experimental observations obtained in the research.

2.5. Coupling WCOT Column with a Trapping Column

The last step of this work was the coupling of the produced WCOT-LC column (5 m × 25 µm i.d. × coating with 2.5% *m*/*v* OV-210) with a packed trapping column (C18 Symmetry 2 cm × 180 µm i.d. × 5 µm). The purpose was to observe how this configuration could impact the WCOT separation capacity. Initially, the trapping column was connected to an empty fused silica tube (1 m × 25 µm i.d.) to verify its ability to separate the target analytes (atrazine, clomazone, and metolachlor). Next, the materials and methods item described the loading conditions and chromatographic separation employed.

The optimization of the sample loading step in the trapping column was performed manually, observing the chromatographic results. Therefore, the first parameter evaluated was the loading time. Initially, 1 min of loading was tested, and the results proved that this was an insufficient time for loading. Thus, the time was increased to 3 min, which proved adequate. The second parameter evaluated was the flow rate of the mobile phase during the elution step (valve in position 2). In this position, the mobile phase passes through the trapping column, eluting the analytes to the WCOT column, where chromatographic separation will occur. As judged by the Knox curve, the optimal flow rate for the WCOT column is between 100–175 nL min^{-1}. Therefore, we tested a flow rate of 100 nL min^{-1} in the elution step. The results demonstrate that this flow was too low to remove analytes from the 5 µm particle-packed trapping column rapidly. According to Knox's plots, for injections into the WCOT column without a trap column, it might be the optimal flow rate. However, higher flows capable of eluting the analytes from a packed bed are required for this application. Therefore, 300 nL min^{-1} was tested. This flow rate was sufficient to elute the analytes.

Figure 5A shows the chromatogram obtained with the single commercial trapping column. As can be seen, the analytes are separated, especially the metolachlor that has a higher retention time. Atrazine and clomazone are still not very well separated at their baseline. Figure 6B shows the chromatogram corresponding to the coupling between the C18 symmetry column and the WCOT. The result demonstrates a better separation between atrazine and clomazone. In addition, the retention times were extended, as the WCOT column has 5 m.

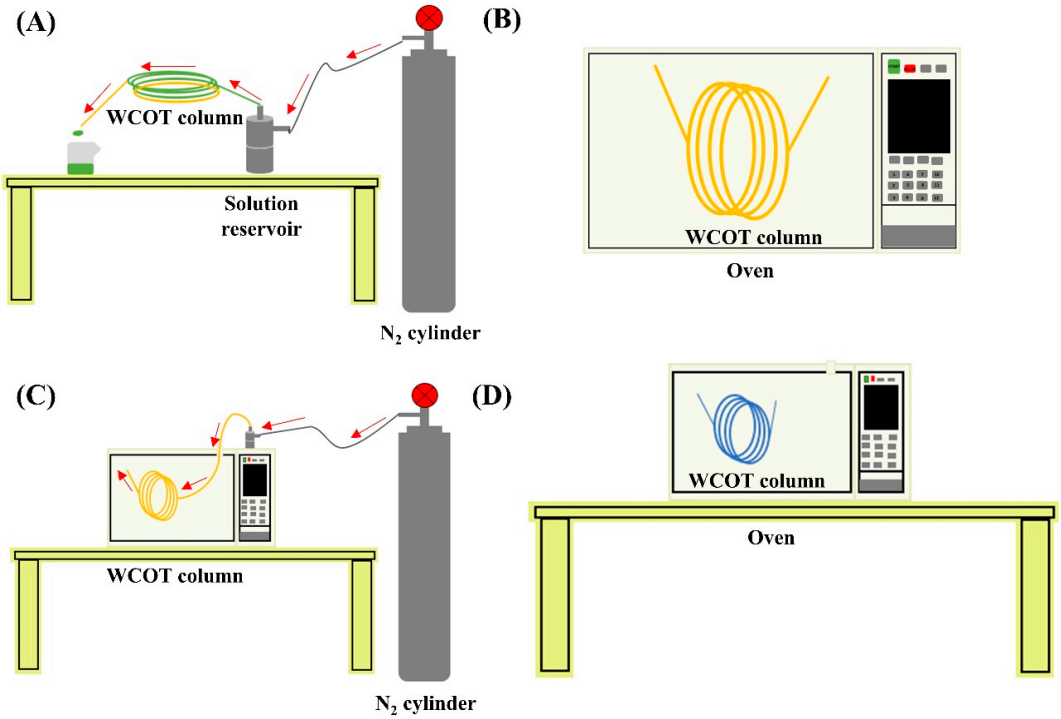

Figure 6. WCOT columns preparation system; (**A**) instrumentation for leaching, solvent washing, and column coating; (**B**) drying step under constant temperature; (**C**) instrumentation for column dehydration process under constant N_2 flow; (**D**) stationary phase film formation step after column coating. The red arrows indicate the path taken by the flow of N_2.

Regarding chromatographic resolution (between clomazone and metolachlor), we started from Rs = 3.6 in the trapping column to Rs = 5.9 in the WCOT column. Therefore, the use of trapping columns together with WCOT columns can be an approach to be explored in future works since, under this configuration, there was an improvement in the separation (visualized between atrazine and clomazone). However, more efforts are required to optimize WCOT columns (preparation and chromatographic conditions) to become competitive columns similar to LC-packed columns in the future.

3. Review of Similar Works

Table 2 summarizes some works reported in the literature on developing WCOT columns applied to LC. As we can see, most of the work was carried out during the 1980s and 1990s, reawakening the scientific community's interest only in 2019, with the development of columns with 2 µm i.d. In Table 3, we see a consensus among works in employing stationary phases of ODS (octadecylsilane) that do not have much selectivity, and the analytical standards are, in their majority, based on PAHs or anthracene derivatives (also a PAH). Furthermore, all analyses were performed on conventional LC-UV-Vis. However, these works (i) do not explain how flows in the µL min^{-1} range are achieved in conventional LC systems; (ii) do not detail the column preparation system used to produce columns with i.d. < 10 µm; and do not present a systematic study to evaluate relevant parameters that may affect column efficiency. Therefore, here lies the difference in our work. In the present work, a step-by-step optimized methodology is used for preparing LC-WCOT columns with stationary phases based on various dimethyl polysiloxane, commonly applied only in gas chromatography. Moreover, the proposed work is supported by a systematic study of the parameters that affect column efficiency. Another differential of our work is the application of WCOT columns prepared with a liquid stationary phase based on dimethyl polysiloxane in nanoLC-ESI-MS/MS systems, with more polar analytes, which deviate from the commonly-used PAHs analysis.

Table 2. WCOT application reports found in the literature.

n°	Stationary Phase	Column Dimension	Analytes	Instrument	Flow Rate	Time	Elution	Year
1	ODS *	3.84 m × 60 μm	Benzene, Naphthalene, Biphenyl	LC-UV	2.2 μL/min	20 min	25:75 ACN/H_2O	1978
2	ODS	20.80 m × 56 μm	Benzene, Biphenyl, and HPAs	LC-UV	1.0 μL/min	90 min	40:60 ACN/H_2O	1978
3	ODS	6.00 m × 100 μm	Resorcinol, Naphthalene, Anthracene	LC-UV	1.1 μL/min	90 min	40:60 ACN/H_2O	1980
4	ODS	5.30 m × 38 μm	Indole-3-acetic acid	LC-UV	1.1 μL/min	12 min	10:90 ACN/acetic acid aqueous solution	1983
5	ODS	22.00 m × 31 μm	HPAs	LC-UV	0.52 μL/min	120 min	ramp from 40 to 70% ACN	1983
6	PS-255 *	2.08 m × 11.6 μm	Anthracene derivatives	LC-UV	0.022 μL/min	40 min	40:60 ACN/H_2O	1987
7	PS-255	1.93 m × 11.3 μm	Anthracene derivatives	LC-UV	not reported	2 min	70: 30 ACN/H_2O	1987
8	$PMSC_{18}$ *	1.44 m × 5.8 μm	Anthracene derivatives	LC-UV	0.013 μL/min	4 min	50:50 ACN/phosphate aqueous solution	1991
9	$PMSC_{18}$	5.80 m × 6.3 μm	Anthracene derivatives	LC-UV	0.0046 μL/min	130 min	50:50 ACN/H_2O	1993
10	ODS	0.80 m × 2.0 μm	Glycine, Isoleucine, Leucine	LC-UV	18 μL/min	7 min	20:80 ACN/ammonium aqueous solution	2019
11	OV-210	5.00 m × 25 μm	Atrazine, Clomazone, Metolachlor	nanoLC-ESI-MS/MS	0.30 μL/min	60 min	Gradient ACN/H_2O	This work

ODS * = octadecylsiloxane/PS-255 * = 1% 1% vinyl/99% DMPS/$PMSC_{18}$ * = polymethyloctadecylsiloxane/OV-210 * = 50% trifluoropropyl/50% DMPS.

Table 3. Optimization of the transitions obtained with the help of the IntelliStart Software (Waters) for the target analytes and their respective cone voltages and collision energy.

Analyte	MM	log P	Precursor Ion (*m*/*z*)	Product Ion (*m*/*z*)	Dwell (s)	Cone (V)	Collision Energy (V)
Atrazine	215.68	2.61	216.06	96.018 103.95	0.512 0.512	22 22	20 26
Clomazone	239.70	2.50	239.93	89.19 124.96	0.152 0.152	50 50	46 16
Metolachor	283.79	3.13	284.00	176.00 252.00	0.152 0.152	20 20	30 20
Oxyfluorfen	361.70	4.73	362.00	140.00 2370.00	0.152 0.152	30 20	50 20

4. Materials and Methods

4.1. Analytical Standards and Reagents

High purity (>99%) analytical standards of clomazone, atrazine, metolachlor, and oxyfluorfen were obtained from Fluka Analytical (St. Louis, MO, USA). Stock solutions were prepared by diluting the standard in methanol to a concentration of 1000 mg L^{-1} and stored in amber bottles at −7 °C. Working solutions were prepared by diluting stock solutions to the concentrations of interest. High purity (>99%) solvents used as the mobile phase were acetonitrile, acquired from Tedia (Fairfield, CT, USA), and water from Merck Millipore Ultrapure Water System (Burlington, VT, USA). Formic acid used as an additive to the mobile phase was purchased from Sigma-Aldrich (St. Louis, MO, USA).

4.2. Chromatographic Apparatus and Analytical Conditions

The WCOT columns were evaluated in a UPLC system consisting of an ACQUITY UPLC liquid chromatograph from Waters (Milford, CT, USA), equipped with an ACQUITY UPLC sample manager and binary solvent pumps, coupled to the XEVO TQ MS tandem mass spectrometer with nano electrospray ionization. Chromatographic analyses were

performed in a partial loop (1 µL), injecting a volume of 500 nL for a concentration of 500 µg L^{-1}, with temperature and flow rate of 21 °C and 300 nL min^{-1}, respectively.

The mass spectrometry detection method was obtained by IntelliStart software (4.1) (XEVO TQ MS optimization tool) in positive ionization mode (ESI+) and multiple reaction monitoring (MRM). For this purpose, each analyte was introduced into the MS/MS by direct infusion at a concentration of 0.5 µg L^{-1}. Furthermore, two transitions were chosen to identify these compounds (Table 3). The calibration conditions ("tunning") for the nano-ESI used in the chromatographic analyzes consisted of capillary and cone voltages of 3.5 kV and 30 V, respectively, and the source temperature was 100 °C.

4.3. Preparation of WCOT Columns

WCOT columns were prepared with fused silica tubes of 50 µm internal diameter and 375 µm outside diameter, purchased from Polymicro Technologies (Phoenix, AZ, USA). Peek sleeves, washers, and ferrules necessary for connecting the column to the UPLC-MS/MS system were purchased from Acore (Sao Paulo, Brazil). The development of WCOT columns can be subdivided into the following stages: tube pretreatment, silanization, stationary phase coating, and film immobilization (cross-linking).

4.3.1. Tube Pretreatment

The fused silica tubing was leached with 2% *v*/*v* HCl solution from Tedia (Fairfield, CT, USA) under nitrogen flow at 80 bar for 5 min. Then, it was heated in an oven at 220 °C for 3 h. Subsequently, the capillary was washed with 1.5 mL of the same hydrochloric acid solution and 1.5 mL of dichloromethane. Afterward, it was dried with nitrogen gas for 30 min. To complete the pretreatment, the column was subjected to a dehydration step in which it was heated at 200 °C for 2 h under a continuous flow of nitrogen gas at 40 bar.

4.3.2. Silanization

After completion of column pretreatment, the capillary was directed to the silanization process with hexamethyldisilazane (HMDS) from Sigma Aldrich (St. Louis, MO, USA). This process consists of the percolation of the silanizing agent for 5 min through the capillary, under nitrogen flow at 80 bar, followed by heating in an oven at 290 °C for 6 h.

4.3.3. Stationary Phase Coating

The column coating was carried out by percolating the stationary phase solution for 30 min under nitrogen flow at 80 bar. Subsequently, the column was heated in an oven at 40 °C for 15 min. The stationary phase solution (2% *m*/*v* solution) was previously prepared by dissolving 40 mg of the liquid phase in 2 mL of a 1:1 dichloromethane/pentane solution.

4.3.4. Film Immobilization

The stationary phase film formed inside the column was immobilized with the azo-tert-butane (ATB) radical initiator obtained from Sigma Aldrich (St. Louis, MO, USA). For this purpose, the ATB was percolated through the column for 5 min and then heated in an oven at 220 °C for 1 h. This process was repeated three times. Figure 6 presents the instrumental part of the development of the columns.

4.4. Screening of Stationary Phases

Five liquid stationary phases were tested to separate the analytical standards mentioned in Section 2.1. OV-73 (5% phenyl 95% DMPS); OV-17 (50% phenyl 50% DMPS); OV-210 (50% trifluoro propyl 50% DMPS—dimethylpolysiloxane); OV-225 (25% cyano 25% phenyl 50% DMPS); and OV-275 (100% cyanopropyl DMPS) were obtained from the Ohio Valley Specialty Company (Marietta, OH, USA). The choice of phases was based on the McReynolds constant, which gives an idea of the polarity of the stationary phase. The screening was performed by injecting a mixture of atrazine, clomazone, and metolachlor (500 µg L^{-1}) under gradient conditions. Separation resolution data between clomazone

and metolachlor analytes (which are the most retained) were computed and plotted on a radar chart.

4.5. Evaluating Parameters That Affect WCOT Columns

After choosing the best stationary phase within the experimental conditions, some parameters that directly affect the efficiency of a column were evaluated. Thus, column length, internal diameter, and film thickness were studied at three different levels for each parameter mentioned (low, medium, and high level). Other parameters, such as mobile phase flow rate, injection volume, and coupling with the trapping column, were evaluated to provide the best operating conditions for the WCOT.

4.5.1. WCOT Column Length

Lengths of 2 m, 5 m, and 8 m were evaluated to determine the most appropriate for our WCOT columns. The other parameters referring to the column remained constant, 50 μm i.d. and stationary phase (2% m/v solution). The number of plates (N) and separation resolution (Rs) data were computed in this experiment, according to Table S1.

4.5.2. WCOT Column Inner Diameter

Three internal diameters were evaluated: 25 μm, 50 μm, and 100 μm, keeping the other column parameters constant. The other parameters referring to the column remained the same (5 m of length and stationary phase coating with 2% m/v solution). The number of plates (N) and width at half height (Wh) data of the chromatographic peak were obtained for this experiment.

4.5.3. Stationary Phase Mass in the Coating

The mass amount of liquid stationary phase used to coat the column directly affects the thickness of the film generated in the column and, consequently, its separation efficiency. Thus, 1.5%, 2%, and 2.5% m/v of the stationary phase (=30 mg, 40 mg, and 50 mg of the liquid phase in 2 mL of solvent) were tested to determine the most efficient. The other parameters referring to the column remained constant; 25 μm i.d. and 5 m long. N data were computed as well.

4.5.4. Optimum Flow Rate of the Mobile Phase

The optimal flow for the WCOT column was evaluated by injecting the analytical standard of clomazone (500 μg L^{-1} and 500 nL of injection volume) in a mobile phase flow range of 100–800 nL min^{-1}. Then, data processing involved plotting the reduced height of the theoretical plate (h) as a function of the reduced linear velocity (v). The equations used for the calculations are in Table S1 in the Supplementary Materials. The molecular diffusion of the analytes in the reversed-phase (Dm = 1.10^{-5} cm^2 s^{-1}) was used in the calculations.

4.5.5. Optimum Injection Volume

Injection volume assessment for WCOT columns was assessed by injecting the clomazone (500 μg L^{-1}) over a 5–500 nL range in partial loop mode (1 μL capacity). The peak area and the number of plates were computed.

4.5.6. Coupling WCOT Column with a Trapping Column

We also evaluate the coupling of a WCOT column to a "trapping" C18 Symmetry column (2 m × 180 μm i.d. × 5 μm, Waters—Milford, CT, USA) through switching valves. Two valves were used for this purpose. In the first moment, which we call position 1, the loop is filled with the sample (in valve 1) and then loaded into the packed trapping column (in valve 2), with the loading mobile phase, which also passes through the WCOT analytical column. In a second moment, which we call position 2, the analytes elute from the trapping column to the WCOT column, with the elution mobile phase, under gradient conditions.

The loading step (when analytes are eluted to the trapping column) was evaluated for 1–3 min, with a mobile phase flow rate of 8 µL min^{-1} and conditions of 99% H_2O (A) and 1% ACN (B) plus 0.1% formic acid. The elution step (when analytes are eluted from the trapping column to the WCOT) was evaluated for a flow between 100–300 nL min^{-1}, under gradient conditions: 0–0.1 min with 1% B, 0.1–0.5 min increases to 60% B and holds up to 21 min, 21–51 min return to 1% B to recondition the WCOT column.

5. Conclusions

The work reported here presented the development and evaluation of selected parameters that affect WCOT-type open tubular columns in nano-LC-ESI-MS/MS systems. The results after all evaluations of some parameters that affect WCOT open tubular columns of stationary phase, length, internal diameter, and optimal flow rate, among others, and the application of the column in line with a trapping column, proved to be satisfactory, considering the limitations—particularly in the instrumentation side—and difficulties of the work. The WCOT column alone presents separation capability, as seen in Figure S1, and under coupling conditions with a trapping column (Figure 6B), it presents the potential to be a new column possibility for LC systems. However, there is still much to study about WCOT columns in LC, as we still face limitations such as liquid film detachment, which leads to column and chromatographic system clogging. In short, this work aimed to show the potential of WCOT columns as a future trend in LC, which still requires greater attention from the scientific community to overcome its limitations. We hope that it will stimulate other research groups to be involved with the theme, thus bringing the WCOT to its deserved position in the top LC columns, as anticipated long ago by the chromatography theory.

Supplementary Materials: The following supporting information can be downloaded at: https://www.mdpi.com/article/10.3390/molecules28135103/s1, Figure S1: Total ion chromatogram obtained from the separation of atrazine, clomazone and metolachor in different WCOT column lengths. (A) L = 2 m. (B) L = 5 m. (C) L = 8 m, Figure S2: Peak broadening for each WCOT column internal diameter, obtained in isocratic mode (80:20 ACN/H2O with 0.1% formic acid) for clomazone (500 µg L^{-1}), Table S1: Equations used for analysis of WCOT columns, and parameter nomenclature, Table S2: Chromatographic resolution data according to WCOT column length, Table S3: Data on the number of theoretical plates obtained for the WCOT column according to length.

Author Contributions: Conceptualization, N.G.P.S.; investigation, N.G.P.S.; visualization, N.G.P.S., D.A.V.M., and F.M.L.; writing-original draft, N.G.P.S. and D.A.V.M.; review and editing, N.G.P.S., D.A.V.M., and F.M.L.; funding acquisition, F.M.L. All authors have read and agreed to the published version of the manuscript.

Funding: The authors are grateful for the financial support from (i) the Coordination for the Improvement of Higher Education Personnel (CAPES—Brazil, Finance Code 001), (ii) the São Paulo Research Foundation (FAPESP—Brazil, Grants 2019/22724-7, 2017/02147-0, 2015/15462-5, 2014/07347-9 and 2019/26263-4), (iii) the National Council for Scientific and Technological Development (CNPq—Brazil, 307293/2014-9; 308843/2019-3), and (iv) the Ministry of Science, Technology, and Innovation (MINCIENCIAS—Colombia, No. 679).

Institutional Review Board Statement: Not applicable.

Informed Consent Statement: Not applicable.

Data Availability Statement: The corresponding author's data supporting this study's findings are available upon reasonable request.

Conflicts of Interest: The authors declare no conflict of interest.

Sample Availability: Samples of the compounds are not available from the authors.

References

1. Mejía-Carmona, K.; Soares da Silva Burato, J.; Borsatto, J.V.B.; de Toffoli, A.L.; Lanças, F.M. Miniaturization of Liquid Chromatography Coupled to Mass Spectrometry. *TrAC Trends Anal. Chem.* **2020**, *122*, 115735. [CrossRef]
2. Nota, G.; Marino, G.; Buonocore, V.; Ballio, A. Liquid-Solid Chromatography with Open Glass Capillary Columns Separation of 1-Dimethylaminonaphthalene-5-Sulphonyl Amino Acids. *J. Chromatogr. A* **1970**, *46*, 103–106. [CrossRef]
3. Guiochon, G.; Claude, L.G. Chapter 8 Methodology Open Tubular Columns. In *Journal of Chromatography Library*; Elsevier: Amsterdam, The Netherlands, 1988; Volume 42, pp. 247–317.
4. Ettre, L.S. MJE Golay and the Invention of Open-Tubular (Capillary) Columns. *J. High Resolut. Chromatogr.* **1987**, *10*, 221–230. [CrossRef]
5. Tsuda, T.; Hibi, K.; Nakanishi, T.; Takeuchi, T.; Ishii, D. Studies of Open-Tubular Micro-Capillary Liquid Chromatography. *J. Chromatogr. A* **1978**, *158*, 227–232. [CrossRef]
6. Yang, F.J. Fused Silica Open Tubular Column for Liquid Chromatography. *J. High Resolut. Chromatogr.* **1980**, *3*, 589–590. [CrossRef]
7. Göhlin, K.; Larsson, M. Narrow (5-50-µm i.d.) Open Tubular Columns in Liquid Chromatography Using Immobilized Polymethyloctadecylsiloxane as Stationary Phase. *J. Microcolumn Sep.* **1991**, *3*, 547–556. [CrossRef]
8. Göhlin, K.; Larsson, M. Study of Polyorganosiloxanes (Native and Solvent Swollen) for the Preparation of Narrow (5-15 Mm I.D.) and Long (1–6 m) Open Tubular Columns in Reversed-Phase Liquid Chromatography. *J. Chromatogr. A* **1993**, *645*, 41–56. [CrossRef]
9. Folestad, S.; Larsson, M. Swollen Polysiloxanes as Stationary Phases in Reversed-Phase Open-Tubular Column Liquid Chromatography. *J. Chromatogr. A* **1987**, *394*, 455–464. [CrossRef]
10. Takeuchi, T.; Ishii, D. Chemically Bonded Octadecylsilane and Polyimine Stationary Phases for Open-Tubular Microcapillary Liquid Chromatography. *J. Chromatogr. A* **1983**, *279*, 439–448. [CrossRef]
11. Hibi, K.; Ishii, D.; Fujishima, I.; Takeuchi, T.; Nakanishi, T. Studies of Open Tubular Micro Capillary Liquid Chromatography. 1. The Development of Open Tubular Micro Capillary Liquid Chromatography. *J. High Resolut. Chromatogr.* **1978**, *1*, 21–27. [CrossRef]
12. Forster, S.; Kolmar, H.; Altmaier, S. Synthesis and Characterization of New Generation Open Tubular Silica Capillaries for Liquid Chromatography. *J. Chromatogr. A* **2012**, *1265*, 88–94. [CrossRef]
13. Knox, J.H.; Gilbert, M.T. Kinetic Optimization of Straight Open-Tubular Liquid Chromatography. *J. Chromatogr. A* **1979**, *186*, 405–418. [CrossRef]
14. Saito, Y.; Jinno, K.; Greibrokk, T. Capillary Columns in Liquid Chromatography: Between Conventional Columns and Microchips. *J. Sep. Sci.* **2004**, *27*, 1379–1390. [CrossRef] [PubMed]
15. Jorgenson, J.W.; Guthrie, E.J. Liquid Chromatography in Open-Tubular Columns: Theory of Column Optimization with Limited Pressure and Analysis Time, and Fabrication of Chemically Bonded Reversed-Phase Columns on Etched Borosilicate Glass Capillaries. *J. Chromatogr. A* **1983**, *255*, 335–348. [CrossRef]
16. Xiang, P.; Yang, Y.; Zhao, Z.; Chen, M.; Liu, S. Ultrafast Gradient Separation with Narrow Open Tubular Liquid Chromatography. *Anal. Chem.* **2019**, *91*, 10738–10743. [CrossRef]
17. Farré-Rius, F.; Henniker, J.; Guiochon, G. Wetting Phenomena in Gas Chromatography Capillary Columns. *Nature* **1962**, *196*, 63–64. [CrossRef]
18. Grob, K. *Making and Manipulating Capillary Columns for Gas Chromatography*, 1st ed.; Dr. Alfred Hüthig Verlag: New York, NY, USA, 1986; Volume 1, ISBN 3778513125.
19. Rajkó, R.; Körtvélyesi, T.; Sebők-Nagy, K.; Görgényi, M. Theoretical Characterization of McReynolds' Constants. *Anal. Chim. Acta* **2005**, *554*, 163–171. [CrossRef]
20. McReynolds, W.O. Characterization of Some Liquid Phases. *J. Chromatogr. Sci.* **1970**, *8*, 685–691. [CrossRef]
21. Parris, N.A. Chapter 3 The Chromatographic Support and Column. In *Journal of Chromatography Library*; Elsevier: Amsterdam, The Netherlands, 1976; Volume 5, pp. 19–41.
22. Forster, S.; Kolmar, H.; Altmaier, S. Performance Evaluation of Thick Film Open Tubular Silica Capillary by Reversed Phase Liquid Chromatography. *J. Chromatogr. A* **2013**, *1283*, 110–115. [CrossRef]
23. Gritti, F.; Guiochon, G. The Current Revolution in Column Technology: How It Began, Where Is It Going? *J. Chromatogr. A* **2012**, *1228*, 2–19. [CrossRef]
24. Poppe, H. Some Reflections on Speed and Efficiency of Modern Chromatographic Methods. *J. Chromatogr. A* **1997**, *778*, 3–21. [CrossRef]

Supplementary information

Development of wall-coated open tubular columns and their application to nano liquid chromatography coupled to tandem mass spectrometry

Natalia G. P. Santos, Deyber A. V. Medina and Fernando M. Lanças *

São Carlos Institute of Chemistry, University of São Paulo, São Carlos 13566-590, Brazil

* Correspondence: flancas@iqsc.usp.br

Table S1. Equations used for analysis of WCOT columns, and parameter nomenclature.

Equation	Parameter nomenclature
Separation resolution $R_s = \frac{tR_2 - tR_1}{\frac{(wb_1 + wb_2)}{2}}$	t_R = retention time (s) t_M = dead time (s) Wb = chromatographic peak base width (s) wh = width at half height of the chromatographic peak (s) L = column length (cm) N = number of theoretical plates (-) dc = column inner diameter (cm) Dm = molecular diffusion of analytes in FM (cm^2/s) Rs = separation resolution (-) H = height plate (cm) h = reduced height plate (-) u_o = mobile phase linear speed (cm/s) v = reduced linear speed (-) N = number of theoretical plates (-)
Height equivalent of a theoretical plate $H = \frac{L}{N}$	
Reduced height for a theoretical plate $h = \frac{H}{N.dc}$	
Mobile phase linear speed $u_o = \frac{L}{tM}$	
Reduced linear speed $v = \frac{u_o.dc}{Dm}$	
Number of theoretical plates $N = 5{,}54\left(\frac{tR}{wh}\right)^2$	

Figure S1. Total ion chromatogram obtained from the separation of atrazine, clomazone and metolachor in different WCOT column lengths. (A) L = 2 m. (B) L = 5 m. (C) L = 8 m.

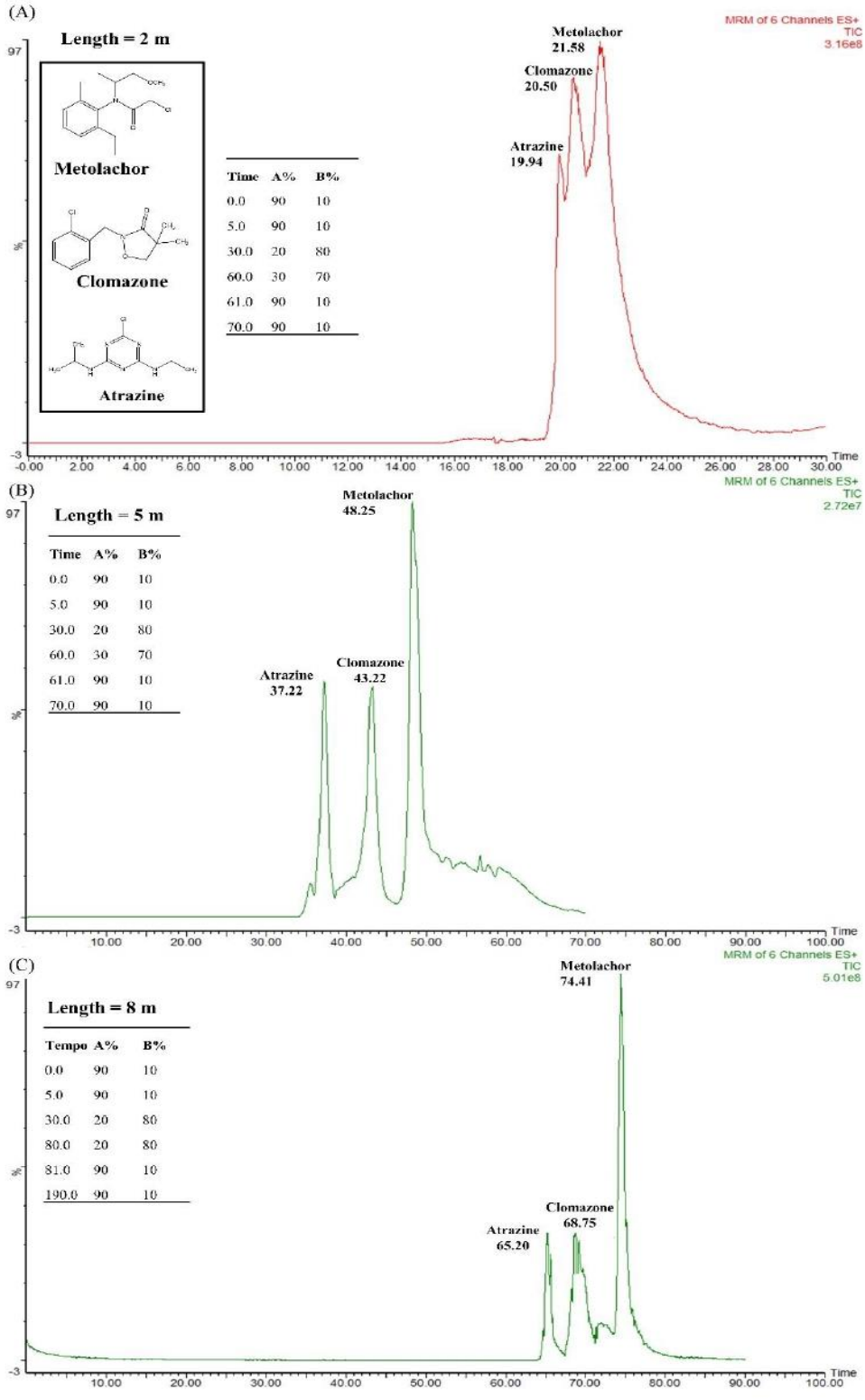

Table S2. Chromatographic resolution data according to WCOT column length.

Length	tR (A)	tR (C)	tR (M)	Wb (A)	Wb (C)	Wb (M)	Rs*
2 m	19.94	20.50	21.48	1.26	1.92	2.16	0.5
5 m	37.62	42.32	48.15	2.07	2.39	2.62	2.1
8 m	65.20	68.74	74.48	1.65	3.04	2.42	2.2

A: atrazine/ C: clomazone/ M: metolachor/ Rs*: between clomazone and metolachor/ t_R (min); Wb (min)

Table S3. Data on the number of theoretical plates obtained for the WCOT column according to length.

Length	tR (C)	Wh (C)	N*	N/m
2 m	20.50	0.189	65.176	32.588
5 m	38.16	0.221	165.173	33.035
8 m	56.91	0.240	311.504	38.938

N*: data calculated for clomazone (500 µg L^{-1}) under isocratic conditions of 80:20 ACN/H_2O plus 0.1% formic acid/ t_R (min); Wh (min)

Figure S2. Peak broadening for each WCOT column internal diameter, obtained in isocratic mode (80:20 ACN/H_2O with 0.1% formic acid) for clomazone (500 µg L^{-1}).

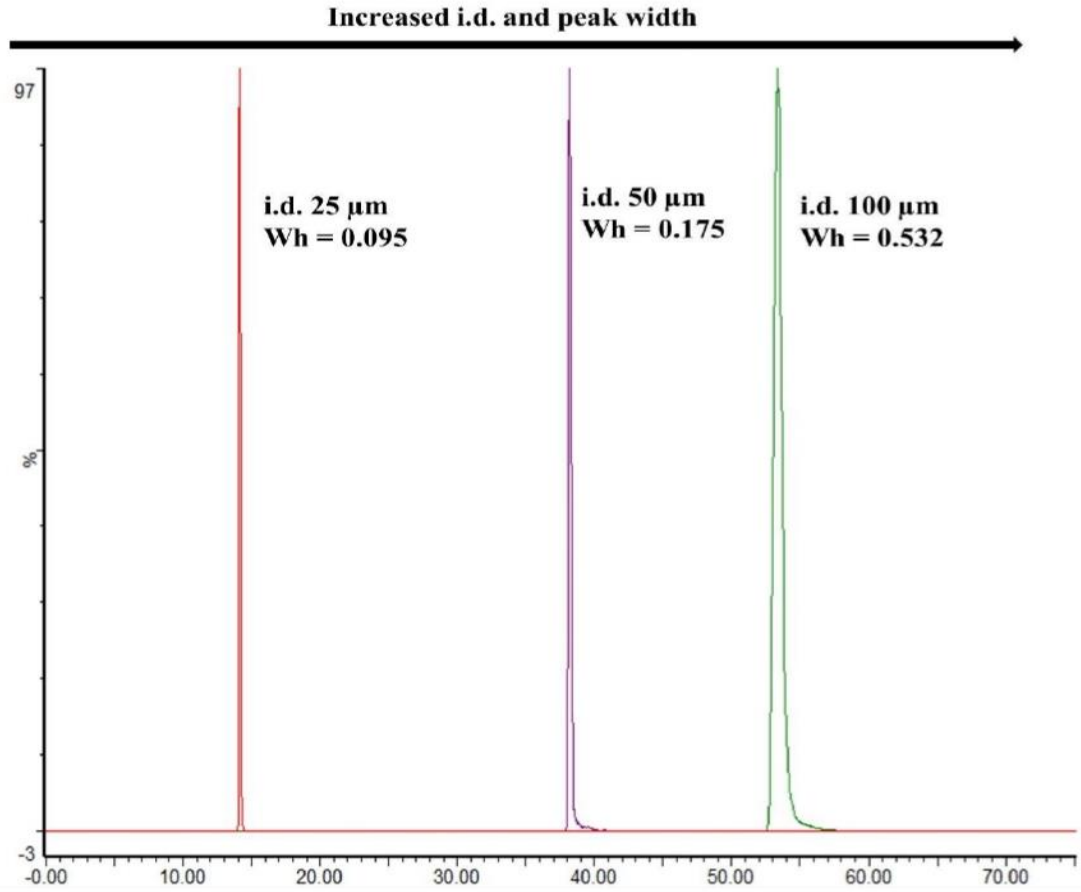

Capítulo 5

Artigo publicado no *Journal of Liquid Chromatography & Related Technologies* (2021)

JOURNAL OF LIQUID CHROMATOGRAPHY & RELATED TECHNOLOGIES
2021, VOL. 44, NOS. 17–20, 862–871
https://doi.org/10.1080/10826076.2022.2110114

Taylor & Francis
Taylor & Francis Group

Current prospects on nano liquid chromatography coupled to electron ionization mass spectrometry (nanoLC-EI-MS)

Deyber Arley Vargas Medina, Natalia Gabrielly Pereira dos Santos, Edvaldo Vasconcelos Soares Maciel, and Fernando Mauro Lanças

Institute of Chemistry of São Carlos, University of São Paulo, São Carlos, Brazil

ABSTRACT

NanoLC consolidates as powerful analytical technology liable to provide improved chromatographic performance and superior detection capabilities. Significant instrumental advances have been accomplished in the last 20 years to make nanoLC instruments more robust, accurate, and amenable for routine analysis. Similarly, new stationary phases and nanoLC formats provide new opportunities for separations at the miniaturized scale. Besides, nanoLC makes the hyphenation with EI-MS feasible, and a series of interfaces and interesting applications have been reported in the last years. Ei-MS offers unparallel identification capabilities, and its coupling with nanoLC has the potential to revolutionize the Performance of LC-MS untargeted studies. This manuscript makes a historical journey through the development of the nanoLC and its hyphenation with the EI-MS, exploring the more outstanding advances in that technology, discussing its scope, and identifying its limitations. We intend to give the reader a current overview of the state of the art of nanoLC and point out perspectives and future lines of advancement and improvement for new research in this area.

KEYWORDS

Electron ionization; liquid chromatography; mass spectrometry; miniaturization; nanoLC

GRAPHICAL ABSTRACT

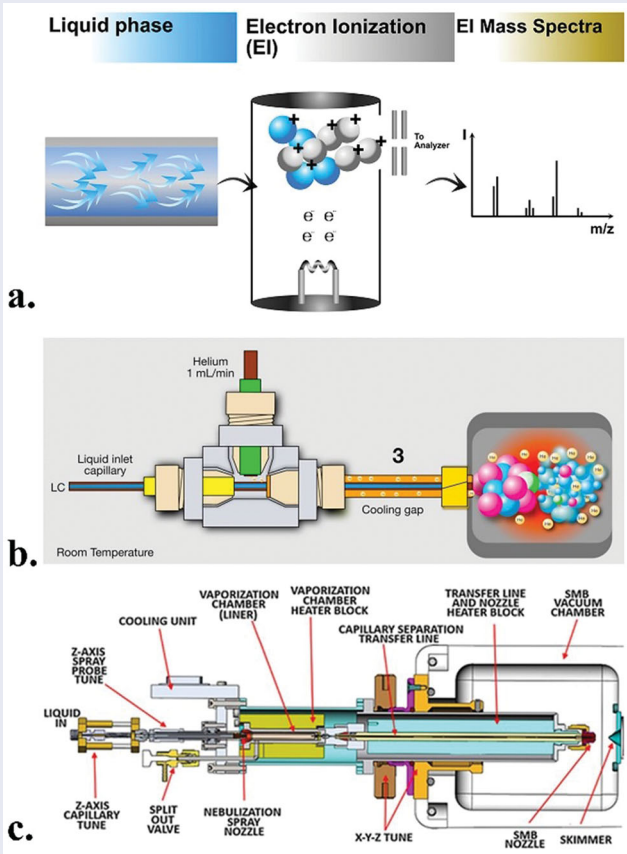

CONTACT Fernando Mauro Lanças flancas@iqsc.usp.br Institute of Chemistry of São Carlos, University of São Paulo, São Carlos, Brazil.

Introduction

Nowadays, the hyphenation of liquid chromatography (LC) with mass spectrometry (LC-MS) is one of the most potent techniques in analytical science. The majority of LC-MS instruments available are hyphenated and operate under atmospheric pressure ionization interfaces, including electrospray (ESI), atmospheric pressure chemical ionization (APCI), and atmospheric pressure photochemical ionization (APPI).[1] Such API-based techniques are recognized as soft ionization procedures, as they are characterized by mainly generating adduct, protonated, or deprotonated quasi-molecular ions.[2] LC-ESI-MS stands out in targeted and untargeted studies because of its sensitivity, robustness in routine analysis, and a good range of analyzable compounds involving small molecules (e.g., pesticides and pharmaceutical drugs) and biomolecules.[3] APCI and APPI are ESI-complementary techniques, especially suggested for small and less polar compounds that are difficult to be ionized through ESI.[4,5]

Although these API techniques have been used successfully, they still possess downsides. For example, ionization of non-polar compounds is a challenging task. They depend on LC mobile phase composition—the presence or absence of salts or other solutes makes them highly susceptible to matrix effects, resulting in analytical signal suppression or enhancement.[6–9] API process barely takes place with fragmentation. Consequently, mass spectra generated do not provide meaningful structural information.[10] With those soft ionization techniques, the obtention of molecular structure is only possible with the aid of in-tandem or high-resolution mass spectrometry (MS/MS and HRMS, respectively).[2] However, despite API-based techniques capable of generating fragmentation spectra, this process usually suffers from non-reproducibility and is influenced by instrumental and operational parameters.[10] Therefore, results generated from analytical methods relying on LC-API-MS instrumentation are not easy to reproduce from lab to lab, or when instruments from different manufacturers must be used for the same purpose.[11]

On the other hand, the last two decades have been marked by significant achievements in LC miniaturization, resulting in the development of reliable instruments for capillary and nanoLC.[12] The well-recognized capillary/nanoflow rate compatibility with ESI-MS promotes analytical sensitivity gains. The development of modern columns and instruments that work at nano flowrates makes the LC and the EI-MS finally compatible. The rich fragments and high reproducible 70 eV spectra characteristic of EI-MS constitute a significant advantage over the API-based techniques.[11] EI-MS is a hard ionization technique whose reproducible fragmentation pattern results in almost a fingerprint-like mass spectrum for each target compound.[11] This feature facilitates the structural elucidation and identification of unknown compounds *via* automated library spectra comparison.[13,14] Besides, mass spectra generated by hard-ionization EI-MS rarely suffer from matrix effects. The high vacuum conditions necessary for electron ionization (EI) extinguish almost any molecule-molecule or molecule-ion interaction; therefore, the matrix effects barely affect mass spectra generated by 70 eV EI-MS.[14] Moreover, the advent of nanoLC and the recent developments focused on interfaces to coupling it with EI-MS have the potential to bridge the gap between LC and gas chromatography (GC), enabling their coexistence in a single instrument capable of analyzing a considerable higher spectrum of target compounds simultaneously.[1,10,11,15,16]

Within such a context, Table 1 gathers important information about hard ionization (EI-MS) and soft ionization techniques (API) to make things clearer to the journal audience—especially to help everyone understand "Why should so much effort be put into attaining compatibility of EI-MS with LC, if ESI-MS is already a well-established technique, and already compatible with LC?"

Taking all this into account, this review aims to present the topic as state-of-art, highlighting the major and promising nanoLC-EI-MS interfaces already available or in implementation, as well as to discuss the future trends alongside possible directions that analytical chemists can take in the coming years for the sake of this scientific field.

Modern nano liquid chromatography

Nano-LC is a microfluidic technique that emerged around the 1990s and has become the most widespread miniaturization of LC developed so far.[12,17,18] It is characterized by a reduced internal diameter (i.d.) of the analytical columns to ~10–100 µm and a flowrate of 50–800 nL/min.[19,20] Columns with an inner diameter of 75 µm columns are the more frequently employed and represent the best compromise between load capacity, separation efficiency, and detectability.[21] The attributes of the technique include higher separation efficiencies and improved sensitivity when coupled to mass spectrometry[19] and an alignment with green chemistry principles due to the reduction in the

Table 1. Main features, advantages, and disadvantages of electron ionization and atmospheric pressure ionization techniques for mass spectrometry.

EI-MS	API-MS
Hard-ionization procedure	Soft-ionization procedure
Extensive molecular fragmentation—fingerprint-like MS spectrum	Limited molecular fragmentation—MS/MS or HRMS for producing structural information is needed
High-vacuum condition	Atmospheric pressure condition
Negligible matrix effect	Highly susceptible to matrix effect
Very reproducible mass spectra	Non-reproducible mass spectra
Library-searchable results	Non-library searchable results
Not compatible with nonvolatile and thermolabile molecules	Ideal for proteins and other biomolecules
Standard technique for coupling with GC	Standard technique for coupling with LC
Complementary set of characteristics	

volume of solvents and stationary phases that are required. Coupled with mass spectrometry through electrospray ionization sources (ESI-MS), improved sensitivity is obtained at nano flowrates as the ionization process is faster and more efficient than with a conventional LC. Similarly, when coupled to EI-MS, the impact of the mobile phase on the ionization process is reduced, and the compatibility of LC and EI-MS is attained.[1]

The enhanced sensitivity characteristic of nanoLC is a consequence of the relationship between the i.d. of the columns and the dilution of the chromatographic band (D). This sample dilution (in the mobile phase) inside the column can compromise the separation efficiency and generate broad peaks. To understand the sample dilution, Equation (1) below is used:[18,20,21]

$$D = \frac{C_o}{C_{\max}} = \frac{\varepsilon \pi r^2 \ (1+k)\sqrt{2\pi LH}}{V_{\text{inj}}} \tag{1}$$

Here, C_o and $C_{\max}$ are the concentration of the injected sample, and at the peak maximum, respectively, k is the retention factor, L is the column length, H is the plate height, r is the radius analytical column, and, V_{inj} is the injection volume. Considering that the column radius is directly proportional to the band dilution, reducing the radius (smaller column i.d.) reduces band dilution. Hence, well-resolved, narrower, and more intense peaks are obtained.

Interest in nanoLC has been growing over the years, either for applications in omics (e.g., proteomics, metabolomics, genomics),[22–24] or more recently, in small molecules.[25–27] Although commercial nanoLC instruments have been available since the end of the 1990s, efforts are still needed to ensure robust instrumentation. When the issue of instrumentation for nanoLC is taken into consideration, the mobile phase pumping system is one of the most critical components and must deliver a precise and stable flow in both isocratic and gradient modes.[21] Therefore, the pumps are combined with flow rate controllers and nanoflow sensors to monitor the accuracy of mobile phase delivery and any leaks that may occur and compromise separation efficiency. These leaks are much more critical on a miniaturized scale, where the low flow rate makes a leak undetectable.

Early nanoL/min flowrates delivery systems were based on conventional HPLC pumps with flow splitters. Nevertheless, this approach leads to considerable solvent wasting and reduced sensitivity with mass-dependent detectors. Nowadays, accurate nanoflow rates are obtained through constant flow pumps (reciprocating and syringe) and constant pressure pumps (pneumatic with or without amplification).[28] Constant-flow pumps employ an electric motor to deliver the mobile phase during the analysis employing a piston. The difference between them is precisely this piston. While the syringe pump employs one piston and generates a non-pulsating flow, the reciprocating pump employs two alternating pistons that generate a pulsating flow.

Consequently, the use of dampers at the pump outlet is necessary to reduce this pulsation. On the other hand, constant pressure pumps use gas to deliver the mobile phase. Pneumatic pumps without amplification contain the mobile phase in a reservoir, with an inlet for the gas and an outlet for the mobile phase connected to the analytical column. In pneumatic pumps with amplification, the gas will exert pressure on a piston to deliver the mobile phase.[28]

Another critical point is introducing the sample into the analytical column. The obtention of narrow peaks makes it necessary to create a short sample plug at the column entrance. Therefore, to avoid any overloading of the column or band broadening, the maximum injection volume of the sample should be determined by Equation (2) below:[29]

$$V_{\max} = 0.36\sqrt{Ld_p} \ d_c^2(k+1) \tag{2}$$

In this equation, L is the column length, d_p is the particle diameter, d_c is the column diameter, and k is the retention factor. Analytes with a low retention factor should be injected in smaller amounts to avoid band broadening and consequent reduction in separation efficiency.

The sample can be introduced into the column using either an injection valve with an internal or external loop or pre-concentration in a trap column.[20] Typically, in nanoLC, trap columns are widely employed for sample preconcentrate and increase sensitivity in the analysis.[30] Moreover, to protect the analytical column from overfilling and clogging. Therefore, a trap column has a larger diameter than the capillary column and larger particles to increase its loading capacity.

Another critical instrumental parameter is the use of proper connection/fitting accessories. Tubes and connections are essential to minimize the extra-column band broadening in nanoLC systems. Therefore it is recommended to use tubes with minor diameters and lengths, and connections should have no dead volume (ZDV).[21,28]

Finally, one of the critical components of nanoLC instrumentation is the nano analytical column. NanoLC columns generally have an i.d. of 75 µm and are usually produced in fused silica tubes. Currently, columns for nanoLC include packed columns, monoliths, microfabricated pillar array columns (µPAC), and open-tubular columns.[31] Packed columns are the usual format, typically employing fully porous 1.7–3.5 µm C18 particles. In other words, there are few stationary phase materials available on the market in the format of nanocolumns, which leads researchers to develop new materials and package their columns in the research laboratory.[32] Monoliths can be an excellent column format for nanoLC, considering the high backpressure generated by packed columns. These columns offer three stationary phase compositions ensuring various selectivity possibilities. Therefore, we have monoliths based on organic polymer, silica, and hybrid materials. In short, the monoliths have a pore structure with different sizes (macropores and mesopores), which ensures a high permeability to the mobile phase, allowing higher flows and reduced analysis time, all at low backpressure.[32–34] However, no monolithic nanoLC columns are commercially available despite their great potential.

A type of column that has been little explored in nanoLC but with great potential for the technique is the open-

tubular columns (OT).[34] These columns are characterized by having a thick film attached to the wall of the fused silica tube, and its interior is empty. Therefore, the OT offers the highest permeability to the mobile phase among all types of columns, ensuring low backpressures, high flows, and rapid analysis. Within the OT column category, there are two possibilities: the porous layer opens tubular columns (PLOT), which have a porous and polymeric film on the wall of the tube, and the wall coated open tubular column (WCOT), which is characterized by coating the column with a liquid film, usually stationary phases characteristic of gas chromatography.[28] Most research into OT is done with PLOT, as it is a column format with a higher loading capacity than WCOT columns. However, some efforts are still needed to understand the operation and production dynamics of OT columns and to further explore their coupling with nanoLC. We can estimate that future research in LC miniaturization will be directed toward this column type.

Despite all these column types, nanoLC features a new chip-based column format that represents the most remarkable evolution in the miniaturization of LC.[35] The microchips couple in a single device, the sampling loop, pre-column, separation analytical column, and detector—detection cell or nanospray emitter for mass spectrometry (MS). In addition, they are characterized by a 2D network of channels, where separation takes place. These channels, in turn, can take the form of particles, monoliths, or open tubes.[36] In other words, microchips can replace any conventional column model with a more robust platform that requires less human handling.[28] As it is still a new technology, many studies need to be done to overcome the limitations found in the coupling between the microchip and the LC system.[37]

NanoLC can be used with a variety of detectors. In the case of the ultraviolet detector, the detection cell needs to be resized to the mobile phase flow rate in the nL/min range to avoid any extra-column band broadening. However, the most suitable detector for the technique, considering its low flow rate, is MS. Several ionization sources can be employed within this niche, being electrospray (ESI) the most common. However, research and instrument manufacturers are working on coupling with electron ionization (EI), and due to its innovative character, this topic will be discussed in the next section.

Modern nanoLC coupled to electron ionization mass spectrometry (nanoLC-EI-MS)

Although nanoLC coupled to MS thought nanoESI sources perform very well, the hyphenation of LC with EI-MS has long been a goal, even before the emergence of the API sources.[38] The LC-EI-MS coupling approaches date back to the end of the 1960s when Tal'roze explored for the first time the direct interfacing of the column eluent into the vacuum region of the EI-MS source.[14] That approach did not succeed, but it boosted the research in this area, and a wide plethora of interfacing strategies emerged between the 1970s and 1980s. Important applications were reported in this period involving interfaces, such as the different versions of the direct liquid introduction (DLI),[14] the mobile belt (MB),[39,40] the monodispersive aerosol generation interface (MAGIC),[14,41] and the particle beam (PB) interface.[41]

The Performance of all those early interfaces was quite limited and characterized by low detectability, a narrow range of applicability, and frequent blockage.[11,14] The main struggle was the incompatibility between high-vacuum operation conditions of the EI-MS source and the high mobile phase flowrates characteristics of the conventional LC.[38] However, the development and exploration of interfaces, such as MAGIC and PB allowed establishing the need to reduce the amount of mobile phase entreating into the ionization source, to achieve suitable analytes ionization. MAGIC evolved in the PB interface, and during the 1990s, PB rapidly progressed toward the Cap-EI, a miniaturized version able to work at micro-flow rates. Cap-EI provided remarkable advances, and at the end of the century, the emergence of the nanoLC finally set the milestone that is making LC and EI-MS hyphenation feasible.

Nowadays, the research in nanoLC-EI-MS hyphenation relays on the exploration of three main interfacing strategies: (i) Direct EI, (ii) liquid electron ionization (LEI), and (iii) Cold EI. Those interfaces have been under continuous research and evolution over the last 20 years and have continuously extended their range of applications toward heavier and more polar compounds. New improvements to those interfaces could probably shortly make nanoLC-EI-MS competitive with nanoLC-API-MS approaches. Figure 1 introduces a schematic representation of those interfaces, and further details about their operation principle, applications, and limitations will be discussed in the following sections.

Direct EI

Currently, Direct EI is the most straightforward, cheap, and affordable approach for nanoLC-EI-MS coupling.[43] Direct EI is a simple strategy that does not require additional interfacing mechanisms and consists of the direct infusion of the nanoLC column effluent into the high-vacuum region of the EI-MS source through a fused silica capillary of inner diameter <25 µm (Figure 1a).[10] Despite its simplicity, this interface has demonstrated suitable sensitivity, and linearity, for the analysis of volatile compounds with low to medium molecular weight.[43]

Although Direct EI was initially configured by incorporating a curve capillary with a cone-shaped tip, further studies demonstrated no significant difference between cone-shaped tips and regular capillaries.[43] However, the inner diameter of the transference capillary strongly influences ionization. Capillaries with an i.d. between 15 and 25 µm have demonstrated suitable Performance.[10] Although there are no reports, further ionization improvements could be obtained by adapting capillaries with lower i.d.

The Performance of the Direct EI interface depends on several instrumental factors. The temperature of the ionization source (150–350 °C) can prevent water freezing at the capillary output and improve the effluent vaporization.

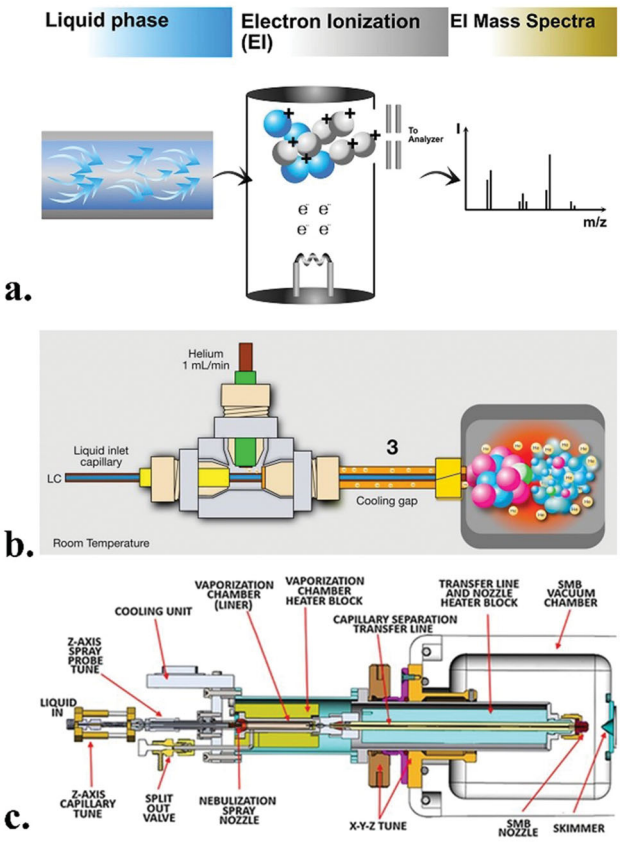

Figure 1. Schematic representation of the modern interfaces for nanoLC-EI-MS coupling. (a) Direct EI interface; (b) liquid electron ionization interface (LEI). Reprinted with permission of Ref.[14] Copyright (2019) Elsevier. (c) Cold EI with supersonic molecular bean interface (SMB). Reprinted with permission of Ref.[42] Copyright © 2011, John Wiley & Sons, Inc.

Similarly, transference tube temperature can positively affect the nebulization process and end premature solvent evaporation and interface clogging.[44] Due to the surface of the ion source material, unspecific adsorption of polar, low-volatile, and thermolabile analytes can lead to excessive peak tailing. Cappiello's research group studied silica, titania, and zirconia-based materials as coating of the stainless-steel ion source.[45] Assessed in the analysis of polycyclic aromatic hydrocarbons (PAHs) and hormones, sources coated with a thin layer of silica provide more intense and narrower chromatographic peaks than other bared or coated sources.

The mobile phase flow rate affects the EI process. The lower the solvent entreated into the ionization source, the higher the signal-to-noise ratio and the better the analyte's detectability. EI occurs under vacuum conditions and just one in ten thousand molecules entering the ionization source is ionized. So, the lower number of solvent molecules competing with the analytes for the ionizing electrons, the better the ionization of the analytes. Besides, solvent molecules can induce chemical ionization, hindering the obtention of library searchable standard 70 eV EI spectra.[46] Modern nanoLC works with flowrates around 500 nL/min, but further improvements in detectability could be obtained by the scale reduction until the pL/min order, with the exploitation of alternative separation media like very narrow open tubular or on-chip microfabricated columns.

Although the quality of the EI spectra is not affected, the mobile composition can also impact the ionization efficiency. The liquid to gas transference depends on mobile phase volatility, viscosity, and surface tension factors. The higher the percentage of organic solvent on the mobile phase, the faster evaporation and higher signal-to-noise responses are obtained.

On the other hand, Direct-EI is less susceptible than API sources to ionization enhancement/suppression due to buffers and other mobile phase additives. Direct EI was the first interface that corroborated the absence of the matrix of mobile phase additives effect in liquid chromatography coupled to EI-MS.[47] Table 2 compares the matrix effects observed for analyzing different compounds from different matrices, employing ESI-MS and EI-MS coupled to liquid chromatography. As observed, EI-MS excels over ESI by the practical null matrix effects.

The Performance of Direct EI was early demonstrated in the analysis of several analytes with different characteristics, such as organochlorine pesticides[48,49] and boronic acids,[50] nitro-polycyclic aromatic hydrocarbons, and human hormones,[51] among many others. More recently, Rigano et al. introduced a new method for determining free fatty acids profile in mussel samples, *via* nanoLC-EI-MS, with Direct-EI interfacing.[52] This strategy avoided the esterification stages typically required for analysis of fatty acids *via* GC-MS, provided detection limits (LODs) in the range between 0.19 and 1.19 μg mg^{-1}, and set the bases for further analysis of lipidomic studies nanoLC-EI-MS. Also recently, Jocelyn et al. introduced a portable nanoLC-EI-MS system for in-field forensic analysis by coupling an Easy-nLC 1000 and a Viking 573 Mass spectrometer using a Direct EI interface.[53] The system allowed the infield determination of fentanyl with a LOD of 1.5 ng/mL.

Although Direct-EI is an easily adaptable and profitable interfacing alternative, this interface still entails some critical shortcomings, such as frequent interface clogging due to premature solvent evaporation and analytes precipitation.

Liquid electron ionization interface (LEI)

Liquid-Electron Ionization Interface (LEI) is the most advanced nanoLC-EI-MS hyphenation technology.[15] This interface uses a specially designed vaporization chamber that separates the column eluent evaporation and the analytes ionization stages.[54] LEI was developed as a modern approach, aiming to overcome the shortcomings of Direct-EI that lead to peak broadening, noise mass spectra, and reduced analytical response.

Studies on Direct-EI showed the need to perform the liquid to gas conversion outside of the ionization source, and this idea gradually led to the development of the LEI. Initially, the Mondello research group and Fasmatech Science and Technology (Athens, Greece) introduced an interface based on a medium-low pressure vaporization/desolvation chamber placed between the column effluent and the EI source. Column effluent vaporizes by heating, and a make-up nitrogen flow promotes the formation of a fine

Table 2 Post-extraction addition ME evaluation on different matrices with ESI–MSMS and Direct-EI–LC-MS. Reprinted with permission of Ref.[47] Copyright © 2011, Wiley.

	Summary of the experimental conditions		ME ± RSD (%)	
Compound	Matrix	Extraction method	LC-ESI-MS/MS	LC-Direct EI-MS
Ibuprofen	Human plasma	LL	64 ± 22	105 ± 5
	Human plasma	SPE	52 ± 14	97 ± 4
Phenacetin	Human plasma	LL	135 ± 14	99 ± 2
	Human plasma	SPE	123 ± 13	101 ± 2
Aldicarb	Fulvic acid artificial matrix	Injected without extraction	53 ± 7	115 ± 6
	River water	SPE	74 ± 8	100 ± 10
Atrazine	Artificial matrix	Injected without extraction	48 ± 6	99 ± 4
	River water	SPE	106 ± 8	105 ± 19
Methomyl	Artificial matrix	Injected without extraction	60 ± 6	101 ± 3
	River water	SPE	110 ± 27	105 ± 5
Propazine	Artificial matrix	Injected without extraction	61 ± 4	99 ± 5
	River water	SPE	74 ± 6	97 ± 13

aerosol, carrying the vaporized molecules to the ionization source by a pressure gradient.[11]

Cappiello et al. recently introduced the first version of LEI, exploring the incorporation of a vaporization micro-channel, where nebulization takes place promoted by fast heating.[54] In this case, the eluate is introduced in the vaporization micro-channel through a 25 µm i.d. fused silica capillary so that fast vaporization occurs upon contact with the heated inner capillary. A helium flow rapidly swept the formed vapors to the ionization source. A Peltier-based cooling system was incorporated at the inlet of the vaporization microchannel to prevent premature solvent evaporation (and possible clogging by analytes precipitation).[15]

This first version of the LEI proved to be more robust than Direct-EI. Nevertheless, the interface continues to be susceptible to frequent capillary blockage mainly due to inefficient separation of the cold and hot zones. Hence, researchers substituted the Peltier plates for a cooling gap between the vaporization and gas-liquid mixing zone (Figure 1b). This approach provided better temperature control, demonstrating superior Performance in preventing premature solvent evaporation and significantly reducing the chances of nebulizer capillary clogging.[15] In recent years, LEI has demonstrated excellent Performance in analyzing pesticides, polycyclic aromatic hydrocarbons, hormones, and phenols, excelling as a promissory tool for the nanoLC-EI-MS analysis of polar and non-polar compounds.[55] This interface has also demonstrated the feasibility of performing untargeted studies, allowing the exploitation of digital spectra libraries and deconvolution software. For example, Figure 2 shows the identification with the aid of deconvolution of Benzo[a]pyrene, during the untargeted analysis, in full scan mode, of a brain sample extract of a sudden infant death syndrome (SIDS) victim.

Recently Cappiello's research group explored the coupling of micro LC with Negative chemical ionization (NCI) and Electron Capture Negative Ionization (ECNI) tandem mass spectrometry (MS/MS) through an LEI interface.[56] Analysis was performed in a 2.1 µm i.d column and a passive post-column splitter allowed to reduce the flow rate from 100 µL/min to 0.5 µL/min before entering the LEI (split ratio 1:200). This approach demonstrated a 100-fold sensitivity increase compared to LC – LEI – MS, with standard 70 eV EI in the determination of dicamba and tefluthrin pesticides in commercial formulations,

As LEI is a new interface, the reported applications are still scarce. At the moment, LEI has exhibited suitable capability for analyzing small polar and non-polar GC amenable molecules, although the developers argue a more extended range of applicability than the exhibited by GC–MS.[55] On the other hand, the dependence of temperature promoted vaporization of LEI could limit its applicability to the analysis of thermolabile or low-volatile compounds.

Cold EI

EI-MS spectra are rich in structural information and amenable for analyte identification *via* library comparison for many compounds. However, in many cases, radical cations formed are so unstable that the standard 70 eV EI spectra do not show molecular ions (or very low intensity). The absence of this information hinders the identification chances and limits the assignment of an elemental formula to the compound. Alternative strategies, such as chemical ionization (CI), field ionization (FI), photoionization (PI), and low electron energy EI have been used as complementary strategies for the obtention of spectra with enhanced molecular ions. CI is the most commonly used and is currently available as an alternative ionization mode in many modern GC-Ms instruments.

On the other hand, although those alternative ionization modes can provide suitable results, Cold EI is the best alternative available to obtain EI spectra with enhanced molecular ions. This technique relies on the ionization of cold molecules in supersonic beams (SMB) with 70 eV electrons, like in standard EI-MS. Cold-EI yields classical 70 eV EI mass spectra, rich in fragments but with intense molecular ions.[57]

Cold EI was introduced in the '90s when Amirav's research discovered the enhancement of the molecular ion of cholesterol and bromopentane upon its cooling in SMB.[58,59] Initially, this technology was exploited in GC-MS and rapidly adapted to coupling miniaturized LC with EI-MS.[20–22]

Cold EI relays on the electron ionization of a fly-through ion source of vibrationally cold sample molecules in supersonic molecular beams (SMB). An SMB is the adiabatic

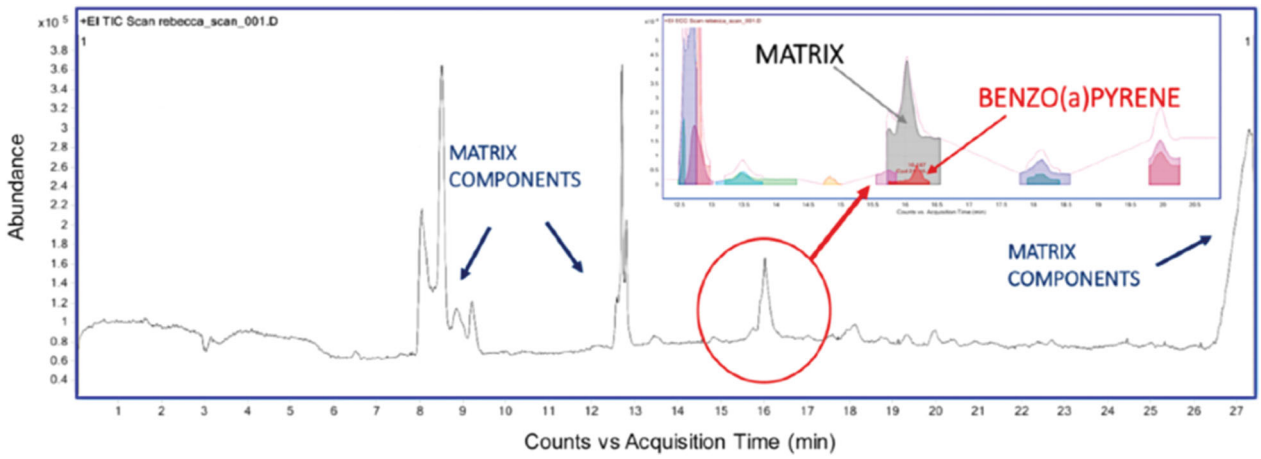

Figure 2. Example of untargeted studies performed employing the LEI. Benzo[*a*]pyrene beneath the large matrix peak at acquisition time 16 min was identified thanks to a deconvolution program and perfect matching of the 70 EV EI Spectra with the NIST library reprinted with permission of Ref.[54] Copyright © 2017, American Chemical Society.

expansion of carrier gas and the sample through a nebulizer—a 100 µm i.d. ceramic-shaped pinhole in the heated transfer line—so that all the molecules are speed-up to the same velocity and a vibrational–rotational cooling results from slow intra-beam collisions. These vibrationally cold sample compounds are skimmed and collimated, and the SMB flies through the ion source, ionizing by 70 eV electrons. The result is Cold EI spectra that exhibit the fragmentation patterns of standard EI but with enhanced molecular ions.[60]

LC-EI-MS with Cold EI was initially accomplished through an interface based on a spray formation at high pressure, soft thermal vaporization, subsequent expansion in a supersonic nozzle, and further ionization.[61] A thermal gradient between the three different heated zones and a make-up flow of helium assisted the supersonic spray formation, preventing premature solvent vaporization. Nevertheless, this first version of the SMB LC-EI MS interface was susceptible to clogging and low robustness and reproducibility.[11]

In 2015, Amirav et al. introduced the most advanced Cold EI interface based on the pneumatic spraying of the LC effluent in a heated nebulization chamber and succeeding ionization of the SMB (Figure 1c).[42] Spray stability was improved by thermal isolation of the vaporization chamber inlet so that the sample spraying could take place at a low temperature (40 °C), whit further vaporization at 300 °C. Vapors are swept toward the SMB nozzle with a helium flow and a capillary flow restrictor.

Like standard EI, Cold EI is practically free of ionization suppression/enhancement due to the matrix effects, and SMB technology can endure high eluent flow rates (up to 250 uL/min). Besides, vibrational cooling occurs without sample/solvent adducts formation. The improved molecular ion of Cols EI spectra provides superior identification capabilities *via* library comparison. Besides, the Tal-Aviv Molecule Identifier (TAMI) software was developed to determine elemental formulas from the enhanced molecular ion isotope abundance patterns of cold EI spectra.[62] SMB technology can provide linear responses up to 5 orders of magnitude rages detection limits below one pg for many compounds and a superior range of applicability than standard EI, allowing the ionization of polar and non-polar compounds with molecular masses up to 700- 800 Da.

According to Amirav's research group, Cold-EI is superior to standard EI.[63] While CI and other "soft" ion sources are complementary alternatives to standard EI, cold EI can substitute EI, applying to the analysis of molecules in a wide range of polarity and molecular weight without complementary ionization modes. Cold EI can provide both standard EI spectra without any instrumental modification or provide Cold EI spectra with enhanced molecular ions.

Cold EI has demonstrated an extended range of applications.[64] Compared to LC-ESI-MS, LC-Cold-EI allowed the ionization of both polar and non-polar compounds. GC-Cold-EI-MS demonstrated improved resolution and performance obtention narrower chromatographic peaks compared with standard GC-EI-MS.

Recently Amirav's research group introduced a hybrid and unified instrument able to unify Gas chromatography (GC) and liquid chromatography (LC) coupled with standard EI-MS and cold EI-MS.[65] The technique unification was accomplished by incorporating a restrictor capillary as an LC interface (for standard EI) or the interface for pneumatic spray formation (for Cold EI) through the transfer line and parallel to the GC capillary column. At µL/min flow rates, the pneumatic spray is thermally vaporized at ambient pressure so that most of the vaporized spray is released to the atmosphere, and just a portion is conducted through the heated flow restriction capillary and goes under SMB, and further, Cold EI.

The system can switch between GC-EI-MS and LC-EI-MS *via* software without any instrumental change to perform GC – MS and EI – LC – MS analyses in a single run and report the results in the same chromatogram. Figure 3 shows a GC/LC hybrid chromatogram obtained in one unified analytical instrument run for a model mixture at the concentration of 10 mg/L for GC compounds and 50 mg/L for LC compounds. Figure 3b illustrates the possibility of obtaining Cold-EI spectra in LC-MS for heavy

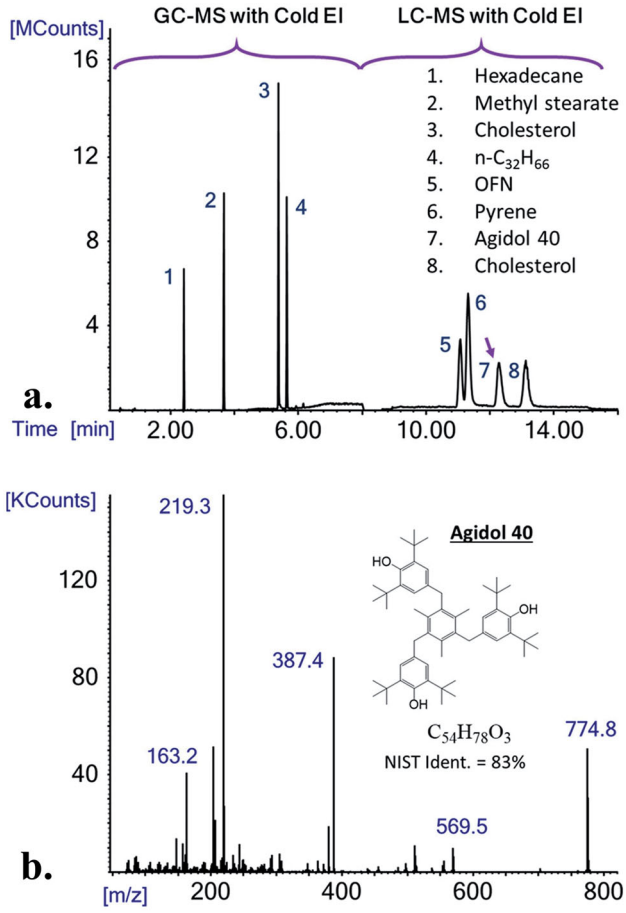

Figure 3. GC–MS with cold EI and EI–LC-MS with cold EI analyses in one unified analytical instrument run for the demonstration that the unified GC–MS with cold EI and EI–LC-MS with a cold EI system (EI–LC/GC–MS–SMB) can operate with software-based mode changing and generate both analyses in one file without any change in hardware assembly or setup. Reprinted with permission of Ref.[65] Copyright © 2020, American Society for Mass Spectrometry.

compounds with the same quality as those obtained *via* GC-MS.[65]

Conclusion

NanoLC coupled to MS is a modern and powerful analytical technique that provides enhanced chromatographic Performance and superior detectability than the observed at a conventional scale. The first commercial instruments for nanoLC were introduced 20 years ago, and since then, the technique has been under continuous evolution. Robust, compact, and portable instruments have been introduced, and the researchers have developed a plethora of new stationary phases and column formats. Nowadays, packed columns with innovative stationary phases, open tubular columns, and microfabricated devices provide a series of separation alternatives to be explored in nanoLC.

On the other hand, although nanoLC coupled to MS through nanoESI sources has demonstrated improved performance in the last 20 years, one of the most outstanding advantages of the miniaturized scale is the possibility to allow the hyphenation with EI-MS instruments. EI-MS exceeds the atmospheric pressure ionization techniques by providing highly reproducible and molar informative mass spectra, its negligible matrix effects, and its potential to unify GC and LC in a single instrument. The LC-EI-MS coupling has been long pursued, even before the development of the ESI sources arose. In the past, incompatibility between the high vacuum condition of EI-MS and the large flowrates characteristics of LC hindered the coupling between the techniques. With the nanoLC technology's rise, those incompatibilities have come to be overcome, and in the last 20 years, three different interfacing strategies have been providing progressive results: (i) Direct EI, (ii) LEI, and (iii) Cold EI. Direct EI is the more simple and easily adaptable but also the less robust approach. LEI is the newer technology and has allowed overcoming many limitations of direct EI and promises a wide range of applicability, including polar and non-polar compounds in a range of molecular masses more extensive than allowed by GC-MS. Nevertheless, the reported applications of this interface are still scarce. Cold EI is a more sophisticated technology but excels as an improved version of the conventional EI, mainly due to its ability to provide mass spectra with enhanced molecular ions, improving the identification capabilities. Recently. Cold EI allowed the first introduction of a GC/LC unified instrument. Although the detection limits are still high, this advance may be opening the door for the advent of unified chromatography. Shortly, we will continue to see new developments in these interfaces, and their association with new advances with new nanoLC instruments and columns could bring new application opportunities and gradually make nanoLC-EI-MS finally competitive with nanoLC-ESI-MS.

Funding

The authors are grateful to the Coordenação de Aperfeiçoamento de Pessoal de Nível Superior—Brazil (CAPES)—Finance Code 001; to FAPESP (Grants 2019/22724-7, 2017/02147-0, 2019/26263-4, 2015/15462-5, 2014/03765-0, and 2014/07347-9); and to CNPq (307293/2014-9 and 308843/2019-3) for the financial support provided for this research and to our laboratory.

References

[1] Vargas Medina, D. A.; Maciel, E. V. S.; de Toffoli, A. L.; Lanças, F. M. Miniaturization of Liquid Chromatography Coupled to Mass Spectrometry. 2. Achievements on Modern Instrumentation for Miniaturized Liquid Chromatography Coupled to Mass Spectrometry. *Trends Anal. Chem.* **2020**, *128*, 115910. DOI: 10.1016/j.trac.2020.115910.

[2] Famiglini, G.; Palma, P.; Termopoli, V.; Cappiello, A.; Tsizin, S.; Seemann, B.; Alon, T.; Fialkov, A. B.; Amirav, A. Electron Ionization LC-MS: What Is It and Why Use It? *Compr. Anal. Chem.* **2018**, *79*, 1–28. DOI: 10.1016/bs.coac.2017.06.008.

[3] Wilm, M. Principles of Electrospray Ionization. *Mol. Cell Proteomics* **2011**, *10*, M111.009407. DOI: 10.1074/mcp.M111.009407.

[4] Leinonen, A.; Kuuranne, T.; Kostiainen, R. Liquid Chromatography/Mass Spectrometry in Anabolic Steroid Analysis? Optimization and Comparison of Three Ionization Techniques: Electrospray Ionization, Atmospheric Pressure Chemical Ionization and Atmospheric Pressure

Photoionization. *J. Mass Spectrom.* **2002**, *37*, 693–698. DOI: 10.1002/jms.328.

[5] Robb, D. B.; Covey, T. R.; Bruins, A. P. Atmospheric Pressure Photoionization: An Ionization Method for Liquid Chromatography–Mass Spectrometry. *Anal. Chem.* **2000**, *72*, 3653–3659. DOI: 10.1021/ac0001636.

[6] Sarkar, P. K.; Prajapati, P. K.; Shukla, V. J.; Ravishankar, B.; Choudhary, A. K. A Timeline of Stable of Isotopes and Mass Spectrometry. *Indian J. Exp. Biol.* **2009**, *47*, 987–992. DOI: 10.1002/mas.

[7] Matuszewski, B. K.; Constanzer, M. L.; Chavez-Eng, C. M. Strategies for the Assessment of Matrix Effect in Quantitative Bioanalytical Methods Based on HPLC-MS/MS. *Anal. Chem.* **2003**, *75*, 3019–3030. DOI: 10.1021/ac020361s.

[8] Antignac, J.-P.; de Wasch, K.; Monteau, F.; De Brabander, H.; Andre, F.; Le Bizec, B. The Ion Suppression Phenomenon in Liquid Chromatography–Mass Spectrometry and Its Consequences in the Field of Residue Analysis. *Anal. Chim. Acta* **2005**, *529*, 129–136. DOI: 10.1016/j.aca.2004.08.055.

[9] Heemskerk, A. A. M.; Busnel, J.-M.; Schoenmaker, B.; Derks, R. J. E.; Klychnikov, O.; Hensbergen, P. J.; Deelder, A. M.; Mayboroda, O. A. Ultra-Low Flow Electrospray Ionization-Mass Spectrometry for Improved Ionization Efficiency in Phosphoproteomics. *Anal. Chem.* **2012**, *84*, 4552–4559. DOI: 10.1021/ac300641x.

[10] Palma, P.; Famiglini, G.; Trufelli, H.; Pierini, E.; Termopoli, V.; Cappiello, A. Electron Ionization in LC-MS: Recent Developments and Applications of the Direct-EI LC-MS Interface. *Anal. Bioanal. Chem.* **2011**, *399*, 2683–2693. DOI: 10.1007/s00216-010-4637-0.

[11] Rigano, F.; Tranchida, P. Q.; Dugo, P.; Mondello, L. High-Performance Liquid Chromatography Combined with Electron Ionization Mass Spectrometry: A Review. *Trends Anal. Chem.* **2019**, *118*, 112–122. DOI: 10.1016/j.trac.2019.05.032.

[12] Šesták, J.; Moravcová, D.; Kahle, V. Instrument Platforms for Nano Liquid Chromatography. *J. Chromatogr. A* **2015**, *1421*, 2–17. DOI: 10.1016/j.chroma.2015.07.090.

[13] Rigano, F.; Arigò, A.; Oteri, M.; La Tella, R.; Dugo, P.; Mondello, L. The Retention Index Approach in Liquid Chromatography: An Historical Review and Recent Advances. *J. Chromatogr. A* **2021**, *1640*, 461963. DOI: 10.1016/j.chroma.2021.461963.

[14] Famiglini, G.; Palma, P.; Termopoli, V.; Cappiello, A. The History of Electron Ionization in LC-MS, from the Early Days to Modern Technologies: A Review. *Anal. Chim. Acta* **2021**, *1167*, 338350. DOI: 10.1016/j.aca.2021.338350.

[15] Termopoli, V.; Famiglini, G.; Palma, P.; Piergiovanni, M.; Rocio-Bautista, P.; Ottaviani, M. F.; Cappiello, A.; Saeed, M.; Perry, S. Evaluation of a Liquid Electron Ionization Liquid Chromatography–Mass Spectrometry Interface. *J. Chromatogr. A* **2019**, *1591*, 120–130. DOI: 10.1016/j.chroma.2019.01.034.

[16] Palma, P.; Pierini, E.; Cappiello, A. LC-MS Interfaces. In *Analytical Separation Science*; Wiley-VCH Verlag GmbH & Co. KGaA: Weinheim, 2015; pp 87–110. DOI: 10.1002/9783527678129.assep005.

[17] Chervet, J. P.; Ursem, M.; Salzmann, J. P. Instrumental Requirements for Nanoscale Liquid Chromatography. *Anal. Chem.* **1996**, *68*, 1507–1512. DOI: 10.1021/ac9508964.

[18] Vissers, J. P.; Claessens, H. A.; Cramers, C. A. Microcolumn Liquid Chromatography: Instrumentation, Detection and Applications. *J. Chromatogr. A* **1997**, *779*, 1–28. DOI: 10.1016/S0021-9673(97)00422-6.

[19] Fanali, S. An Overview to Nano-Scale Analytical Techniques: Nano-Liquid Chromatography and Capillary Electrochromatography. *Electrophoresis* **2017**, *38*, 1822–1829. DOI: 10.1002/elps.201600573.

[20] Fanali, S. Nano-Liquid Chromatography Applied to Enantiomers Separation. *J. Chromatogr. A* **2017**, *1486*, 20–34. DOI: 10.1016/j.chroma.2016.10.028.

[21] Gama, M. R.; Collins, C. H.; Bottoli, C. B. G. Nano-Liquid Chromatography in Pharmaceutical and Biomedical Research. *J. Chromatogr. Sci.* **2013**, *51*, 694–703. DOI: 10.1093/chromsci/bmt023.

[22] Wilson, S. R.; Vehus, T.; Berg, H. S.; Lundanes, E. Nano-LC in Proteomics: Recent Advances and Approaches. *Bioanalysis* **2015**, *7*, 1799–1815. DOI: 10.4155/bio.15.92.

[23] Chetwynd, A. J.; David, A. A Review of Nanoscale LC-ESI for Metabolomics and Its Potential to Enhance the Metabolome Coverage. *Talanta* **2018**, *182*, 380–390. DOI: 10.1016/j.talanta.2018.01.084.

[24] Li, Y.; Bouza, M.; Wu, C.; Guo, H.; Huang, D.; Doron, G.; Temenoff, J. S.; Stecenko, A. A.; Wang, Z. L.; Fernández, F. M. Sub-Nanoliter Metabolomics via Mass Spectrometry to Characterize Volume-Limited Samples. *Nat. Commun.* **2020**, *11*, 1–16. DOI: 10.1038/s41467-020-19444-y.

[25] Mirabelli, M. F.; Wolf, J. C.; Zenobi, R. Pesticide Analysis at Ppt Concentration Levels: Coupling Nano-Liquid Chromatography with Dielectric Barrier Discharge Ionization-Mass Spectrometry. *Anal. Bioanal. Chem.* **2016**, *408*, 3425–3434. DOI: 10.1007/s00216-016-9419-x.

[26] Lanckmans, K.; Van Eeckhaut, A.; Sarre, S.; Smolders, I.; Michotte, Y. Capillary and Nano-Liquid Chromatography-Tandem Mass Spectrometry for the Quantification of Small Molecules in Microdialysis Samples: Comparison with Microbore Dimensions. *J. Chromatogr. A* **2006**, *1131*, 166–175. DOI: 10.1016/j.chroma.2006.07.090.

[27] D'Orazio, G.; Rocchi, S.; Fanali, S. Nano-Liquid Chromatography Coupled with Mass Spectrometry: Separation of Sulfonamides Employing Non-Porous Core-Shell Particles. *J. Chromatogr. A* **2012**, *1255*, 277–285. DOI: 10.1016/j.chroma.2012.03.032.

[28] Nazario, C. E. D.; Silva, M. R.; Franco, M. S.; Lanças, F. M. Evolution in Miniaturized Column Liquid Chromatography Instrumentation and Applications: An Overview. *J. Chromatogr. A* **2015**, *1421*, 18–37. DOI: 10.1016/j.chroma.2015.08.051.

[29] Natsume, T.; Yamauchi, Y.; Nakayama, H.; Shinkawa, T.; Yanagida, M.; Takahashi, N.; Isobe, T. A Direct Nanoflow Liquid Chromatography-Tandem Mass Spectrometry System for Interaction Proteomics. *Anal. Chem.* **2002**, *74*, 4725–4733. DOI: 10.1021/ac020018n.

[30] Sanders, K. L.; Edwards, J. L. Nano-Liquid Chromatography-Mass Spectrometry and Recent Applications in Omics Investigations. *Anal. Methods* **2020**, *12*, 4404–4417. DOI: 10.1039/d0ay01194k.

[31] Wilson, S. R.; Olsen, C.; Lundanes, E. Nano Liquid Chromatography Columns. *Analyst* **2019**, *144*, 7090–7104. DOI: 10.1039/c9an01473j.

[32] Asensio-Ramos, M.; Fanali, C.; D'Orazio, G.; Fanali, S. *Nano-Liquid Chromatography*, in: Liquid Chromatography Fundamentals and Instrumentation 2nd ed.; Elsevier Inc: Amsterdam, 2017; Vol. 1. DOI: 10.1016/B978-0-12-805393-5.00027-0.

[33] Hernández-Borges, J.; Aturki, Z.; Rocco, A.; Fanali, S. Recent Applications in Nanoliquid Chromatography. *J. Sep. Sci.* **2007**, *30*, 1589–1610. DOI: 10.1002/jssc.200700061.

[34] Mejía-Carmona, K.; Soares da Silva Burato, J.; Borsatto, J. V. B.; de Toffoli, A. L.; Lanças, F. M. Miniaturization of Liquid Chromatography Coupled to Mass Spectrometry: 1. Current Trends on Miniaturized LC Columns. *Trends Anal. Chem.* **2020**, *122*, 115735. DOI: 10.1016/j.trac.2019.115735.

[35] Pattanayak, P.; Singh, S. K.; Gulati, M.; Vishwas, S.; Kapoor, B.; Chellappan, D. K.; Anand, K.; Gupta, G.; Jha, N. K.; Gupta, P. K. Microfluidic Chips: Recent Advances, Critical Strategies in Design, Applications and Future Perspectives. *Microfluid. Nanofluid.* **2021**, *25*, 1–28. DOI: 10.1007/S10404-021-02502-2.

[36] Vargas Medina, D. A.; Maciel, E. V. S.; Lanças, F. M. Miniaturization of Liquid Chromatography Coupled to Mass Spectrometry. 3. Achievements on Chip-Based LC-MS Devices. *Trends Anal. Chem.* **2020**, *131*, 116003. DOI: 10.1016/j.trac.2020.116003.

[37] Vasconcelos Soares Maciel, E.; de Toffoli, A. L.; Sobieski, E.; Domingues Nazário, C. E.; Lanças, F. M. Miniaturized Liquid Chromatography Focusing on Analytical Columns and Mass Spectrometry: A Review. *Anal. Chim. Acta* **2020**, *1103*, 11–31. DOI: 10.1016/j.aca.2019.12.064.

[38] Vargas Medina, D. A.; Pereira dos Santos, N. G.; da Silva Burato, J. S.; Borsatto, J. V. B.; Lanças, F. M. An Overview of Open Tubular Liquid Chromatography with a Focus on the Coupling with Mass Spectrometry for the Analysis of Small Molecules. *J. Chromatogr. A* **2021**, *1641*, 461989. DOI: 10.1016/j.chroma.2021.461989.

[39] McFadden, W. H.; Schwartz, H. L.; Evans, S. Direct Analysis of Liquid Chromatographic Effluents. *J. Chromatogr. A* **1976**, *122*, 389–396. DOI: 10.1016/S0021-9673(00)82261-X.

[40] Hayes, M. J.; Lankmayer, E. P.; Vouros, P.; Karger, B. L.; McGuire, J. M. Moving Belt Interface with Spray Deposition for Liquid Chromatography/Mass Spectrometry. *Anal. Chem.* **1983**, *55*, 1745–1752. DOI: 10.1021/ac00261a024.

[41] Cappiello, A. Is Particle Beam an Up-to-Date LC-MS Interface? State of the Art and Perspectives. *Mass Spectrom. Rev.* **1996**, *15*, 283–296. DOI: 10.1002/(SICI)1098-2787(1996)15:5 < 283::AID-MAS1 > 3.0.CO;2-E.

[42] Seemann, B.; Alon, T.; Tsizin, S.; Fialkov, A. B.; Amirav, A. Electron Ionization LC-MS with Supersonic Molecular Beams-the New Concept, Benefits and Applications. *J. Mass Spectrom.* **2015**, *50*, 1252–1263. DOI: 10.1002/jms.3695.

[43] Cappiello, A.; Famiglini, G.; Mangani, F.; Palma, P. A Simple Approach for Coupling Liquid Chromatography and Electron Ionization Mass Spectrometry. *J. Am. Soc. Mass Spectrom.* **2002**, *13*, 265–273. DOI: 10.1016/S1044-0305(01)00363-4.

[44] Flender, C.; Wolf, C.; Leonhard, P.; Karas, M. Nano-Liquid Chromatography-Direct Electron Ionization Mass Spectrometry: Improving Performance by a New Ion Source Adapter. *J. Mass Spectrom.* **2011**, *46*, 1004–1010. DOI: 10.1002/jms.1981.

[45] Riboni, N.; Magrini, L.; Bianchi, F.; Careri, M.; Cappiello, A. Sol-Gel Coated Ion Sources for Liquid Chromatography-Direct Electron Ionization Mass Spectrometry. *Anal. Chim. Acta* **2017**, *978*, 35–41. DOI: 10.1016/j.aca.2017.04.026.

[46] Cappiello, A.; Famiglini, G.; Pierini, E.; Palma, P.; Trufelli, H. Advanced Liquid Chromatography-Mass Spectrometry Interface Based on Electron Ionization. *Anal. Chem.* **2007**, *79*, 5364–5372. DOI: 10.1021/ac070468l.

[47] Cappiello, A.; Famiglini, G.; Palma, P.; Pierini, E.; Termopoli, V.; Trufelli, H. Direct-EI in LC-MS: Towards a Universal Detector for Small-Molecule Applications. *Mass Spectrom. Rev.* **2011**, *30*, 1242–1255. DOI: 10.1002/mas.20329.

[48] Famiglini, G.; Palma, P.; Termopoli, V.; Trufelli, H.; Cappiello, A. Single-Step LC/MS Method for the Simultaneous Determination of GC-Amenable Organochlorine and LC-Amenable Phenoxy Acidic Pesticides. *Anal. Chem.* **2009**, *81*, 7373–7378. DOI: 10.1021/ac9008995.

[49] Famiglini, G.; Palma, P.; Pierini, E.; Trufelli, H.; Cappiello, A. Organochlorine Pesticides by LC-MS. *Anal. Chem.* **2008**, *80*, 3445–3449. DOI: 10.1021/ac8000435.

[50] Flender, C.; Leonhard, P.; Wolf, C.; Fritzsche, M.; Karas, M. Analysis of Boronic Acids by Nano Liquid Chromatography-Direct Electron Ionization Mass Spectrometry. *Anal. Chem.* **2010**, *82*, 4194–4200. DOI: 10.1021/ac1004585.

[51] Cappiello, A.; Famiglini, G.; Mangani, F.; Palma, P.; Siviero, A. Nano-High-Performance Liquid Chromatography-Electron Ionization Mass Spectrometry Approach for Environmental Analysis. *Anal. Chim. Acta* **2003**, *493*, 125–136. DOI: 10.1016/S0003-2670(03)00868-7.

[52] Rigano, F.; Albergamo, A.; Sciarrone, D.; Beccaria, M.; Purcaro, G.; Mondello, L. Nano Liquid Chromatography Directly Coupled to Electron Ionization Mass Spectrometry for Free Fatty Acid Elucidation in Mussel. *Anal. Chem.* **2016**, *88*, 4021–4028. DOI: 10.1021/acs.analchem.6b00328.

[53] Abonamah, J. V.; Eckenrode, B. A.; Moini, M. On-Site Detection of Fentanyl and Its Derivatives by Field Portable Nano-Liquid Chromatography-Electron Lonization-Mass Spectrometry (NLC-EI-MS). *Forensic Chem.* **2019**, *16*, 100180. DOI: 10.1016/j.forc.2019.100180.

[54] Termopoli, V.; Famiglini, G.; Palma, P.; Piergiovanni, M.; Cappiello, A. Atmospheric Pressure Vaporization Mechanism for Coupling a Liquid Phase with Electron Ionization Mass Spectrometry. *Anal. Chem.* **2017**, *89*, 2049–2056. DOI: 10.1021/acs.analchem.6b04646.

[55] Cappiello, A. The Benefits of a Liquid-Electron Ionization Liquid Chromatography-Mass Spectrometry Interface. *LCGC* **2019**, *32*, 330–331.

[56] Cappiello, A.; Termopoli, V.; Palma, P.; Famiglini, G.; Saeed, M.; Perry, S.; Navarro, P. Liquid Chromatography–Electron Capture Negative Ionization–Tandem Mass Spectrometry Detection of Pesticides in a Commercial Formulation. *J. Am. Soc. Mass Spectrom.* **2022**, *33*, 141–148. DOI: 10.1021/jasms.1c00307.

[57] Margolin Eren, K. J.; Elkabets, O.; Amirav, A. A Comparison of Electron Ionization Mass Spectra Obtained at 70 EV, Low Electron Energies, and with Cold EI and Their NIST Library Identification Probabilities. *J. Mass Spectrom.* **2020**, *55*, e4646. DOI: 10.1002/jms.4646.

[58] Beams, S. M. Electron Impact Mass Spectrometry of Cholesterol in Supersonic Molecular Beams. *J. Phys. Chem.* **1990**, *94*, 5200–5202.

[59] Amirav, A. Electron Impact and Hyperthermal Surface Ionization Mass Spectrometry in Supersonic Molecular Beams. *Org. Mass Spectrom.* **1991**, *26*, 1–17.

[60] Amirav, A.; Fialkov, A. B.; Margolin Eren, K. J.; Neumark, B.; Elkabets, O.; Tsizin, S.; Alexander Gordin, T. A. Gas Chromatography–Mass Spectrometry (GC–MS) with Cold Electron Ionization (EI): Bridging the Gap between GC–MS and LC-MS. *Spectrosc. Suppl.* **2021**, *18*, 5–15.

[61] Granot, O.; Amirav, A. LC-MS with Electron Ionization of Cold Molecules in Supersonic Molecular Beams. *Int. J. Mass Spectrom.* **2005**, *244*, 15–28. DOI: 10.1016/j.ijms.2005.04.003.

[62] Alon, T.; Amirav, A. Isotope Abundance Analysis Methods and Software for Improved Sample Identification with Supersonic Gas Chromatography/Mass Spectrometry. *Rapid Commun. Mass Spectrom.* **2006**, *20*, 2579–2588. DOI: 10.1002/rcm.2637.

[63] Amirav, A.; Fialkov, A. B.; Gordin, A.; Elkabets, O.; Margolin Eren, K. J. Cold Electron Ionization (EI) Is Not a Supplementary Ion Source to Standard EI. It Is a Highly Superior Replacement Ion Source. *J. Am. Soc. Mass Spectrom.* **2021**, *32*, 2631–2635. DOI: 10.1021/jasms.1c00241.

[64] Tsizin, S.; Bokka, R.; Keshet, U.; Alon, T.; Fialkov, A. B.; Tal, N.; Amirav, A. Comparison of Electrospray LC-MS, LC-MS with Cold EI and GC–MS with Cold EI for Sample Identification. *Int. J. Mass Spectrom.* **2017**, *422*, 119–125. DOI: 10.1016/j.ijms.2017.09.006.

[65] Tsizin, S.; Fialkov, A. B.; Amirav, A. Electron Ionization Mass Spectrometry for Both Liquid and Gas Chromatography in One System without the Need for Hardware Adjustments. *J. Am. Soc. Mass Spectrom.* **2020**, *31*, 1713–1721. DOI: 10.1021/jasms.0c00136.

Capítulo 6

Artigo publicado no *Electrophoresis*, 2022

Received: 27 December 2021 | Revised: 5 April 2022 | Accepted: 27 April 2022

DOI: 10.1002/elps.202100392

ELECTROPHORESIS

REVIEW

Electron ionization mass spectrometry: Quo vadis?

Edvaldo Vasconcelos Soares Maciel | **Natalia Gabrielly Pereira dos Santos** | **Deyber Arley Vargas Medina** | **Fernando Mauro Lanças**

Institute of Chemistry of São Carlos, University of São Paulo, São Carlos, São Paulo, Brazil

Correspondence
Fernando Mauro Lanças, Institute of Chemistry of São Carlos, University of São Paulo, São Carlos, SP, Brazil.
Email: flancas@iqsc.usp.br

Color online: See the article online to view Figures 4 and 5 in color.

Funding information
Coordenação de Aperfeiçoamento de Pessoal de Nível Superior, Grant/Award Number: 001; FAPESP, Grant/Award Numbers: 2019/22724-7, 2017/02147-0, 2019/26263-4, 2015/15462-5, 2014/03765-0, 2014/07347-9; CNPq, Grant/Award Numbers: 307293/2014-9, 308843/2019-3

Abstract

Mass spectrometry (MS) is a fundamental technique to identify compounds by their mass-to-charge ratio. It is known that MS can only detect target compounds when they are converted to ions in the gas phase. The ionization procedure is considered one of the most critical steps, and there are distinct techniques for it. One of them is electron ionization (EI), a widely used hard-ionization technique capable of generating several ions due to the excess energy employed. The existence of distinct ionization mechanisms turns EI capable of producing a fingerprint-like spectrum for each molecule. So, it is an essential technique for obtaining structural information. EI is often combined with chromatography to obtain a practical introduction of pretreated samples despite its excellent performance. EI–MS has been applied coupled with gas chromatography (GC) since the 1960s as both are very compatible. Currently, analytes of interest are more suitable for liquid chromatography (LC) analysis, so there are researchers dedicated to developing suitable interfaces for coupling LC and EI–MS. EI excels, as a reliable technique to fill the gap between GC and LC, possibly allowing them to coexist in a single instrument. In this work, the authors will present the fundamentals of EI–MS, emphasizing the development over the years, coupling with gas and LC, and future trends.

KEYWORDS
electron ionization, gas chromatography, liquid chromatography, mass spectrometry, unified chromatography

1 | INTRODUCTION: EI–MS PRIMORDIUM

Mass spectrometry (MS) was introduced at the beginning of the 1990s following some experiments by Thomson about cathodic rays and further studies of Aston [1, 2]. MS operates as a detection technique in which a gaseous phase containing the compounds of interest—as ions—is formed and separated further, according to their mass-to-charge ratio, with the support of electric and magnetic fields. During that period, the discrimination of isotopes was a topic of great interest, and to study that

Abbreviations: APCI, atmosphere pressure chemical ionization; APPI, atmosphere pressure photoionization; Cap–EI, capillary-EI interface; CID, collision-induced dissociation; Direct–EI, Direct-EI interface; DLI, direct liquid introduction interface; EI, electron ionization; ESI, electrospray ionization; GC, gas chromatography; HPLC, high-performance liquid chromatography; HRMS, high-resolution mass spectrometry; LC, liquid chromatography; m/z, mass-to-charge ratio; MAGIC, monodisperse aerosol generation interface for chromatography; MB, mobile belt interface; MS, mass spectrometry; MS/MS, tandem mass spectrometry; NIST, National Institute of Standards and Technology; PB, particle beam interface; SMB, supersonic molecular beam; UV–Vis, ultraviolet detector.

scientists-produced positive ions by heating a metal wire coated with the target element [1, 3]. The initial developments over electron ionization (EI) emerged from this interest, precisely with Dempster in 1918 at the University of Chicago. He showed that a determined sample could produce positively charged ions if an electron beam were accelerated and further shocked by it [4]. Here, the well-recognized terminologies of electron-impact ionization and EI have their roots. By definition, EI consists of bombarding a determined sample with an energy-defined electron beam for transferring energy to the sample, causing it to ionize.

After these pioneering experiments on the EI process, several scientists began interested in the topic—recognizing the importance and potential that this technique would represent for the production of ions and a subsequent identification of them. It is worth mentioning that the following cited works are considered essential contributions to the field. They presented original experiments and interfaces, which helped EI become an established technique for producing ions and as a source for MS [4]. In 1922, Smith created an ion source capable of controlling the acceleration and energy of the electron beam partially, which could identify doubly charged mercury species from its predecessors as well as had used this source to study ions from several other elements [5]. In 1929, Bleakney proposed a novel design of EI source to collimate the electron beam, which can prevent interference between electrons and is principally able to produce a linear source of ions with similar density to be further analyzed [6]. Even so, there were still significant problems in the EI sources, such as the necessity for an all-metal machine-like EI ionization source. Furthermore, these initial works have their ionization chambers primarily made in a single piece of glass, making maintenance or replacements difficult when problems emerge. In addition, the observed varying energy of the electron beam, which hindered ionization efficiency and resolution to producing electron beam with constant energy, was a key goal at that time. Lastly, the demand for compact size EI sources was a challenge, once most designs did not favor the construction of compact instruments, mainly due to their demand for large power supply units (e.g., batteries). Up to the 1980s, several other scientists contributed to overcoming these EI-related downsides, being the most notables Smith and Scott [7, 8], Finkelstein [9], Brink [10], Nier [11, 12], Coggeshall and Jordan [13], Clarke [14], Marmet and Kerwin [15], Simpson [16], Kuyatt and Simpson [17], Fox [18], and Liebmann [19].

These previously cited works contributed to the development of several EI sources, resulting in those MS instruments that we are still using and establishing EI as a widely used technique nowadays. Also, the development of theoretical modeling at the beginning of the 1950s contributed positively to the topic. With the advent of these mathematical models and digital computers, scientists could predict optimized source designs and parameters, getting overall high ionization efficiencies [20, 21]. Finally, it is worth mentioning that EI–MS instruments currently in use (like those coupled with chromatography [GC]) are still based on the works of Nier [11, 12] and Brink [10].

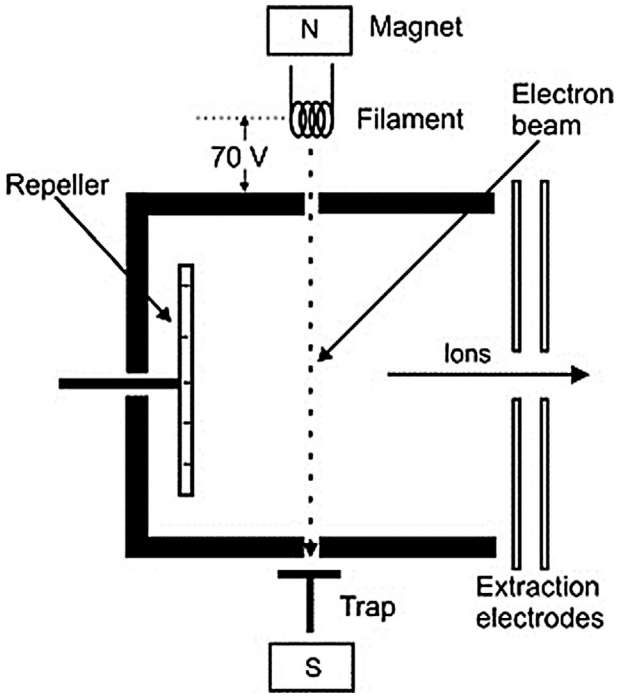

FIGURE 1 Schematic illustration of an ionization chamber used in electron ionization–mass spectrometry instruments. *Source*: Copyright from Ref. [22] with the permission of Elsevier

1.1 | Electron ionization source and phenomena

The "heart" of an EI–MS instrument is the ion source. Figure 1 shows an illustration of a typical arrangement for it—which is a small heated place inside the vacuum region of the instrument (~10-mm length, 1–2 cm^3 in volume), containing a heated filament of tungsten or rhenium, a repeller plate, a trap electrode, small magnet, and a plate-like structure of electrodes at the end of the source [22]. Although sample effluent passes within the ion source, the perpendicular electron beam is sped up from the superior hot filament to the inferior trap electrode at a potential of about 70 V. The electron beam intercepts the sample molecules at a specific angle, triggering the ionization [23]. Theoretically, this intersection angle between the electron and the molecular beams of analytes should be

perpendicular. However, they exhibited subtle variations depending on the target molecules and the design and components of the EI ionization chamber. It is worth mentioning that the magnet causes the electron beam to assume a spiral-like trajectory that increases contact with the sample. Also, the variation between the electrical potential of the repeller plate and extraction electrodes is responsible for focalizing and ejecting the ions toward the mass analyzer [22].

Upon collision with the electron beam, the sample molecules absorb energy, ionize, and then release electrons, forming single- or multiply charged positive ions. Depending on the amount of energy transferred from the electron beam to the sample, the ionization can take different reaction pathways, resulting in variable types and ions formed from the target molecule [23]. However, being independent of the mechanism, they are intramolecular without external interferences, which partly explains the negligible matrix effect and the requirement for vacuum conditions [24]. Complementarily, the high electric potential of the electron beam (70 V) is another parameter contributing to non-observable matrix effects over the ionization efficiency, as we are talking about a high-energized electron beam—this also explains why EI is considered a hard-ionization technique [24]. Commonly, molecules will undergo (i) a loss of a neutral molecular fragment; (ii) an elimination of a charged radical; and (iii) intramolecular rearrangement. According to Lifshitz and Märk [25], the following equations illustrate some reaction pathways for direct ionization (e_{ej}: electrons ejected from the molecule; e_{sc}: electrons scattered from the beam):

$$AB + e \rightarrow AB^{(+\cdot)} + e_{ej} + e_{sc} \quad \text{(single ionization)} \qquad (1)$$

$$AB + e \rightarrow AB^{2+} + 2e_{ej} + e_{sc} \quad \text{(double ionization)} \qquad (2)$$

$$AB + e \rightarrow AB^{n+\cdot} + ne_{ej} + e_{sc} \quad \text{(multiple ionization)} \qquad (3)$$

Besides direct ionization, there are other phenomena in which electrons are ejected sequentially from the sample or the molecular ion decays, as shown in the following equations:

$$AB^{+*} + e_{ej} + e_{sc} \rightarrow A^{\cdot +} + B^{\cdot} + e_{ej} + e_{sc}$$

(metastable fragmentation) (4)

$$AB^{+*} + e_{ej} + e_{sc} \rightarrow AB^{\cdot +} + h\nu + e_{ej} + e_{sc}$$

(radioative fragmentation) (5)

$$AB + e_{sc} \rightarrow A + B^{-} \text{ or } A^{-} + B$$

(dissociative electron attachment) (6)

Metastable fragmentation is unimolecular dissociations taking place out of the ionization source, during the ion's flight from the ion source, through the mass analyzer, to the detection device. This process occurs in the virtue of the internal energy gained by the ion within the ion source. Metastable ions can be detected in double-focusing mass spectrometers and appear in the mass spectra as low intensity and broad peaks, covering several mass units and with an apparent mass $M2/M1- M2$, the mass of the ion product of the inflight fragmentation, and $M1$, the mass of the precursor ion [26].

On the other hand, EI can also lead to negatively charged ions (anions). Electrons can also lead to dissociative electron attachment of molecules in a resonance state, possessing enough lifetime (e.g., nuclear-excited Feshbach resonance, electronically excited Feshbach resonance, or Shape resonance) [27]. An electron can temporarily be "held up" in a resonant state of the molecule, causing autoionization, leading to a vibrational excitation state, or molecule dissociation with the formation of negatively charged species of small-to-moderate kinetic energies, as schematized in Equation (V) [28]. At last, tough with less probability, ions excited by the magnetic field of the bombarding electrons, possessing an excess of energy, can release it by radiative stabilization (emission of photons), as represented in Equation (VI).

These different ionization mechanisms in EI–MS make this technique capable of creating an almost fingerprint-like spectrum for each sample and target molecule [25]. Furthermore, EI often generates several corresponding ions for a target molecule, making it an essential analytical tool for obtaining rich structural information about unknown compounds. Considering that ionization is crucial during MS analysis, it is imperative to understand how this process is performed and which techniques are used. The conversion of molecules to ions is an essential tool in all mass spectrometric–based techniques and directly affects the quality of the mass spectrum. As already introduced in the historical section, EI is a popular and pioneer method to perform such a process. It is usually performed under a high-energetic electron beam of 70 V. As a consequence of the high EI process, it is considered a hard-ionization technique, being productive and reproducible as this amount of energy is enough to ionize molecules in an effective and reproducible pattern that creates a fingerprint-like pattern mass spectrum.

2 | THE GC–EI–MS HOOKUP

Despite the well-recognized efficiency of EI–MS in generating ions, it must be used in combination with a sample introduction technique to ensure that vapor phase molecules reach the ion source [29]. In this case, EI coupled with GC has been tested since the 1960s. Initially, the scientists started using packed columns that required different MS coupling interfaces, such as jet separators [30], membrane separators [31], and effusion separators [32]. In the 1980s, scientists were able to use fused-silica capillary GC columns directed inserted into the EI ionization chamber [33]. It is worth mentioning that this hyphenation was a revolutionary milestone in developing the modern analytical sciences. The development of the EI sources was a determinant factor for the quick consolidation of GC–MS as a powerful technique once EI–MS proved itself as a reproducible and effective way to perform ionization (underscored in the previous section).

GC can separate many target molecules within a single sample—a desirable feature in analytical chemistry—delivering a cleaner sample extract to the EI mass spectrometer. That aspect is particularly relevant because isolated molecules from the GC effluent reach the ion source at unique times, favoring the ionization efficiency as the competition between them and interfering compounds for ionizable regions in the electrospray ionization (ESI) tip is decreased. Also, by delivering a pretreated extract, we favor the lifetime of the mass spectrometer. It is worth keeping in mind that EI–MS works under vacuum conditions, and ionization is performed mainly by thermionic-based processes, so using it for thermally stable and volatile molecules is good and matches precisely with GC requirements. This complementary set of upsides for EI–MS and GC boosted their combined applications and contributed to the widespread of these two techniques. Also, the development of capillary analytical columns to work at low gas flow rates favored the GC–EI–MS coupling, as they met the high-vacuum requirements of EI sources. Nowadays, GC–EI–MS is applied successfully in many essential areas, such as bioanalytical chemistry, environmental analysis, food analysis, and toxicology [34–36]. Although GC–EI–MS has been employed in many cases, the fact that there is a broad range of other compounds of interest not suitable for gas chromatography has prompted scientists since the 1970s to achieve suitable hyphenation between liquid chromatography (LC) and EI–MS [37]. Snyder et al. stated that only approximately 20% of organic molecules are GC-compatible without any modification (e.g., derivatization), reinforcing the necessity of LC-based analytical instruments [38].

EI is a powerful and highly molecular informative technique. Compared to ESI and other atmospheric pressure ionization (API) techniques, EI is a hard-ionization mode that provides characteristics of mass spectra, with highly reproducible fragmentation patterns, which allows automated analytes identification capabilities via library comparison [37]. Although potent informatics tools based on high-resolution (HR) and tandem ESI–MS have emerged in the last years, the overall performance of EI–MS is still better in most cases. Moreover, as ionization occurs under vacuum conditions, EI–MS offers substantial matrix effects mitigation [24, 37]. Besides, EI can allow the unification of GC and LC in a single instrument.

Due to its molecular information advantages, an efficient hyphenation of LC and EI–MS has been attracting the continuous interest of researchers and instrument manufacturers. Nonetheless, coupling LC to EI–MS is a challenging task because of some incompatibilities between them, such as the liquid nature of the mobile phase—principally when it enters the high-vacuum condition inside the EI ion source—and the high working pressure of LC instruments. However, several LC–EI–MS coupling interfaces have been reported since the 1970s, some of them even commercialized for a period [39, 40]. Nevertheless, it is worth mentioning that such attempts did not achieve the expected success, mainly because of the high mobile phase flow rate used in conventional LC instruments—operating at the range of ml/min [38, 41]. Additionally, the development of other LC-amenable ionization techniques for MS since the 1980s, like the outstanding ESI, hampered, even more, the use and the research focused on the development of LC–EI–MS coupling interfaces [41].

Considering the significant points highlighted for EI–MS, with the well-recognized efficiency of LC in analyzing a broad range of molecules, it was expected that researchers continued insisting on creating a suitable coupling between these techniques. So, things started to change positively with the advent of miniaturized LC, especially capillary and nanoLC. These new modes of LC require significantly lower mobile phase flow rates than those used in conventional LC, favoring a more suitable transition for the LC eluent when entering the EI ionization source. The following sections will present and discuss the most notable achievements in LC–EI–MS interfaces throughout the years, their pros and cons, and detailed contextualization of the topic for the journal audience.

3 | LC–EI–MS COUPLING: INTERFACE DEVELOPMENT AND ADVANCES

The coupling between LC and EI–MS has been studied for several decades to overcome the incompatibility between the techniques. The most challenging aspect is

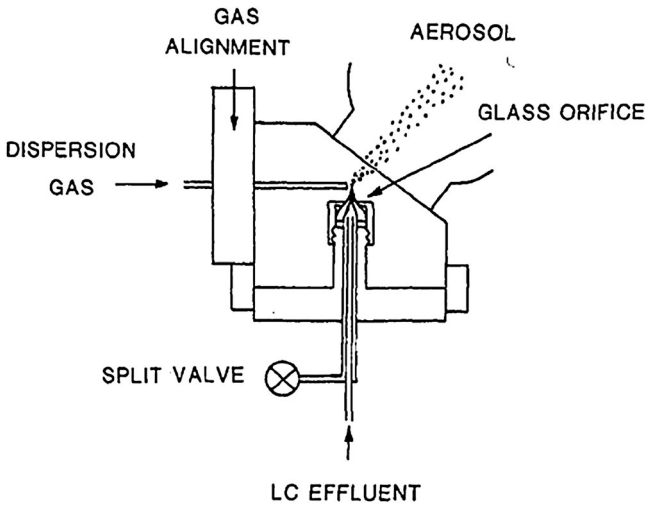

FIGURE 2 (A) MAGIC interface; (B) schematic of the nebulization process at the PB interface. MAGIC, monodisperse aerosol generation interface for chromatography; PB, particle beam interface. *Source*: (A) Copyright with the permission of the American Chemical Society from Ref. [46]; (B) Reprinted with the permission of Ref. [47]. Copyright (2001) John Wiley & Sons, Inc

the incompatibility between the LC mobile phase and the high-vacuum condition of EI–MS [40, 42]. The pioneer columns developed for LC operated at flow rates in the ml/min, which is enough to break the vacuum, making the LC–EI–MS coupling unfeasible. However, advances in the miniaturization of LC (reduction of the internal diameter of analytical columns) are turning this hyphenation increasingly possible.

The history of the coupling between LC and EI–MS consists of a series of interfaces developed to introduce the LC effluent into the EI ionization source. The first attempt dates back to 1960, with the work of Tal'roze [43], who proposed a direct LC–EI–MS coupling. However, this first approach was unsuccessful [40]. In the 1970s, the first commercial interface, called moving belt (MB) [44, 45], was proposed. In this case, the LC eluent is sprayed onto the surface of a belt, where it evaporates at atmospheric pressure. The analytes present on the belt are transferred to the ionization source (EI–MS) assisted by subsequent vacuum chambers. Upon reaching the source, they are heated and volatilized for later ionization. The MB interface was commercialized until around the 1980s, despite several drawbacks reported, such as significant carryover, applicability only for compounds with a boiling point above 300°C, and poor mechanical resistance.

In 1984, Willoughby and Browner proposed a new interface based on a monodisperse aerosol generation interface for LC (MAGIC) (Figure 2A) [46]. This interface was designed with the same purpose as MG—removing the mobile phase from the LC before introducing the analytes into the EI source. In short, the LC effluent at a mobile phase flow rate of around 0.1–0.5-ml/min passes through a small-diameter glass orifice to generate a fine liquid jet. This liquid jet is broken by natural Rayleigh forces, forming uniform drops (aerosol), which are dispersed by a gas flow toward the desolvation chamber. The solvent evaporates at atmospheric pressure, and then the analyte particles are introduced into the EI–MS, assisted by a multistage moment separator [37].

MAGIC is considered a prototype for the particle beam interface (PB), widely used during the 1990s [40, 47]. It is worth mentioning that PB results from the technical evolution of the previous MAGIC interface and the methods it was based upon. In short, PB comprises a nebulizer—in which the aerosol is formed—the desolvation chamber, and the multistage separator. The generation of aerosol in the nebulizer (thermal and pneumatic type) occurs spontaneously by combining an adequate mobile phase flow rate and physical dimensions of the fused silica capillaries. In general, these capillaries had internal diameters smaller than 50 μm, acting as the tip of the nebulizer, where the aerosol was generated (Figure 2B) [47, 48]. Conversely, in the MAGIC interface, this aerosol was formed by the instability of the tiny liquid jet.

The PB interface was a significant advance for coupling LC and EI–MS. It presented simplicity, reliability, and diversity of applications and principally assisted in providing good quality mass spectra for the structural identification of unknown compounds [47]. However, the technique was again limited to compounds with some volatility and thermal stability. Additionally, PB showed poor linear range, low reproducibility and sensitivity for polar compounds, and nonworking conditions when mobile phases with high water content were employed, leading to incomplete desolvation of target compounds [49].

Considering these limitations, Cappiello and Bruner developed in 1993 a PB-based interface for operating at micro-flow rates, known as Cap-EI, also known as micro-PB [50]. In this case, micro-LC columns worked with mobile phase flow rates between 1 and 5 μl/min [51]—an order of magnitude lower than that employed for PB. Cap-EI is very similar to PB, keeping the same design. However, some adaptations were made in the nebulizer to overcome the problems of poor linear range and sensitivity [52]. Therefore, a high-velocity gas flow (helium or nitrogen) was introduced coaxially with the flow of the analytical column eluent, generating a pneumatic nebulization. Through this configuration, Cap-EI generates a fine and homogeneous aerosol with smaller particles than PB, making the analytes more concentrated before entering the ionization source. In addition, the aerosol droplets are smaller because the gas present in the

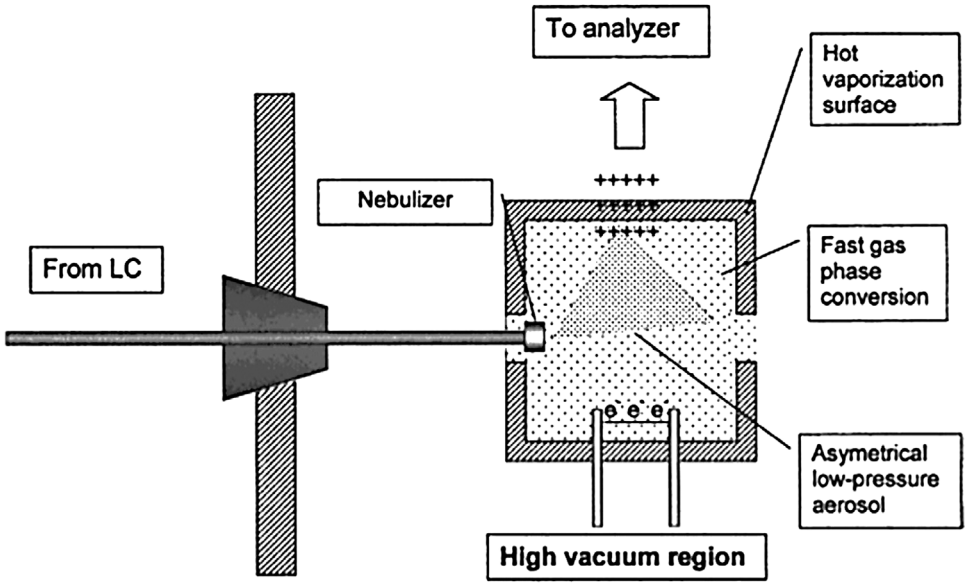

FIGURE 3 Direct-EI interface proposed by Cappiello. EI, electron ionization. *Source*: Reprinted with the permission of Ref. [52]. Copyright (2001) John Wiley & Sons, Inc

nebulizer is forced through a ring-shaped restriction, which increases its velocity, facilitating the fractionation of the LC effluent [52].

Several works have been proposed with Cap-EI, presenting satisfactory results in terms of reproducibility, sensitivity, and selectivity [24]. Another significant advance brought by Cap-EI was the possibility of using buffers as mobile phase additives, and other modifiers, without compromising the ionization of the analytes [53]. The merits of this interface were demonstrated in the analysis of several classes of compounds such as coumarins [54]; drugs and hormones [53]; acidic, basic, and neutral pesticides [55–57], phenols [58]; aflatoxins [59]; and explosives [60] in different matrices.

From another approach, an alternative interface was proposed by Amirav and Granot, known as supersonic molecular beam or Cold-EI MS [61–64]. This interface follows a different perspective from the interfaces proposed so far. In Cold-EI, the LC eluate is vaporized in a deactivated glass tube thermally insulated by an aluminum cooling block. This vaporization process takes place at a temperature of 300°C. Then, the sample is transferred with helium or nitrogen gas to a supersonic nozzle through a 300-μm fused silica capillary. In this supersonic nozzle, the vibrational cooling of the analytes takes place, which is subsequently ionized in the EI source—in this case, as vibrationally cold molecules. The advantage of Cold-EI is that it generates a mass spectrum with little fragmentation and a well-defined molecular ion, which is very useful for identification purposes. According to the Amirav Research Group, Cold-EI is not a complementary ion source to standard EI, but it is superior to standard EI. Cold-EI produces conventional EI mass spectra with improved molecular ions, enhancing the detectability and identification capabilities. Besides, Cold-EI possesses a wide range of analyzable compounds, including heavier molecules, and can also reduce ion source–related degradation or peak tailing problems [65].

Following technological advances in LC miniaturization, the Direct-EI interface appeared in the early 2000s due to the work of Professor Cappiello. Although the Cap-EI interface uses micro-LC columns, Direct-EI employs nanoLC columns, operating in mobile phase flow rates between 100 and 400 nl/min [49, 66]. Direct-EI (Figure 3) receives this designation because the LC effluent is introduced directly into the EI source without external devices [42]. Therefore, this new advance guarantee simplicity, increased sensitivity, reproducibility, low detection limits, linearity, and a wide application range for low-to-medium molecular weight compounds. According to Cappiello's studies [49] using caffeine analytical standards, propanil, and vitamin K, linearity data were obtained with a correlation coefficient equivalent to $R = 0.998$. The reproducibility evaluated for consecutive injections on the same day showed a relative standard deviation of 8%, 3.8%, and 7.4%, respectively, and the limit of detection was in the order of 0.1, 0.05, and 0.1 ng/L.

Direct-EI is an interface that transfers the analytical column effluent into the ionization source through a fused silica capillary of 25 or 50-μm i.d. Like the interfaces already discussed, Direct-EI follows the same principles: nebulization of the eluate, with subsequent formation of an aerosol

(under high-vacuum conditions), followed by rapid solvent desolvation, solute volatilization, and ionization. Therefore, it is a compact and straightforward technique [67].

In several works proposed by Cappiello to understand the Direct-EI, it was observed that the temperature of the ionization source (between 150 and 300°C) is an essential factor in promoting the volatilization of analytes and avoiding the freezing of the LC effluent in the nebulizer. Furthermore, experimental data show that lower mobile flow rates lead to a higher signal-to-noise ratio and improved ionization efficiency. An explanation for this can be that the existence of fewer solvent molecules reduces the competition of interfering molecules with the analyte for ionizable regions in the ionization chamber. Therefore, the maximum mobile phase flow rate that the interface supports is approximately 1.5 µl/min. Then, the solvent molecules can compromise the ionization of the analytes. As a consequence, the EI spectra may show chemical ionization interferences [51]. In addition, the composition of the mobile phase was another analyzed parameter as the surface tension and volatility of the mobile phase can compromise the evaporation and quality of the aerosol. Fortunately, Direct-EI tolerates the most frequently used mixtures of MeCN/H_2O, MeOH/H_2O, buffers, and other additives used to facilitate ionization.

Direct-EI enables the analysis of target molecules hard to be ionized by API (LC–API–MS), or those requiring derivatization steps for being analyzed through GC–MS, for example. Therefore, Direct-EI LC–MS becomes an alternative to these difficulties encountered, having already been applied by Cappiello in analyzing organochlorine pesticides [68, 69] and boronic acids [48]. In short, Direct-EI enables the unification of LC and EI advantages for analyzing specific compounds.

Termopoli and coworkers more recently introduced a new interface [70] called liquid EI (LEI). This new interface was developed through a modern approach, aiming to overcome some challenges of Direct-EI, which, despite its excellent contributions to the advancement of LC–EI–MS coupling, still have limitations: (i) The analysis of compounds at low concentration levels in complex matrices is still challenging; (ii) capillaries in the interface are susceptible to blockages by premature solvent evaporation, as the nebulization and vaporization process occurs within the ion source; (iii) undesired adsorption and thermal degradation over the metallic surface of the ion source lead to peak broadening; (iv) interferences in the EI spectrum due to chemical ionization; and (v) reduced chromatographic response.

Therefore, LEI was proposed recently, offering a new approach for fast converting the eluate from the liquid to the gaseous phase. The new interface comprises a liquid–gas connector, a cooling gap, and a liquid-to-gas conversion zone called a micro-channel of vaporization (Figure 4) [71]. The analytical column eluate is introduced into the liquid–gas connector via an inlet capillary with an internal diameter of 25–50 µm. Inside this device, the mixture between the mobile phase and the helium gas takes place, which will help in the vaporization of the sample and transport it to the ion source. This inlet capillary will connect to the micro-channel of vaporization, passing through the cooling gap (fused silica capillary up to 5 cm in length). The gap prevents the heat from the micro-channel from diffusing to the previous region, where the gas–liquid connector is located.

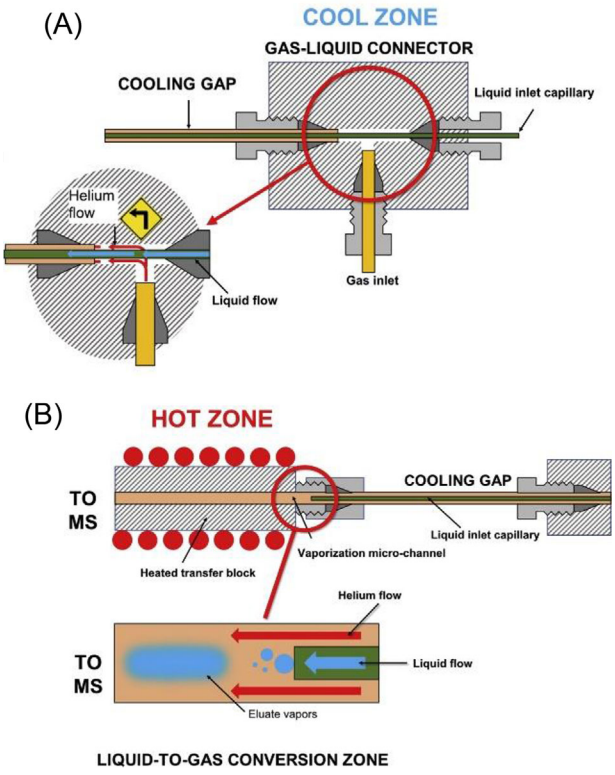

FIGURE 4 Detailed illustration of LEI interface proposed by Termopoli et al.: (A) liquid–gas connector placed in the cold zone; (B) cooling gap and liquid-to-gas conversion zone called a micro-channel of vaporization, where the hot zone starts, just before EI–MS entrance. EI, electron ionization; LEI, liquid electron ionization; MS, mass spectrometry. *Source*: Reprinted with the permission of Ref. [71]. Copyright (2019) Elsevier

The micro-channel of vaporization receives this denomination, as it is a very narrow fused silica capillary and heated to a high temperature of 400°C. The inlet capillary is introduced 2 mm into this micro-channel, and the eluate is vaporized upon contacting the heated inner surface and then forwarded to the high-vacuum ionization source [71]. As it is a new interface, few LEI-based works are reported in the literature. So, there is a need to explore this interface better, mainly because future perspectives

and new developments are driven by advances in nanoLC, which is the current basis for hyphenation between LC and EI.

4 | EI–MS: QUO VADIS?

Nowadays, EI excels as a feasible ionization technique for GC–MS and LC–MS. Coupled with GC, EI–MS is a mature technique, and its merits in analyzing molecules with low-to-medium polarity and molecular weights up to ≈1000 Da have been demonstrated for more than 50 years. Of note, GC–EI–MS is a well-consolidated technique that hardly visualizes future lines of advancement in this area.

EI performance is affected by the design and operational mechanisms of the source. For this reason, EI sources have evolved in the last 70 years to become more efficient and sensitive. However, to the best of our knowledge, there is no modern literature on the design of the EI source, and developments in EI–MS sources are mainly communicated in patents. In brief, the performance of the EI–MS source depends on (i) the current supplied to the filament to heat it to incandescent (filament current), (ii) the rate of electron emission from the filament (emission current), and (iii) the number of electrons available in the chamber for ionization (ionizing current) and frequently can be expressed as the sample ion current (I^+), which is a measure of the ionization rate:

$$I^+ = \beta Q_i L\,[N]\,I_e \tag{7}$$

where β is the extraction efficiency, Q_i is the total ionizing cross section, L is the effective ionizing path length, $[N]$ the concentration of the sample molecules, and I_e the ionizing current. Q_i depends on the molecular structure of the analyte and is the reason by which the standard EI spectra are obtained with electron beans of 70 eV of energy. De Broglie's wavelength of the electrons with the energy around 70 eV matches the average length of most of the covalent bonds in organic molecules (~ 0.14 nm), so energy transference is very efficient. Furthermore, around 70-V electron kinetic energy, small electron velocity changes do not significantly impact the ionization efficiency.

The other parameters in the previous equation depend on other experimental factors: β improves by increasing the repeller and acceleration voltage; L is inversely proportional to the magnetic field and can be increased by using a weak magnetic field. I_e is considered the most crucial parameter to enhance the sample ion current and depends on the source's current filament and geometrical characteristics [72].

From the instrumental point of view, the EI source's performance depends on the electron–molecule interactions and the capability to transfer ions to the mass analyzer [73]. EI sources' sizes have been drastically reduced, becoming more efficient in the generation and transference of ions, so that EI–MS sensitivity has been improving by one order of magnitude in the last years [74]. In addition, compact sources are easier to pump, and the analytes are introduced and removed faster, so the extraction of the ions into the analyzer occurs more efficiently. The illuminated volume has also been improved by increasing the number of electron entrances or incorporating multiple filaments. EI source manufacturers also have looked for more inert materials to minimize the analyte's surface adsorption, reducing the noise and providing more robustness and sensitivity. In addition, more efficient heating systems (such as the dual heater design) have been incorporated to prevent condensation and adsorption of the sample molecules onto the ion volume, lens stack, and RF lens, preventing contamination [73].

In addition, modern EI sources are compact, quickly assembled, and replaceable for exchange and cleaning without breaking high-vacuum conditions. Thanks to those developments in EI sources miniaturization—associated with the developments on low-thermal mass GC systems, smaller high-performance batteries, and the advances in instrumentation miniaturization, in general—several GC–EI–MS techniques exist currently on the market, and almost all the GC–MS manufacturers have their portable GC–MS for on-field applications. To increase detection and identification capabilities, most of the EI–MS instrument manufacturers have dedicated themselves to the development of multimode sources, combining various ionization modes, such as EI, positive chemical ionization, and negative chemical ionization in one easy-to-use source [75]. Modern EI–MS sources allow the ionization mode via software, in a single click, and with no instrumental adjustment. Besides, multimode sources merging EI or CI with single-photon ionization in one instrument have also been described as an alternative for acquiring orthogonal structural information for target compounds [76, 77].

Perhaps, the most outstanding advantage of the EI–MS is its unparalleled capability to generate automated searchable and comparable mass spectra for fast and confident analyte identification. However, in treating very complex samples, the limited resolving power of the separation techniques—even with two-dimensional approaches—does not allow the maximum utilization of EI–MS identification capabilities. Hence, EI–MS data analysis benefits from informatics tools and machine learning approaches that allow deconvoluting mass spectra of overlapped chromatographic peaks [78]. Current developments focus on simulating in silico mass spectra for comparison purposes or [79] performing molecular networks of full scan GC–MS

data for improved annotation/identification of unknown compounds in complex samples [80]. Those tools are now expanding the boundaries of the untargeted studies, and although their applications are based on the GC–EI–MS analysis, their eventual association to the nanoLC–EI–MS advances could bring new insights in LC–MS analysis.

Coupled with nanoLC, EI–MS expands the range of applicability of the LC–MS, allowing the analysis of non-ESI ionizable compounds and even exceeding the range of applicability of the atmosphere pressure chemical ionization and atmosphere pressure photoionization. In addition, EI–MS can ionize polar and nonpolar compounds. Therefore, nanoLC–EI–MS has the potential to enable the simultaneous analysis of non-GC and non-ESI compounds. For example, apolar compounds can be analyzed via GC–MS but hardly via LC–ESI–MS. Without previous derivatization, some thermolabile compounds can be analyzed by LC–ESI–MS but not via GC–MS. The analysis of mixtures containing nonpolar and thermolabile compounds would not be feasible by GC–MS or LC–ESI–MS but could be done by nanoLC–EI–MS.

Direct-EI and LEI are the more straightforward and promising alternatives to nanoLC–EI–MS interfacing. Direct-EI does not require major instrumental modifications and can easily be adapted to any GC–MS instrument by substituting the 100-μm transfer tube with a ≤25-μm i.d. capillary [49, 81]. The applicability of this interface has been explored in the last 20 years with relevant results in target and untargeted studies, demonstrating a significant mitigation of the ionization suppression or enhancement effects due to the matrix effects. Besides, Direct-EI has demonstrated excellent suitability for developing portable nanoLC–EI–MS instruments for infield analysis [82]. Nevertheless, Direct-EI is not yet a robust enough interface for routine applications. Premature solvent evaporation, analytes precipitation, and water-freezing frequently clog the transference capillary, requiring vacuum breaks for tube substitution. Applications of Direct-EI are still limited to some classes of compounds, including pesticides [83], hormones [81], boronic acids [48], fatty acids [84], vitamin K [49], a few pharmaceuticals [85], and some opioids [82].

The use of transference tubes with a small i.d. (<10 μm) could expand the applicability of this interface and improve its detection limits. However, that approach can also entail a considerable increase in the backpressure of the system and more specialized connection hardware. Perhaps for those reasons, to the better of our knowledge, no reports describe the use of very narrow capillaries for nanoLC–EI–MS interfacing via Direct-EI. An alternative could come from using open tubular (OT) LC [29]. At the moment, all the descriptions of Direct-EI interfacing published rely on nanoLC-packed columns. However, OT columns do not require interfacing tubes and can be inserted directly into the ionization source. Recently, a series of OTLC columns with an i.d. of <10 μm—including columns with 2.0-μm i.d. able to work at pl/min flow rates—have been introduced, demonstrating high peak capacity and performance for proteomics [86, 87]. The coupling of those columns directly on the EI–MS source, with zero dead volume contribution, and the significant reduction of the mobile phase flow rate up to the pl/min scale has the potential to make the LC–EI–MS interfacing finally competitive with GC–MS and LC–ESI–MS, providing improved detectability and a more extended range of applicability.

LEI is the modern and more advanced approach for nanoLC–EI–MS interfacing, and its developers foresee that interface could be commercially available shortly. Despite being a more complex interface than Direct-EI, LEI was designed to be easily adaptable to any GC–MS instrument, with minor instrumental modifications and no contribution to band broadening or any notable alteration of the mass spectra. Like Direct-EI, LEI generates reproducible and library comparable EI spectra for automated identification purposes, but with superior sensitivity, a range of applications, and robustness. In addition, LC–LEI–MS provides mass spectra comparable with the obtained ones via GC–MS but in a more extensive range of polarity and molecular weights.

The liquid-to-gas analytes transference in the LEI process relies on a pneumatic vaporization micro-channel that can be heated up to 400°C, which, although designed for fast heat transference and liquid phase vaporization, can be susceptible to thermal degradation of thermolabile analytes, limiting, to some extent, the applicability of the interface. Future research in LEI could find a faster and more efficient vaporization mechanism that avoids thermal degradation and enlarges the range of applicability to thermolabile and larger molecules.

The potential of the Direct-EI and the LEI to provide matrix-effect-free MS analysis generates the opportunity to develop fast methods for direct injection of raw samples without previous chromatographic separation, similarly as performed in ambient ionization MS. Direct insertion probes for introducing solids into EI–MS have been available since the mid-1960s, and it is an available option in most modern GC–MS instruments [88]. Direct insertion probes are stainless steel shafts that allow the insertion of a few micrograms of analytes without EI–MS vacuum breaking. The analyte can be introduced into a sample vial or crucible from which evaporates or sublimes into the ion source or as a solution or suspension applied over a thin wire loop or pin, directly exposed to the electron beam [88].

Direct-EI and LEI could become complementary tools for the direct introduction of liquid samples without prejudice of the filament time life or instrument wellness. This approach has been explored by the Cappiello Research Group in recent years, demonstrating to be a competitive strategy for the unequivocal detection of target compounds via selected ion monitoring (SIM) or multiple reaction monitoring [89, 90]. In this way, fast, reliable, matrix-effects-free, and sensitive methods for quantitative determinations were obtained. Furthermore, EI–MS in SIM or full scan modes could represent a cheaper and more straightforward alternative for targeted studies via direct sample introduction than tandem (MS/MS) or HR MS.

In the studies of the Cappiello Research Group on direct sample introduction, samples were pumped to the EI–MS source using flow injection analysis (FIA) systems or high-performance liquid chromatography pumps. Bear in mind that those systems dispense the use of the chromatographic column, and then the backpressure becomes negligible; it is worth asking if it is possible to develop EI–MS systems for direct sample introduction that uses the MS vacuum pump to propel the sample into ionization source? That approach could significantly reduce the instrumental requirements, enabling the development of cheap, fast, and miniaturized EI–MS-based systems (even in a chip format). Developing those external pumps free systems could be an exciting research topic in the future of EI–MS.

Finally, one of the most outstanding characteristics of the EI–MS is its potential to allow the coexistence of GC and LC—and even supercritical fluid chromatography—in a single instrument. Unified chromatography has long been hypothesized, and developing an instrument liable to perform gas and liquid analysis is a current goal for academics and instrument manufacturers [91]. Interfaces such as LEI and Cold-EI—or Direct-EI with packed columns—easily turn a GC–MS into an LC–MS, compatible with both chromatography modes. Cold-EI was developed as a GC–MS interface liable to enhance molecular ions and improve the identification potentialities [92] and then explored in LC–EI–MS [63]. Cold-EI allows combining GC and LC techniques by integrating two instruments and easy switching between GC and LC. Also, LEI could allow the integration of GC–MS and LC–MS without major instrumental modifications. For example, the effluent of the GC columns could be used as a nebulization gas line in nanoLC–ELI–MS mode. Hence coupling a nanoLC and a GC instrument, the same chromatographic modes will be available in the same instruments.

Recently, the Amirav Research Group introduced an instrument that combines GC–EI–MS and LC–EI–MS [93]. The system quickly switches between the two modes from the same software without any instrumental modification, even allowing GC–MS and LC–MS data acquisition in the same chromatogram and using conventional or Cold-EI. Despite having high concentrations, the authors demonstrated the possibility to acquire highly reproducible and comparable EI spectra via GC–MS and LC–MS (Figure 5). Unified GC/LC instruments could reduce costs in analytical facilities and bring new insights into methods development, such as exploiting temperature gradient in LC separations.

Finally, beyond the coupling with GC and LC, modern GC–EI–MS instruments are equipped with sample probes that allow the direct introduction of solid samples and low-to-medium boiling liquids, expanding considerably the range of applicability of this technique for characterization, elucidation, and identification of unknown compounds [24].

5 | CONCLUDING REMARKS

EI was the first ionization technique developed for MS analysis. The technique was created at the beginning of the 20th century, and its coupling with GC at the end of the 1960s was a significant milestone for developing the modern analytical sciences. This boosted the consolidation of GC–MS as a robust and routine analytical technique faster than LC–MS. Nowadays, EI is the most used ionization technique for GC–MS and provides some advantages compared to other ionization techniques available. EI is a hard ionization technique that provides highly reproducible mass spectra, allowing the automated identification of the analytes by spectra comparison. Even in the absence of reference spectra, EI–MS can provide more structural information that the obtained via ESI with HR or tandem MS analyzers. Unlike the API techniques, the EI process does not rely on the analytes' polarity nor acid/basic character so that EI can allow the analysis of molecules in a range of polarity superior to other currently available ionization techniques. According to Cappiello, polar and nonpolar compounds—such as sugars and hydrocarbons, respectively—could be simultaneously analyzed by EI–MS in a single run [94].

Because EI–MS takes place under vacuum conditions, the ionization process and the recorded mass spectra are not affected by the matrix effect. For this reason, LC–EI–MS-effective coupling has been a significant focus for many analytical chemists. Although hindered in the past due to the incompatibility between the techniques, current developments in nanoLC make the LC–EI–MS coupling a feasible idea. Nowadays, interfaces such as Cold-EI, Direct-EI, and LEI are showing excellent performance combined with nanoLC, even producing EI spectra comparable to those obtained via GC–MS. Due to these

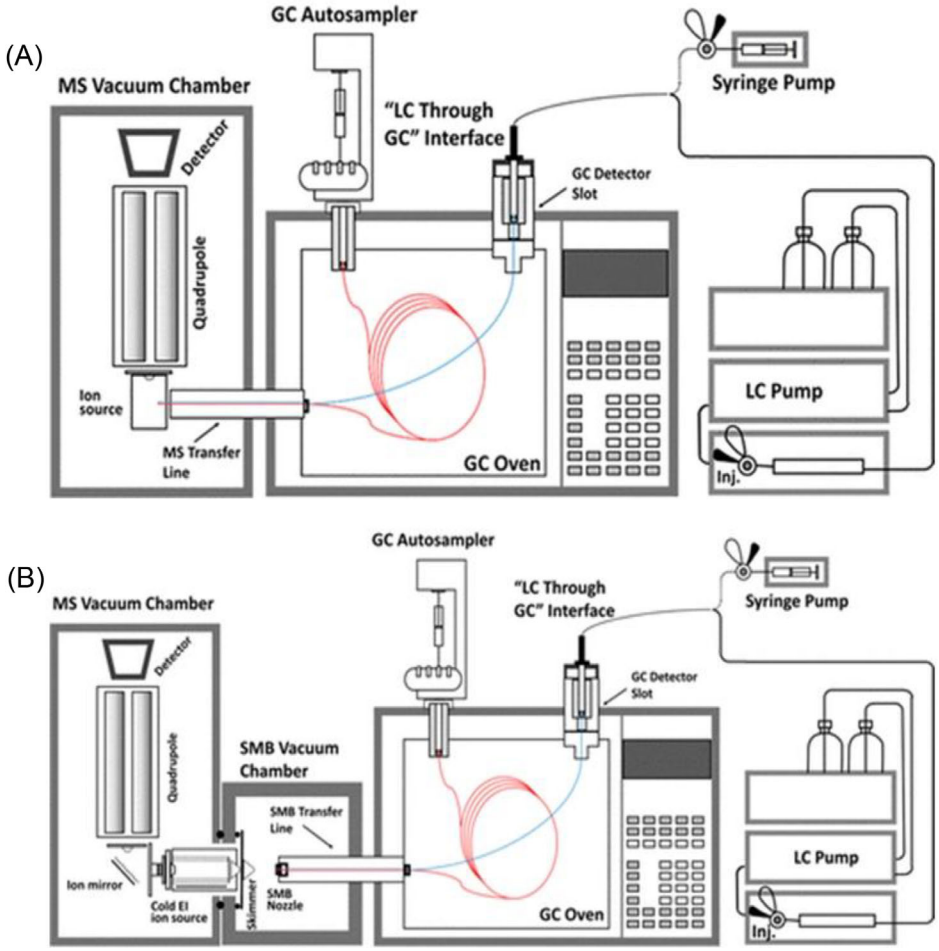

FIGURE 5 Schematic illustration of the unified GC–MS and LC–MS, employing (A) conventional EI–MS and (B) Cold EI–MS. EI, electron ionization; GC, gas chromatography; LC, liquid chromatography; MC, mass spectrometry. *Source*: Reprinted with the permission of Ref. [93]. Copyright (2020), American Society for Mass Spectrometry

developments, now EI–MS has the potential to allow the coexistence of GC and LC—and even supercritical fluid chromatography—in a single instrument. Furthermore, EI–MS can simultaneously analyze LC and GC amenable compounds, and interfaces such as Cold-EI, Direct-EI, and LEI can operate with gas or liquid mobile phase, enabling an integration of the nanoLC and GC instruments and the switching between techniques without major instrumental modifications. In the near future, we will probably see unified chromatography systems employing EI as the main ionization mode.

ACKNOWLEDGMENTS

The authors are grateful to the Coordenação de Aperfeiçoamento de Pessoal de Nível Superior—Brazil (CAPES)—Finance Code 001; to FAPESP (Grant nos. 2019/22724-7, 2017/02147-0, 2019/26263-4, 2015/15462-5, 2014/03765-0, and 2014/07347-9); and to CNPq (307293/2014-9 and 308843/2019-3) for the financial support provided for this research and to our laboratory.

CONFLICT OF INTEREST

The authors have declared no conflict of interest.

AUTHOR CONTRIBUTION

Deyber Arley Vargas Medina: conceptualization, writing—original draft,
Edvaldo Vasconcelos Soares Maciel: conceptualization, writing—original draft,
Fernando Mauro Lanças: funding, supervision, writing—original draft,
Natalia Gabrielly Pereira dos Santos: conceptualization, writing—original draft.

DATA AVAILABILITY STATEMENT

The data that support the findings of this study are available from the corresponding author upon reasonable request.

ORCID

Fernando Mauro Lanças https://orcid.org/0000-0002-8711-5905

REFERENCES

1. Beynon JH, Morgan RP. The development of mass spectroscopy: an historical account. Int J Mass Spectrom Ion Phys. 1978;27(1):1–30.
2. Thomson JJ. XIX. Further experiments on positive rays. London, Edinburgh, Dublin Philos Mag J Sci. 1912;24(140):209–53.
3. Morris PJT. From classical to modern chemistry: the instrumental revolution. In: Morris PJT, editor. From classical to modern chemistry: the instrumental revolution. Cambridge: Royal Society of Chemistry in association with the Science Museum; 2002.
4. Traeger JC. The development of electron ionization. In: The encyclopedia of mass spectrometry. Amsterdam: Elsevier; 2016. p. 77–82.
5. Smyth DH. A new method for studying ionising potentials. Proc R Soc London, Ser A Contain Pap Math Phys Character. 1922;102(716):283–93.
6. Bleakney W. A new method of positive ray analysis and its application to the measurement of ionization potentials in mercury vapor. Phys Rev. 1929;34(1):157–60.
7. Smith LP, Scott GW. Conditions for producing intense ionic beams. Phys Rev. 1939;55(10):946–53.
8. Scott GW. Focused beam source of hydrogen and helium ions. Phys Rev. 1939;55(10):954–9.
9. Finkelstein AT. A high efficiency ion source. Rev Sci Instrum. 1940;11(3):94–7.
10. Brink GO. Electron bombardment molecular beam detector. Rev Sci Instrum. 1966;37(7):857–60.
11. Nier AO. A mass spectrometer for routine isotope abundance measurements. Rev Sci Instrum. 1940;11(7):212–6.
12. Nier AO. A mass spectrometer for isotope and gas analysis. Rev Sci Instrum. 1947;18(6):398–411.
13. Coggeshall ND, Jordan EB. An experimental mass spectrometer. Rev Sci Instrum. 1943;14(5):125–9.
14. Clarke EM. Ionization probability curves using an electron selector: results on N_2^+, N^+, Xe^{++}. Can J Phys. 1954;32(12):764–74.
15. Marmet P, Kerwin L. An improved electrostatic electron selector. Can J Phys. 1960;38(6):787–96.
16. Simpson JA. High resolution, low energy electron spectrometer. Rev Sci Instrum. 1964;35(12):1698–704.
17. Kuyatt CE, Simpson JA. Electron monochromator design. Rev Sci Instrum. 1967;38(1):103–11.
18. Fox RE, Hickam WM, Grove DJ, Kjeldaas T. Ionization in a mass spectrometer by monoenergetic electrons. Rev Sci Instrum. 1955;26(12):1101–7.
19. Liebmann G. An improved method of numerical ray tracing through electron lenses. Proc Phys Soc Sect B. 1949;62(12):753–72.
20. Dahl DA. SIMION for the personal computer in reflection. Int J Mass Spectrom. 2000;200(1–3):3–25.
21. Werner HW. A study of a mass spectrometer ion source by means of computer-calculated ion trajectories. J Phys E. 1974;7(2):115–21.
22. Harvey DJ. Mass spectrometric detectors for gas chromatography. In: Gas chromatography. Amsterdam: Elsevier; 2021. p. 399–424.
23. Gross JH. Electron ionization and chemical ionization. In: Reference module in chemistry, molecular sciences and chemical engineering. Amsterdam: Elsevier; 2018.
24. Vargas Medina DA, Soares Maciel EV, Lúcia de Toffoli A, Lanças FM. Miniaturization of liquid chromatography coupled to mass spectrometry. 2. Achievements on modern instrumentation for miniaturized liquid chromatography coupled to mass spectrometry. TrAC Trends Anal Chem. 2020;128:115910.
25. Lifshitz C, Märk TD. Mass spectrometry, ionization theory. In: Encyclopedia of spectroscopy and spectrometry. Amsterdam: Elsevier; 2017. p. 748–57.
26. Versluis C, Staaij AVD, Stokvis E, Heck AJR, Craene BD. Metastable ion formation and disparate charge separation in the gas-phase dissection. J Am Soc Mass Spectrom. 2001;305(00):329–36
27. Mirsaleh-Kohan N, Robertson WD, Compton RN. Electron ionization time-of-flight mass spectrometry: historical review and current applications. Mass Spectrom Rev. 2008;27(3):237–85.
28. Munro JJ, Harrison S, Fujimoto MM, Tennyson J. A dissociative electron attachment cross-section estimator. J Phys Conf Ser. 2012;388(PART 1).
29. Vargas Medina DA, Pereira Dos Santos NG, Da Silva Burato JS, Borsatto JVB, Lanças FM. An overview of open tubular liquid chromatography with a focus on the coupling with mass spectrometry for the analysis of small molecules. J Chromatogr A. 2021;1641:461989.
30. Ryhage R. Use of a mass spectrometer as a detector and analyzer for effluent emerging from high temperature gas liquid chromatography columns. Anal Chem. 1964;36(4):759–64.
31. Simpson CF, Gough TA. Gas chromatography – mass spectroscopy interfacial systems. CRC Crit Rev Anal Chem. 1972;3(1):1–40.
32. Fock W. Gas chromatograph/mass spectrometer interface. Analysis of the molecular effusion separator. Anal Chem. 1975;47(14):2447–50.
33. Gruber B, David F, Sandra P. Capillary gas chromatography-mass spectrometry: current trends and perspectives. TrAC – Trends Anal Chem. 2020;124:115475.
34. Jordan-Sinisterra M, Lanças FM. Microextraction by packed sorbent of selected pesticides in coffee samples employing ionic liquids supported on graphene nanosheets as extraction phase. Anal Bioanal Chem. 2022;414:413–23.
35. Alsenedi KA, Morrison C. Determination and long-term stability of twenty-nine cathinones and amphetamine-type stimulants (ATS) in urine using gas chromatography – mass spectrometry. J Chromatogr B. 2018;1076:91–102.
36. Rontani J-F. Use of gas chromatography-mass spectrometry techniques (GC-MS, GC-MS/MS and GC-QTOF) for the characterization of photooxidation and autoxidation products of lipids of autotrophic organisms in environmental samples. Molecules. 2022;27(5):1629.
37. Rigano F, Tranchida PQ, Dugo P, Mondello L. High-performance liquid chromatography combined with electron ionization mass spectrometry: a review. TrAC – Trends Anal Chem. 2019;118:112–22.
38. Snyder JW, Kirkland JJ, Dolan JJ. Introduction to modern liquid chromatography, third edition. J Am Soc Mass Spectrom. 2011;22(1):196.
39. Abian J. The coupling of gas and liquid chromatography with mass spectrometry. J Mass Spectrom. 1999;34(3):157–68.

40. Famiglini G, Palma P, Termopoli V, Cappiello A. The history of electron ionization in LC-MS, from the early days to modern technologies: a review. Anal Chim Acta. 2021;1167:338350.
41. Niessen WMA. Progress in liquid chromatography – mass spectrometry instrumentation and its impact on high-throughput screening. J Chromatogr A. 2003;1000(1–2):413–36.
42. Palma P, Famiglini G, Trufelli H, Pierini E, Termopoli V, Cappiello A. Electron ionization in LC-MS: recent developments and applications of the direct-EI LC-MS interface. Anal Bioanal Chem. 2011;399(8):2683–93.
43. Tal'roze VL, Karpov GV, Gordetskii IG, Vladimir S. Capillary systems for the introduction of liquid mixtures into an analytical mass spectrometer. Russ J Phys Chem. 1968;42: 1658–64.
44. Mcfadden WH, Schwartz HL, Evans S. Direct analysis of liquid chromatographic effluents. J Chromatogr A. 1976;122(C):389–96.
45. Hayes MJ, Lankmayer EP, Vouros P, Karger BL, Mcguire JM. Moving belt interface with spray deposition for liquid chromatography/mass spectrometry. Anal Chem. 1983;55(11):1745–52.
46. Willoughby RC, Browner RF. Monodisperse aerosol generation interface for combining liquid chromatography with mass spectroscopy. Anal Chem. 1984;56(14):2626–31.
47. Cappiello A. Is particle beam an up-to-date LC-MS interface? State of the art and perspectives. Mass Spectrom Rev. 1996;15(5):283–96.
48. Flender C, Leonhard P, Wolf C, Fritzsche M, Karas M. Analysis of boronic acids by nano liquid chromatography-direct electron ionization mass spectrometry. Anal Chem. 2010;82(10):4194–200.
49. Cappiello A, Famiglini G, Mangani F, Palma P. A simple approach for coupling liquid chromatography and electron ionization mass spectrometry. Am Soc Mass Spectrom. 2002;13(01):265–73.
50. Cappiello A, Bruner F. Micro flow rate particle beam interface for capillary liquid chromatography/mass spectrometry. Anal Chem. 1993;65(9):1281–7.
51. Cappiello A, Famiglini G, Pierini E, Palma P, Trufelli H. Advanced liquid chromatography-mass spectrometry interface based on electron ionization. Anal Chem. 2007;79(14):5364–72.
52. Cappiello A, Famiglini G, Mangani F, Palma P. New trends in the application of electron ionization to liquid chromatography? mass spectrometry interfacing. Mass Spectrom Rev. 2001;20(2):88–104.
53. Cappiello A, Famiglini G, Rossi L, Magnani M. Use of nonvolatile buffers in liquid chromatography/mass spectrometry: advantages of capillary-scale particle beam interfacing. Anal Chem. 1997;69(24):5136–41.
54. Cappiello A, Famiglini G, Mangani F, Tirillini B. Analysis of coumarins by micro high-performance liquid chromatography-mass spectrometry with a particle beam interface. J Am Soc Mass Spectrom. 1995;6(2):132–9.
55. Cappiello A, Famiglini G, Bruner F. Determination of acidic and basic/neutral pesticides in water with a new microliter flow rate LC/MS particle beam interface. Anal Chem. 1994;66(9):1416–23.
56. Cappiello A, Famiglini G. Analysis of thermally unstable compounds by a liquid chromatography/mass spectrometry particle beam interface with a modified ion source. Anal Chem. 1995;67(2):412–9.
57. Cappiello A, Famiglini G, Mangani F, Angelino S, Gennaro MC. Simultaneous determination of acidic and basic-neutral pesticides in water at ppt concentration level by ion-interaction micro-HPLC/MS. Environ Sci Technol. 1999;33(21):3905–10.
58. Cappiello A, Famiglini G, Mangani F, Careri M, Lombardi P, Mucchino C. Liquid chromatographic-mass spectrometric determination of phenolic compounds using a capillary-scale particle beam interface. J Chromatogr A. 1999;855(2):515–27.
59. Cappiello A, Famiglini G, Tirillini B. Determination of aflatoxins in peanut meal by LC/MS with a particle beam interface. Chromatographia. 1995;40(7–8):411–6.
60. Cappiello A, Famiglini G, Lombardozzi A, Massari A, Vadalà GG. Electron capture ionization of explosives with a microflow rate particle beam interface. J Am Soc Mass Spectrom. 1996;7(8):753–8.
61. Amirav A, Granot O. Liquid chromatography mass spectrometry with supersonic molecular beams. J Am Soc Mass Spectrom. 2000;11(6):587–91.
62. Granot O, Amirav A. LC-MS with electron ionization of cold molecules in supersonic molecular beams. Int J Mass Spectrom. 2005;244(1):15–28.
63. Seemann B, Alon T, Tsizin S, Fialkov AB, Amirav A. Electron ionization LC-MS with supersonic molecular beams-the new concept, benefits and applications. J Mass Spectrom. 2015;50(11):1252–63.
64. Granot O, Amirav A. Electron ionization LC–MS with supersonic molecular beams. Adv LC–MS Instrum. 2007;72:45–64.
65. Amirav A, Fialkov AB, Gordin A, Elkabets O, Margolin Eren KJ. Cold electron ionization (EI) is not a supplementary ion source to standard EI. It is a highly superior replacement ion source. J Am Soc Mass Spectrom. 2021;32(11):2631–5.
66. Famiglini G, Palma P, Termopoli V, Cappiello A, Tsizin S, Seemann B, et al. Electron ionization LC-MS. In: Comprehensive analytical chemistry. Amsterdam: Elsevier Ltd; 2018. p. 1–28.
67. Cappiello A, Famiglini G, Mangani F, Palma P. A simple approach for coupling liquid chromatography and electron ionization mass spectrometry. J Am Soc Mass Spectrom. 2002;13(3):265–73.
68. Famiglini G, Palma P, Termopoli V, Trufelli H, Cappiello A. Single-step LC/MS method for the simultaneous determination of GC-amenable organochlorine and LC-amenable phenoxy acidic pesticides. Anal Chem. 2009;81(17):7373–8.
69. Famiglini G, Palma P, Pierini E, Trufelli H, Cappiello A. Organochlorine pesticides by LC-MS. Anal Chem. 2008;80(9):3445–9.
70. Termopoli V, Famiglini G, Palma P, Piergiovanni M, Cappiello A. Atmospheric pressure vaporization mechanism for coupling a liquid phase with electron ionization mass spectrometry. Anal Chem. 2017;89(3):2049–56.
71. Termopoli V, Famiglini G, Palma P, Piergiovanni M, Rocio-Bautista P, Ottaviani MF, et al. Evaluation of a liquid electron ionization liquid chromatography-mass spectrometry interface. J Chromatogr A. 2019;1591:120–30.
72. Dass C. Fundamentals of contemporary mass spectrometry. Hoboken, NJ: John Wiley & Sons, Inc.; 2007. 591 p.
73. Forum MS. Mass spectrometry forum electron ionization sources : the basics the ion source is the heart of the mass spectrometer. In the ion source, ions are created. 2006;21:14–8.

74. Famiglini G, Palma P, Termopoli V, Cappiello A, Tsizin S, Seemann B, et al. Electron ionization LC-MS: what is it and why use it?. Compr Anal Chem. 2018;79:1–28.
75. Sakamoto Y. Technical Report Usefulness of Smart EI /CI Ion Source Which Enables Both EI and CI Mode Measurements with the Same Ion Source. Available from: https://www.shimadzu.com/an/literature/gcms/jpo218057.html (accessed on 22 February 2022)
76. Schepler C, Sklorz M, Passig J, Famiglini G, Cappiello A, Zimmermann R. Flow injection of liquid samples to a mass spectrometer with ionization under vacuum conditions: a combined ion source for single-photon and electron impact ionization. Anal Bioanal Chem. 2013;405(22):6953–7.
77. Hua L, Wu Q, Hou K, Cui H, Chen P, Wang W, et al. Single photon ionization and chemical ionization combined ion source based on a vacuum ultraviolet lamp for orthogonal acceleration time-of-flight mass spectrometry. Anal Chem. 2011;83(13):5309–16.
78. Behrends V, Tredwell GD, Bundy JG. A software complement to AMDIS for processing GC-MS metabolomic data. Anal Biochem. 2011;415(2):206–8.
79. Ji H, Deng H, Lu H, Zhang Z. Predicting a molecular fingerprint from an electron ionization mass spectrum with deep neural networks. Anal Chem. 2020;92(13):8649–53.
80. Aksenov AA, Laponogov I, Zhang Z, Doran SLF, Belluomo I, Veselkov D, et al. Auto-deconvolution and molecular networking of gas chromatography-mass spectrometry data. Nat Biotechnol. 2021;39(2):169–73.
81. Cappiello A, Famiglini G, Mangani F, Palma P, Siviero A. Nano-high-performance liquid chromatography-electron ionization mass spectrometry approach for environmental analysis. Anal Chim Acta. 2003;493(2):125–36.
82. Abonamah JV, Eckenrode BA, Moini M. On-site detection of fentanyl and its derivatives by field portable nano-liquid chromatography-electron ionization-mass spectrometry (nLC-EI-MS). Forensic Chem. 2019;16:100180.
83. Cappiello A, Famiglini G, Palma P, Mangani F. Trace level determination of organophosphorus pesticides in water with the new direct-electron ionization LC/MS interface. Anal Chem. 2002;74(14):3547–54.
84. Rigano F, Albergamo A, Sciarrone D, Beccaria M, Purcaro G, Mondello L. Nano liquid chromatography directly coupled to electron ionization mass spectrometry for free fatty acid elucidation in mussel. Anal Chem. 2016;88(7):4021–8.
85. Cappiello A, Famiglini G, Palma P, Pierini E, Termopoli V, Trufelli H. Direct-EI in LC-MS: towards a universal detector for small-molecule applications. Mass Spectrom Rev. 2011;30(6):1242–55.
86. Xiang P, Yang Y, Zhao Z, Chen M, Liu S. Ultrafast gradient separation with narrow open tubular liquid chromatography. Anal Chem. 2019;91(16):10738–43.
87. Chen A, Liu S, Yang Y, Xiang P. Liquid chromatographic separation using a 2 μm i.d. open tubular column at elevated temperature. Anal Chem. 2021;93(10):4361–4.
88. Gross JH. Mass spectrometry: a textbook. 2nd ed. Berlin: Springer;2011.
89. Famiglini G, Termopoli V, Palma P, Cappiello A. Liquid chromatography-electron ionization tandem mass spectrometry with the direct-EI interface in the fast determination of diazepam and flunitrazepam in alcoholic beverages. Electrophoresis. 2016;37(7–8):1048–54.
90. Cappiello A, Famiglini G, Palma P, Pierini E, Trufelli H, Maggi C, et al. Application of nano-FIA-Direct-EI-MS to determine diethylene glycol in produced formation water discharges and seawater samples. Chemosphere. 2007;69(4):554–60.
91. Silva MR, Andrade FN, Fumes BH, Lanças FM. Unified chromatography: fundamentals, instrumentation and applications. J Sep Sci. 2015;38:3071–83.
92. Amirav A, Gordin A, Poliak M, Fialkov AB. Gas chromatography-mass spectrometry with supersonic molecular beams. J Mass Spectrom. 2008;43(2):141–63.
93. Tsizin S, Fialkov AB, Amirav A. Electron ionization mass spectrometry for both liquid and gas chromatography in one system without the need for hardware adjustments. J Am Soc Mass Spectrom. 2020;31(8):1713–21.
94. Cappiello A. The benefits of a liquid-electron ionization liquid chromatography – mass spectrometry interface. LCGC. 2019;32(6):330–1.

How to cite this article: Maciel EVS, Pereira dos Santos NG, Vargas Medina DA, Lanças FM. Electron ionization mass spectrometry: Quo vadis?. Electrophoresis. 2022;1–14. https://doi.org/10.1002/elps.202100392

Capítulo 7

Artigo publicado no *Journal of Separation Science,* 2022

Received: 31 March 2023 | Revised: 16 June 2023 | Accepted: 20 June 2023

DOI: 10.1002/jssc.202300214

JOURNAL OF SEPARATION SCIENCE

RESEARCH ARTICLE

Microextraction by packed sorbent of *N*-nitrosamines from Losartan tablets using a high-throughput robot platform followed by liquid chromatography-tandem mass spectrometry

Natalia Gabrielly Pereira dos Santos | **Deyber Arley Vargas Medina** | **Fernando Mauro Lanças**

Sao Carlos Institute of Chemistry, University of Sao Paulo, Sao Carlos, São Paulo, Brazil

Correspondence
Fernando Mauro Lanças, University of Sao Paulo, Sao Carlos Institute of Chemistry, Sao Carlos - SP, Brazil.
Email: flancas@iqsc.usp.br

Funding information
Coordination for the Improvement of Higher Education Personnel; National Council for Scientific and Technological Development, Grant/Award Numbers: 307293/2014-9, 308843/ 2019-3; the São Paulo Research Foundation (FAPESP), Grant/Award Numbers: 2019/22724-7, 2017/02147-0, 2015/15462-5, 2014/07347-9, 2019/26263-4

The development of a fast, cost-effective, and efficient microextraction by packed sorbent setup was achieved by combining affordable laboratory-repackable devices of microextraction with a high-throughput cartesian robot. This setup was evaluated for the development of an analytical method to determine *N*-nitrosamines in losartan tablets. *N*-nitrosamines pose a significant concern in the pharmaceutical market due to their carcinogenic risk, necessitating their control and quantification in pharmaceutical products. The parameters influencing the performance of this sample preparation for *N*-nitrosamines were investigated through both univariate and multivariate experiments. Microextractions were performed using just 5.0 mg of carboxylic acid-modified polystyrene divinylbenzene copolymer as the extraction phase. Under the optimized conditions, the automated setup enabled the simultaneous treatment of six samples in less than 20 min, providing reliable analytical confidence for the proposed application. The analytical performance of the automated high-throughput microextraction by the packed sorbent method was evaluated using a matrix-matching calibration. Quantification was performed using ultra-high-performance liquid chromatography-tandem mass spectrometry with chemical ionization at atmospheric pressure. The method exhibited limits of detection as low as 50 ng/g, good linearity, and satisfactory intra-day (1.38–18.76) and inter-day (2.66–20.08) precision. Additionally, the method showed accuracy ranging from 80% to 136% for these impurities in pharmaceutical formulations.

KEYWORDS
losartan, microextraction, *N*-nitrosamines, pharmaceutical impurities, sample automatization

Article Related Abbreviations: API, active pharmaceutical ingredients; EF, enrichment factors; EMA, European Medicines Agency; FDA, Food and Drug Administration; GO@SiO_2, sílica-coated with graphene oxide; MEPS, microextraction by packed sorbent; NDEA, *N*-nitrosoethylamine; NDIPA, *N*-nitrosodipropylamine; NDMA, *N*-nitrosodimethylamine; NEIPA, *N*-nitrosoethylisopropylamine; SiO_2-NH_2, aminopropyl-silica; X-CW-PS/DVB, carboxylic acid-modified polystyrene divinylbenzene copolymer.

1 | INTRODUCTION

Sartans are a representative class of inhibitors and angiotensin II receptor blockers widely used for the treatment of hypertension [1], which is the most significant risk factor for cardiovascular disease globally [2, 3]. The incidence of hypertension in individuals aged 30−79 years doubled between 1990 and 2019 [4], so sartans are becoming among the most commonly consumed drugs in the world. These medicines are currently under strict surveillance and control because of recent reports of their contamination with *N*-nitrosamines [5, 6]. From 2018 to the present, several sartans lots (and other pharmaceutical drugs) have been recalled owing to the presence of *N*-nitrosamine class impurities [7–10]. For example, from more than 1400 batches of medicines collected, ∼24% (324) were of Losartan (Figure S1A) [11]. *N*-nitrosamines are genotoxic chemical carcinogens that are metabolized by cytochrome P450 and converted to diazonium ions, which can interact with DNA causing mutations (Figure 1SB) [12].

According to the Food and Drug Administration (FDA) and the European Medicines Agency (EMA), contamination of pharmaceuticals with *N*-nitrosamines can occur in different stages of the manufacturing process (API synthesis, formulation, packaging, etc.) [13]. However, many researchers consider the synthetic routes for producing active pharmaceutical ingredients (API) as the primary source of *N*-nitrosamines. For example, sartans have a tetrazole ring in their chemical structure, so their synthesis requires sodium nitrite (nitrosating agent) and solvents such as dimethylformamide, *N*-methyl pyrrolidone, diisopropylethylamine, and triethylamine. Those reagents are a source of secondary and tertiary amines that can produce *N*-nitrosamines during the synthetic process [14] (Figure S1C).

FDA and EMA established acceptable intake limits (AI) of *N*-nitrosamines, corresponding to 96.0 ng/day for *N*-nitrosodimethylamine (NDMA) and *N*-nitroso-*N*-methyl-4-aminobutyric acid, and 26.5 ng/day for *N*-nitrosodiethylamine (NDEA) and the other *N*-nitrosamines [5, 6]. Nevertheless, the concentration for each impurity in a formulation can vary depending on the dosage of each sartan. The higher the API dosage, the lower the acceptable concentration of *N*-nitrosamine. So, the development of analytical methods for quantifying and identifying *N*-nitrosamines at low concentrations present in complex matrices is currently highly demanded.

N-nitrosamines are typically determined by GC-MS or LC-MS using the simple diluting and shooting approach [15–20]. Although fast and straightforward, that methodology entails the injection of dirty extracts into the chromatographic system and can lead to column clogging, instrument contamination, and carry-over effects. Therefore, an appropriate methodology for routine monitoring of *N*-nitrosamines should be accompanied by an efficient sample preparation technique [21–23].

SPE has been proposed as a sample preparation technique for determining nitrosamines from pharmaceutical formulations. For example, an SPE method using two cartridges with different sorbents (cationic ion exchange resin and carbon) was employed to eliminate the matrix effect and pre-concentrate the *N*-nitrosamines; however, the procedure was laborious, time-consuming, and used large amounts of organic pollutant solvents [15]. In a faster and more selective alternative, *N*-nitrosamines have been determined by direct derivatization in the matrix, with dansyl chloride and fluorenylmethoxycarbonyl, before the LC analysis with fluorescence detection [13]. However, this approach not only entails the same risk of diluting and shooting but also involves additional stages that make the procedure intricate and susceptible to errors.

This study aimed to develop a new, fast, and efficient microextraction by packed sorbent (MEPS) approach for identifying *N*-nitrosamines in pharmaceutical matrices while addressing limitations associated with the dilute and shoot approach. These limitations include strong matrix effects, carryover due to the presence of tablet constituents, and the potential for accumulation leading to clogging of analytical columns, LC tubing, or the ESI source. As an alternative to overcome these challenges, we are introducing an analytical approach based on the use of cost-effective laboratory-repackable MEPS syringes and the automation of the technique using a high-throughput cartesian robot. The combination of the automated MEPS setup with UHPLC-MS/MS analysis resulted in a fast, productive, straightforward, and reliable, analytical strategy for determining pharmaceutical impurities.

2 | MATERIALS AND METHODS

2.1 | Standards and reagents

The high purity (>99%) analytical standards of *N*-nitrosodimethylamine (NMDA), NDEA, *N*-nitrosoisopropylethylamine (NEIPA), *N*-nitrosodiisopropylamine (NDIPA) were obtained from Clearsynth (Toronto, CA). The stock solution at 500 mg/L was prepared by diluting the standard in methanol and then stored in an amber bottle at −7°C. Working solutions were obtained by diluting the stock solution to the desired concentration.

HPLC grade methanol was purchased from Tedia (Fairfield, USA), and the Merk Millipore system provided the ultrapure water (Burlington, USA). Formic acid from Sigma Aldrich (St Louis, USA) was used as a solvent additive.

2.2 | Samples

Losartan tablets (200 mg total mass and 50 mg of API) were purchased at a local market. Losartan tablets were converted to powder using a porcelain mortar and pestle. The resulting powder was fortified to the desired concentration with the *N*-nitrosamine stock solution (ng nitrosamines/g of tablet) and dried to room temperature. Soon after, it was transferred to a falcon tube (15 ml) and dissolved with a 2% HCl solution (2 ml, pH 1,0). For better dissolution, the sample was vortexed for 2 min. After that, the sample was centrifuged (5000 rpm for 10 min), and 1.5 ml of the supernatant containing the *N*-nitrosamines was collected. This process is outlined in Figure S5.

2.3 | Microextraction by packed sorbent

High-throughput MEPS of *N*-nitrosamines was performed using a laboratory-made multi-syringe robot (Figure S2.). One-milliliter syringes were packed with 5.0 mg of extraction phase, trapped between two polypropylene frits. The syringes were then installed in the robotic system. An Arduino sketch was developed for the automated execution of all the MEPS stages, with their respective volumes and aspiring/dispensing cycles. Initially, the MEPS syringe is introduced into the sample (microtube) for the sampling process. Several sample aspiration/dispensing cycles are performed to enable the interaction of the analytes with the extraction phase. Then, the robot moves to the next position and washes the packed bed with water to remove the matrix interferents and selectively retain the targeted analytes. In the sequence, analytes sorbed in the extractor phase are eluted with an elution solvent (in aspiration/dispensing cycles). Finally, the MEPS syringe goes through the cleaning process with a suitable solvent to remove traces of analytes or matrix constituents in the packed bed. An illustrative video showing the automated MEPS procedure is available at https://www.youtube.com/watch?v = 4gJTuKV1ZIY.

2.4 | Optimization of microextraection by packet sorbent

2.4.1 | Extractor phase and sample dissolution solvent

Florisil, carboxylic acid-modified polystyrene divinylbenzene copolymer (X-CW-PS/DVB), aminopropyl silica (SiO_2-NH_2), charcoal, and C18 were obtained from Sigma-Aldrich (St Louis, USA). Silica-coated with graphene oxide (GO@SiO_2) was synthesized in our laboratory, according to the methodology described in [24]. These materials were first evaluated to choose the best sorbent for *N*-nitrosamines. According to the results, a mixed extraction phase containing 80% X-CW-PS-DVB and 20% charcoal was also further evaluated. Water and 2% HCl solution (2 ml, pH 1.0) were tested as the solvent for the tablet's dissolution during the sample's pretreatment.

2.4.2 | Univariate analysis of syringe conditioning

After selecting the best sample dissolution solvent and the extractor phase for MEPS, a study of the conditioning of the sorbent was carried out. Therefore, we studied whether there would be a need to condition the sorbent in water before starting the extraction or not. For that, a test without conditioning was performed, and a test with conditioning (condition: 10 cycles of 100 μl of acidified water). The other MEPS steps followed the standard conditions: sampling (15 cycles of 500 μl), elution with methanol (12 cycles of 50 μl), and cleaning (3 cycles of 300 μl), which were individually optimized as described in the next item 2.4.3.

2.4.3 | Optimization of the sampling and elution steps

Sampling and elution steps were optimized through a central composite experiment design. This is a design in which the experimental region takes the form of an eight-pointed star. Each variable is assessed in five levels, with the central point (0,0) in the star's center and whose normalized coordinates range between -$\sqrt{2}$, −1, 1, and $\sqrt{2}$. The number of aspiring/dispensing cycles and the volume of sample or solvent pumped through the packed bed were evaluated. The number of aspiring/dispensing cycles varied in the experimental region between 1(-$\sqrt{2}$) and 19 ($\sqrt{2}$) cycles in both procedure steps (sampling and elution). The pumped volume was assessed in the range between 100 μl (-$\sqrt{2}$) and 500 μl ($\sqrt{2}$) for the sampling stage and 50 μl (-$\sqrt{2}$) and 150 μl ($\sqrt{2}$) for the elution stage. The complete experimental design is presented in the supplementary information (Table S1).

The cleaning step was determined by performing cleaning cycles with methanol and monitoring the presence of *N*-nitrosamines in the post-cleaning extract (by HPLC-UV). If no traces of the analytes were found, the syringe would be suitable for the next MEPS extraction.

2.5 | Analytical instrumentation

2.5.1 | HPLC-UV/Vis analysis

During the optimization of the MEPS procedure, samples were analyzed in a Shimadzu (Kyoto, JP)

high-performance liquid chromatography model 20A Prominence, equipped with two LC-20AD pumps, a SIL-20A sampler, a CTO-20A column oven, and an SPD 20A UV-Vis detector. Analyzes were performed with a Phenomenex Luna Phenyl-Hexyl column (150 mm x 3.00 mm x 3 μm) at 50°C, 0.6 ml/min flow rate, in isocratic mode using H_2O-MeOH (70:30 v/v) as mobile phase. The monitored wavelengths were 235 and 245 nm.

2.5.2 | UHPLC-MS/MS analysis

The analytical validation step was carried out in an ultra-performance system consisting of a UPLC Acquity system coupled with a triple quadrupole detector of the XEVO TQ-MS type fitted with an ESI/APCI interface, all from Waters (Milford, USA). Chromatographic separation was performed on an Agilent Poroshell Phenyl-Hexyl column (100 mm x 2.1 mm x 2.7 μm) at 50°C, 10 μl partial loop injection using as mobile phase a mixture of H_2O-MeOH (70:30 v/v) plus 0.1% formic acid at a 0.2 ml/min flow rate. The gradient consisted of: (0–2 min) with 5% B, followed by a linear increase in 3 min to 30% B. Then, it was kept isocratic until 8 min with 30% B. Finally (8–10 min) decreases up to 5% B and remains isocratic up to 12 min. *N*-nitrosamines were detected in the positive mode in APCI, with 250°C vaporization temperature, a voltage of 1.3 μA, and 130°C in the ion transfer tube. Some tests were also performed using ESI in positive mode, but the APCI source was chosen due to its higher sensitivity for the investigated analytes. Under ESI conditions, nitrogen gas was used as the desolvation gas at 400°C and a flow rate of 600 L/H. The source temperature was set at 150°C. The transitions and their respective cone and collision energy (Table S2) were manually determined. For each analyte, two product ions were determined, with the highest-intensity ion selected as the quantification transition, and the lowest-intensity ion selected as the qualification transition. Figure S3 shows an example of a total ion chromatogram obtained for the injection of standard aqueous solution (500 ng/ml) under selected conditions.

3 | RESULTS AND DISCUSSION

3.1 | Study of microextraction by packet sorbent influencing parameters

MEPS is a multistage procedure that relies on various categorical and continuous variables to achieve optimal efficiency. These variables include: i) the nature of the extraction phase, ii) the amount of packed sorbent used, and iii) the total volume of sample/solvents (number of aspiring/dispensing cycles and volume) pumped through the packed bed. Therefore, in order to determine the best MEPS conditions, we conducted a stepwise approach. First, we selected the appropriate sorbent and solvents through univariate experiments. Then, we identified the most influential process stages and examined their impact on extraction performance through multivariate experiments.

3.2 | Selection of the extraction phase and sample loading conditions

For the selection of the MEPS sorbent, extraction syringes were prepared by packing 5.0 mg of the extraction phase between two polypropylene frits, as illustrated in Figure S2. The amount of 5.0 mg was chosen to ensure complete and uniform coverage of the transversal area of the syringe with all the tested extraction phases. This choice not only secured effective extraction but also aligned with the environmentally friendly aspect of microextraction by minimizing solvent and sorbent consumption.

Aqueous solutions of targeted *N*-nitrosamines were prepared, and aliquots of 1.5 ml (the robot is compatible with vials of 1.5 and 2.0 ml) were subjected to a preliminary fast MEPS procedure. In this procedure, 500 μl of solvent/sample was aspirated/dispensed in a sequence of 5 cycles at each stage. Although the employed syringe has a volume of 1.0 ml, considering the construction characteristics, the limiting factor in the speed of the method is the time taken by the robot to perform each aspirating/dispensing cycle. To minimize overall time, we opted to perform cycles of 500 μl instead of 1.0 ml. The use of five cycles in this preliminary stage was established as a suitable parameter to obtain measurable analytical responses with fast extractions.

To the best of our knowledge, there are no previous reports describing the use of MEPS for the determination of *N*-nitrosamines. However, some previous studies have employed SPE with various stationary phases, including charcoal (US Environmental Protection Agency Method 521 [25]), hydrophilic-lipophilic balanced resins (Oasis PRiME HLB) [26], activated carbon [17], and strong-cation exchange phases [15]. In this part of the study, we investigate the efficacy of stationary phases with different polarity and interaction mechanisms in extracting *N*-nitrosamines from complex samples such as pharmaceutical matrices. Therefore, we evaluated the performance of various MEPS sorbents, namely Florisil, X-CW-PS/DVBSiO2-NH2, charcoal, GO@SiO2, C18, and a mixture of charcoal and weak cation exchange phase in an 80:20 ratio (Figure 1A).

Normal phase-type sorbents, such as florisil and SiO_2-NH_2, primarily retain analytes through dipole-dipole and

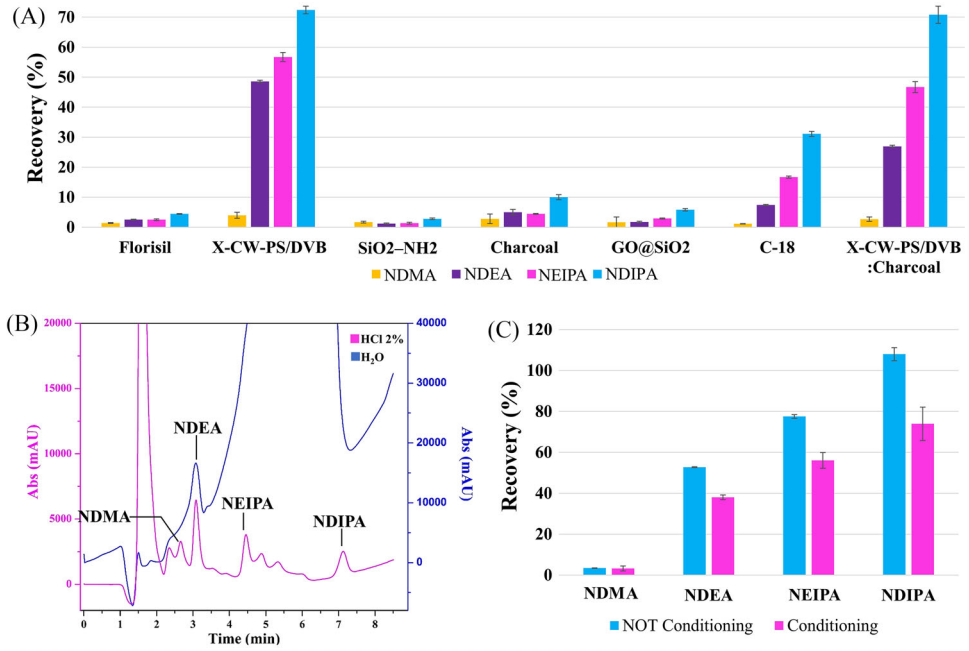

FIGURE 1 Univariate study of some influencing microextraction by packed sorbent (MEPS) performance parameters. (A) selection of the extraction phase; (B) Effect of the sample media; (C) Effect of the conditioning stage.

hydrogen bonding interactions. As expected, these sorbents showed poor uptake capability for *N*-nitrosamines from aqueous samples. However, when a hydrophobic sorbent like C18 was used, the recovery of NDEA, NEIPA, and NDIPA (the most non-polar tested *N*-nitrosamines) increased by 2- to 6-fold, indicating the crucial role of hydrophobic interactions in *N*-nitrosamine uptake. Phases containing carbon allotropes (charcoal and GO@SiO_2) exhibited slightly improved recovery of NMDA compared to the normal or C18 phases, likely due to the establishment of π–π interactions.

In this study, the best retention of *N*-nitrosamines, on chromatography analysis, was observed when a phenylhexyl stationary phase was used. However, the overall best extraction performance was achieved using X-CW-PS/DVB as the sorbent material. X-CW-PS/DVB is a mixed-mode stationary phase capable of interacting with diverse organic compounds through ion exchange involving counterion displacement from the resin phase, electrostatic interaction between ionic functional groups, and physical adsorption involving van der Waals and π-π interactions between non-ionic hydrophobic moieties of the analyte and the polymer backbone of the resin.

Although the cationic behavior of some *N*-nitrosamines, such as NDMA and some of its precursors, has been previously documented, weak cation exchange sorbents remain neutral at neutral and low pH. Thus, we believe that the extraction of *N*-nitrosamines involves a mixed interaction mode, possibly mainly involving ion exchange and π-π interactions. However, other structural factors such as porosity or pore size of the extraction phase can also play an important role.

Finally, as an attempt to improve the uptake of NMDA (the least extracted analyte), we also tested a mixture of X-CW-PS/DVB: charcoal (80:20). However, no significant difference from using pure X-CW-PS/DVB was observed. Consequently, we selected X-CW-PS/DVB as the MEPS sorbent for method development.

The choice of sample dissolution solvent had a notable impact on the extraction of *N*-nitrosamines from losartan tablets. When the tablets were suspended in ultrapure water, a significant amount of the API and excipients were co-extracted, resulting in a low analytical signal for *N*-nitrosamine detection using UV-Vis. In contrast, the addition of 2% HCl (pH 1.0) led to the precipitation of a considerable portion of the API due to its low solubility at acidic pH [27]. This approach effectively removed a portion of the tablet matrix, as shown in the chromatograms depicted in Figure 1B. However, matrix effects arising from the tablet composition, specifically the presence of excipients, posed a significant challenge when analyzing impurities. Therefore, in this stage, to develop the MEPS procedure and assess the extraction influencing parameters using HPLC-UV-Vis, we used acidified aqueous solutions of *N*-nitrosamines. Subsequently, we validated the method using a matrix-matched calibration approach involving controlled spiked losartan tablets.

3.3 | Microextraction by packet sorbent procedure

3.3.1 | Conditioning

Depending on the sorbent used and the specific application, the MEPS procedure can involve additional stages such as conditioning, washing, or drying in addition to sampling and elution. Conditioning stages are particularly important when silica-based phases are employed. Conditioning serves to remove impurities and activate the sorbent surface, enhancing the interaction between the analytes and the functional groups present in the phase. However, for polymeric phases, this activation stage may not be necessary, and loading the sample onto a dried phase does not necessarily affect retention [28].

In the case of the X-CW-PS/DVB polymer sorbent used in this study, including a conditioning stage with acidified water (the same solvent used for sample dissolution) did not result in any significant difference in the analytical response for the more polar NDMA. However, it negatively impacted the recovery of NDEA, NEIPA, and NDIPA (Figure 1C). Conditioning the sorbent with water led to the deposition of a thin layer of water over the X-CW-PS/DVB, thereby hindering the further interaction of the more hydrophobic analytes with the phase. Consequently, we decided not to include conditioning stages in the development of the MEPS procedure.

3.3.2 | Sampling

MEPS is a limited process due to the maximum capacity of the sorbent to retain analytes, which is typically a few milligrams. This retention capacity is dependent on the total volume of the sample that is passed through the packed bed. The total sample volume passed through the sorbent is determined by the relationship between the volume of the sample that is pumped and the number of aspiration/dispensing cycles performed during the MEPS procedure.

To determine the optimal balance between these parameters, we conducted a multivariate experiment, as outlined in the experimental section (Supporting information). The results of this experiment, including surface responses and their first derivatives, are depicted in Figure 2. The surface responses provide insight into the effects of varying the number of cycles and sample volume on the MEPS process.

The chromatographic response exhibited a greater increase with the pumped volume compared to the number of aspiration-dispensing cycles. However, analysis of the first derivative revealed that for most tested analytes, the maximum response was achieved when using 12.5 cycles at low sample volumes (100 µl). The surface responses indicated that both variables increased concurrently until reaching a saturation point at approximately 19 cycles and 500 µl of the sample. However, experimental data indicated a non-significant increase in analytical response beyond 15 cycles. Consequently, to maximize the response within the shortest possible time, we determined that utilizing 15 cycles and 500 µl of the sample was the optimal condition for the sampling stage.

3.3.3 | Elution

An appropriate elution solvent for the MEPS of *N*-nitrosamines should be strong enough to allow the complete removal of the analytes from the sorbent, in just a few microliters, avoiding the dilution of the extracts. In previous SPE methods, solvents such as ammonium acetate buffer (pH 9.5) have been used to uptake *N*-nitrosamines from hydrophilic-lipophilic balance phases [26]. In addition, methanol and dichloromethane have been employed in liquid-phase microextraction [28]. Considering these antecedents and to guarantee compatibility with the HPLC method, we selected pure methanol as the elution solvent.

The elution performance in the method is determined by finding a compromise between the volume of solvent passing through the packed bed and the number of aspiration/dispensing cycles. Figure S4 illustrates the surface responses, which show the chromatographic area as a function of the number of aspiration/dispensing cycles and the volume of the elution solvent. As expected, using a higher volume of solvent leads to a more diluted extract, resulting in a lower analytical response. Therefore, we established the volume for analyte elution at 50 µl.

Furthermore, the analytical response exhibited an exponential increase in the number of elution cycles for the more polar analytes (NDMA and NDEA), with the maximum point exceeding the experimental region. In the case of NEIPA and NDIPA, the maximum responses were observed at approximately 12.5 cycles. To achieve a favorable compromise for the uptake of all the studied analytes, we selected 12 aspiration/dispensing cycles for the elution stage.

3.4 | Analytical performance of the offline robot-assisted MEPS-LC-MS/MS method

As mentioned in Section 3.1.1, the matrix effect due to tablet composition is critical in determining *N*-nitrosamines in pharmaceutical formulations. Therefore,

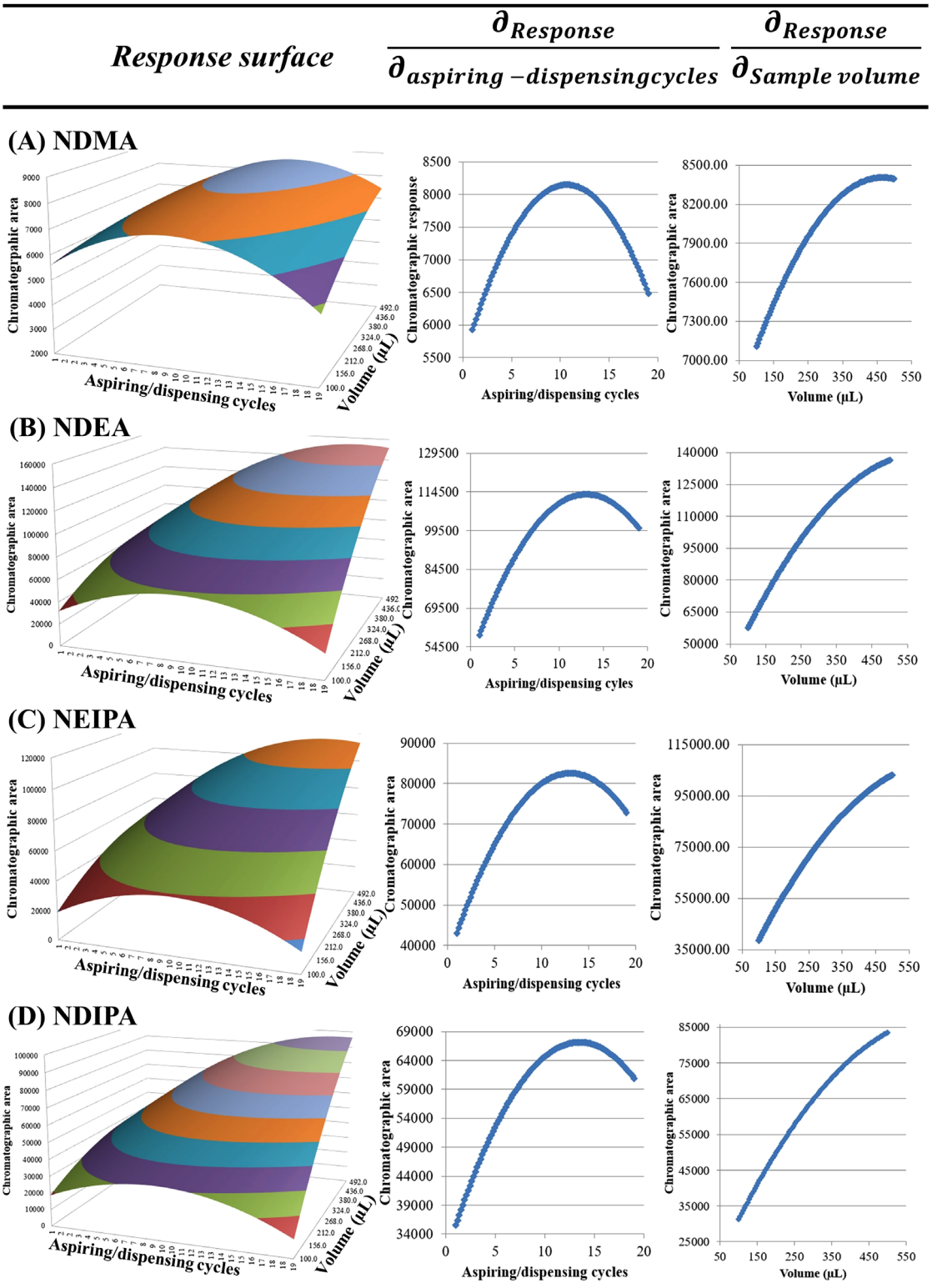

FIGURE 2 Surface response for the sampling step as a function of aspiration/dispensing cycles and sample volume for (A) *N*-nitrosodimethylamine (NDMA); (B) *N*-nitrosodiethylamine (NDEA); (C) *N*-nitrosoisopropylethylamine (NEIPA); and (D) *N*-nitrosodiisopropylamine (NDIPA).

to assess the figures of merit of the MEPS method using the matrix-matched calibration approach, a highly selective detection technique such as MS/MS should be used. Before the development of multiple reaction monitoring (MRM) detection methods, we assessed the effect of matrix effects on the ionization of *N*-nitrosamines via two different ionization systems: ESI and APCI. APCI (Figure 3A) provided better detectability than ESI (Figure 3B) when

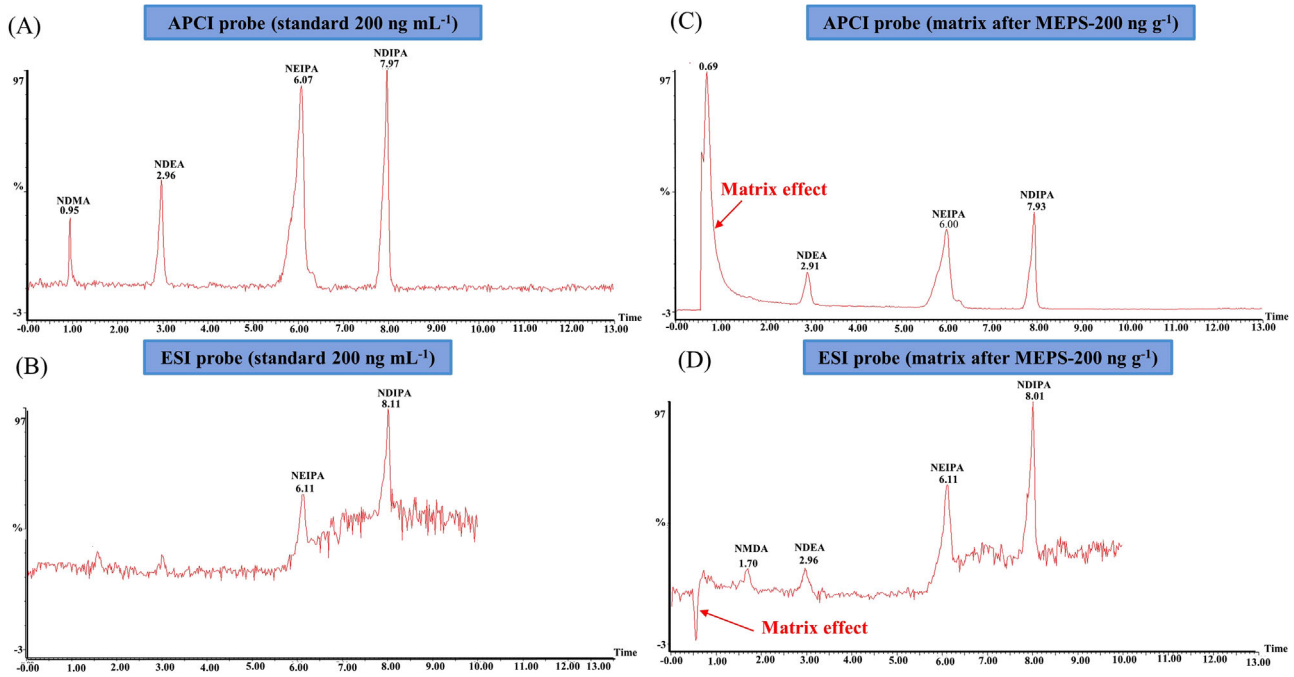

FIGURE 3 Comparative of the ionization performance employing ESI and APCI sources. (A) total ion chromatogram (TIC) obtained for the injection of a standard solution of nitrosamines at 200 ng/ml, using the APCI source; (B) TIC obtained for the injection of a standard solution of nitrosamines at 200 ng/ml, using the ESI source; (C) TIC obtained for the injection of a microextraction by packed sorbent (MEPS) extracts from losartan tablet spiked at 200 ng/g, using the APCI source; (D) TIC obtained for the injection of a MEPS extracts from losartan tablet spiked at 200 ng/g, using the ESI source.

standard aqueous solutions of *N*-nitrosamines (200 ng/ml) were injected.

APCI also provided better detectability than ESI when MEPS extracts of the spiked losartan tablets (spiked with 200 ng g^{-1} of *N*-nitrosamine analytical standards) were injected (Figure 3C,D). However, although the impact was lower than that previously observed using UV-Vis detection, matrix effects were also observed for both ionization modes. Tablet excipients generate a prominent band at the dead time when APCI is used, causing ionization suppression in the ESI source. Because the targeted analytes were detected in MRM acquisition mode, chromatographic areas were selectively estimated from the extracted ion chromatogram of the transitions specifically monitored for each analyte.

The analytical performance of the proposed method, after MEPS optimization, was assessed by Using the APCI source and evaluating the figures of merit, such as LOD, LOQ, linearity, enrichment factors (EFs), extraction recovery, precision (%RSD), and accuracy (% recovery), under the guidelines of the International Conference on Harmonization (ICH Q2) [29].

Linearity, LOD, and LOQ were evaluated by considering the AI limits of *N*-nitrosamines regulated by various regulatory agencies around the world: FDA (USA), EMA (EU), and Brazilian Nacional Agency of Health Surveillance (ANVISA, BR) [5, 6, 30]. There is a consensus between the AI limits for each impurity and their conversion into concentration (ppm), dividing it by the dose of API present in the drug. Table S3 presents the allowed concentrations of *N*-nitrosamines in losartan tablets.

The LOD and LOQ were determined experimentally by sequential injection of MEPS extracts of decreasing concentrations (ng *N*-nitrosamine/g of tablet) until signal-to-noise ratios of 3:1 and 10:1 were obtained, respectively. Although it would be possible to obtain specific values for each analyte by fine-tuning, we set 50 ng/g as a suitable value to guarantee the simultaneous detection of all analytes. Similarly, at 80 ng/g, all analytes could be quantified with suitable analytical confidence. Linearity was assessed within a range spanning from the LOQ of the method to 120% above the highest allowable limit for the active ingredient (AI). To determine the upper limit of the calibration curve, we calculated the maximum daily intake limit by dividing the accepted concentration of *N*-nitrosamine by the mass of the active pharmaceutical ingredient. Subsequently, we identified the value that exceeds this limit by 120%. Consequently, we established a range of up to 2400 ng/g for the calibration curve.

Calibration curves were plotted by measuring the areas of the chromatographic peaks corresponding to MEPS extracts (in triplicate) at five concentration levels, and

determination coefficients (r^2) higher than 0.99 were obtained in all cases (Table 1).

EF was estimated at three concentrations and defined as the ratio between the concentration of the analytes in the methanolic extract from MEPS and the spiked concentration in the tablet ($EF = C_{MEPS\ extract}/C_{tablet}$). Analytes concentration in the MEPS extract was measured from a calibration curve using standard methanolic solutions. The method provides *EFs* < 1 for NDMA, indicating that the concentration of this analyte in the MEPS extract is lower than its concentration in the spiked tablet. The extraction process involved preliminary stages of tablet suspension in acidified water, centrifugation, and filtration. Therefore, not 100 % of the analytes spiked on the tablet are transferred to the aqueous extract and submitted to MEPS. NDMA is also the least retained analyte in the phenyl-hexyl column and coelutes with a part of the matrix interferents, so its ionization is affected to a greater extent by the charge competition phenomena than the other analytes. The EFs serve as a measure of the performance of the MEPS (X-CW-PS/DVB) procedure. This implies that, for instance, in the case of NDEA, the MEPS method yielded a final extract for injection into the LC-MS/MS system that was 2.2 times more concentrated compared to what would have been achieved simple using the dilute and shoot approach.

The extraction recovery can be understood as a measure of the number of moles of each analyte extracted ($n_{MEPS\ extract}$) regarding the number of moles in the sample (n_{tablet}). *ERs* were estimated as 100 times the product of the *EF* by the phase ratio ($Mass_{MEPs\ extract}/Mass_{tablet}$), according to eq. (1):

$$ER = \left[\frac{n_{MEPS\,extract}}{n_{tablet}}\right] * 100 = \left[\frac{C_{MEPS\,extract} * Mass_{MEPS\,Extract}}{C_{tablet} * Mass_{tablet}}\right] * 100 = \left[\frac{Mass_{MEPS\,extract}}{Mass_{tablet}}\right] EF * 100 \quad (1)$$

For NEIPA and NDIPA *ERs* > 100 % were observed The analytical responses depend on the effects of the matrix interferent over the sample preparation step and the ionization of the analyte in the ESI source. Enhancement of the ionization due to the matrix effects (*ME*) can explain the overestimation in the percentage of the extracted number of moles. *MEs* were calculated 100 times the ratio between the slope of the matrix-matched calibration and the solvent curve. *MEs* show that NDMA ionization is hindered by the coelution of that analyte with the remaining tablet constituents. Also, *MEs* cause enhancing of the ionization of NDEA, NEIPA, and NDIPA, leading to higher

TABLE 1 Analytical performance of the developed microextraction by packed sorbent (MEPS)-UHPLC-APCI-MS/MS method.

Analyte	LOD (ng/ml)	Linear range (ng/ml)	$y = mx + b$			EF			ER (%)			ME (%)
			m	*b*	r^2	100 ng/ml	500 ng/ml	2400 ng/ml	100 ng/ml	500 ng/ml	2400 ng/ml	
NDMA	50	80–2400	0.5435	11.808	0.9938	0.3 ± 0.0	0.5 ± 0.1	0.6 ± 0.1	8.5 ± 0.5	11.5 ± 1.7	14.6 ± 3.4	58.8
NDEA	50	80–2400	33.961	−149.02	0.9887	2.2 ± 0.1	2.5 ± 0.1	2.5 ± 0.1	54.5 ± 1.9	59.9 ± 1.8	60.8 ± 2.0	152.7
NEIPA	50	80–2400	179.5	−1816.4	0.9983	5.9 ± 0.2	4.2 ± 0.1	4.3 ± 0.1	144.1 ± 21.8	103.2 ± 4.2	103.8 ± 2.7	181.0
NDIPA	50	80–2400	59.313	4020.3	0.9876	7.4 ± 0.3	5.9 ± 0.6	3.9 ± 0.6	179.7 ± 5.4	142.9 ± 8.5	95.2 ± 15.1	210.6

Abbreviations: NDEA, *N*-nitrosoethylamine; NDIPA, *N*-nitrosodipropylamine; NDMA, *N*-nitrosodimethylamine; NEIPA, *N*-nitrosoethylisopropylamine.

TABLE 2 Precision and accuracy of the developed microextraction by packed sorbent (MEPS)-UHPLC-APCI-MS/MS.

	Intra-day RSD (%)			Inter-day RSD (%)			Accuracy (%)		
Analyte	100 ng/ml	500 ng/ml	2400 ng/ml	100 ng/ml	500 ng/ml	2400 ng/ml	100 ng/ml	500 ng/ml	2400 ng/ml
NDMA	6.59	2.67	18.76	5.65	8.08	7.10	134.7	95.3	108.0
NDEA	6.35	2.56	1.38	4.42	9.41	20.08	129.3	109.3	101.3
NEIPA	9.64	2.07	1.86	12.00	19.82	2.66	135.8	98.6	97.9
NDIPA	2.83	6.35	8.64	2.83	3.17	2.66	91.5	116.3	87.2

Abbreviations: NDEA, *N*-nitrosoethylamine; NDIPA, *N*-nitrosodipropylamine; NDMA, *N*-nitrosodimethylamine; NEIPA, *N*-nitrosoethylisopropylamine.

analytical responses that the observed for the injection of a standard solution prepared in the solvent.

Precision and accuracy were also assessed from matrix-matched samples at three sample concentration levels of 100, 500, and 2400 ng/g — covering the low, medium, and high regions of the calibration curve — and for assays performed in triplicate (Table 2). RSD data were obtained for the inter-day and intra-day (two consecutive days) precision assays. The accuracy of the method was evaluated at the same concentration levels. The experimental and theoretical concentrations obtained from the matrix-matched calibration curve were compared. The RSD varied between 2% and 21%, indicating suitable intra- and inter-day method precision. The accuracy ranged between 87% and 136%, indicating that the method was capable of predicting and estimating the concentration of the tested samples.

Table S4 presents a comparison between the developed automated MEPS method and seven previous studies that focused on analytical methods for determining *N*-nitrosamines in pharmaceutical formulations of sartans. The majority of these studies employed the dilute and shoot approach, which entails diluting the sample (API or finished product) in a solvent and directly injecting it into the chromatographic system [31]. However, the dilute and shoot methods have inherent limitations that may render them unsuitable for routine analysis. These limitations include strong matrix effects, column or tube clogging, instrument contamination, and carry-over effects. Although increasing the dilution ratio can help mitigate the impact of matrix constituents associated with the dilute and shoot approach, it may also hinder method detectability [32].

To overcome the drawbacks of the dilute and shoot approach, alternative sample preparation techniques have been proposed. For example, some studies have employed SPE after suspending the tablet in water or an organic solvent. This approach helps reduce API contamination, system ion suppression, and the presence of high molecular weight polymers that contribute to clogging. However, this strategy, although providing outstanding detectability for nine *N*-nitrosamines, is laborious, time-consuming, and not sustainable. It involves two consecutive stages of solid-liquid extraction and two additional SPE steps using different cartridges, such as strong cation exchange and charcoal. Moreover, relatively large amounts of pollutant chlorinated solvents were used, contradicting the principles of green analytical chemistry.

Another strategy to mitigate matrix effects is the use of derivatization steps, enabling the use of a fluorescence detector and improving selectivity. However, these methods introduce complexity to the analysis and reduce analytical throughput. Additionally, derivatization increases chemical consumption and generates more waste, compromising the sustainability of the developed methods.

This study introduces a straightforward and high-throughput approach that provides suitable detectability for the proposed applications while maintaining a high sample throughput. The use of laboratory-made syringes in the MEPS technology makes it more affordable and allows for reusability (more than 150 times per device). Furthermore, these MEPS devices can be easily packed and repacked indefinitely with any commercial or experimental extraction phase.

Previously reported LODs ranged from < 1.0 up to 460 ng/g, depending on the analyte and technique employed. In comparison, the LOD provided by the automated MEPS setup can be considered competitive. Considering the default class-specific Threshold of Toxicological Concern for nitrosamines in pharmaceuticals, which can reach values up to > 90 ng/day, our method is deemed appropriate for determining *N*-nitrosamine contamination in tablets.

4 | CONCLUDING REMARKS

This paper describes, for the first time, the combined use of affordable laboratory-repackable MEPS devices with a high-throughput cartesian robot for the development of fast, cost-effective, and efficient MEPS methods. The setup was evaluated in the development of a method for the determination of *N*-nitrosamines from drug tablets, enabling the simultaneous treatment of up to six samples in less than 20 min, and proving to be a profitable and competitive analytical tool for routine analysis.

For MEPS, solid losartan tablets were converted into the liquid phase by suspending them in acidified water, resulting in lower matrix effects compared to suspending them in pure water. Among the various extraction phases tested, including florisil, C18, SiO_2-NH_2, charcoal, and GO@SiO_2, the X-CW-PS/DVB sorbent demonstrated superior extraction capability for *N*-nitrosamines. The retention of *N*-nitrosamines in the extraction phase appears to be closely related to the establishment of ion exchange, π–π, and hydrophobic interactions.

Optimization of the sampling and elution stages using multivariate techniques revealed that MEPS efficiency is influenced by factors such as the volume pumped through the packed bed and the number of aspirating/dispensing cycles performed during these stages. After experimentation, the best compromise between recovery and analysis time was achieved by performing the sample stage in 15 aspirating/dispensing cycles of 500 μl of the sample and eluting in 12 cycles of 50 μl.

The figures of merit of the developed MEPS method were determined using matrix-matching calibration and LC-MS/MS. APCI showed higher analytical responses than ESI in both cases when injecting aqueous solutions of *N*-nitrosamine standards and MEPS extracts from losartan tablets. However, both sources are susceptible to matrix effects due to the complex composition of the losartan tablets. Matrix interference caused ionization suppression with the ESI source and ionization enhancement with the APCI source. Therefore, matrix-matched calibration is essential to ensure confident and robust analytical results.

The obtained figures of merit demonstrate that the method provides sufficient detectability and analytical confidence for the proposed application. The automated setup offers a practical, fast, straightforward, and reliable analytical tool for the determination of contaminants and impurities in pharmaceutical products. Although it was not possible to apply the method to the determination of *N*-nitrosamines in recalled losartan tablets, the proposed method can be considered suitable for routine analysis of real samples.

ACKNOWLEDGEMENTS

This work was funded by i) the Coordination for the Improvement of Higher Education Personnel (CAPES—Brazil, Finance Code 001), ii) the São Paulo Research Foundation (FAPESP—Brazil, Grants 2019/26263-4, 2019/22724-7, 2017/02147-0, 2015/15462-5 and 2014/07347-9), and iii) the National Council for Scientific and Technological Development (CNPq—Brazil, 307293/2014-9; 308843/ 2019-3).

CONFLICT OF INTEREST STATEMENT

The authors declare no conflict of interest.

DATA AVAILABILITY STATEMENT

The corresponding author's data supporting this study's findings are available upon reasonable request.

ORCID

Fernando Mauro Lanças https://orcid.org/0000-0002-8711-5905

REFERENCES

1. Messerli FH, Bangalore S, Bavishi C, Rimoldi SF. Angiotensin-converting enzyme inhibitors in hypertension. J Am Coll Cardiol. 2018;71:1474–82.
2. Al-Makki A, DiPette D, Whelton PK, Murad MH, Mustafa RA, Acharya S, et al. Hypertension pharmacological treatment in adults: a World Health Organization guideline executive summary. Hypertension 2022;79:293–301.
3. Mills KT, Stefanescu A, He J. The global epidemiology of hypertension. Nat Rev Nephrol. 2020;16:223–37.
4. Zhou B, Carrillo-Larco RM, Danaei G, Riley LM, Paciorek CJ, Stevens GA. Worldwide trends in hypertension prevalence and progress in treatment and control from 1990 to 2019: a pooled analysis of 1201 population-representative studies with 104 million participants. Lancet. 2021;398:957–80.
5. Food and Drug Administration. Control of nitrosamine impurities in human drugs. Guidance for Industry. 2021.
6. European Medicines Agency. Assessment report: Nitrosamine impurities in human medicinal products. EMA. 2020;5:1–90.
7. Chang S-H, Chang C-C, Wang L-J, Chen W-C, Fan S-Y, Zang C-Z, et al. A multi-analyte LC-MS/MS method for screening and quantification of nitrosamines in sartans. J Food Drug Anal. 2020;28:292–301.
8. Ardiana F, Suciati IG. Profiles of drug substances, excipients and related methodology. Cambridge, MA: Academic Press; 2015.
9. Srinivasan V, Sivaramakrishnan H, Karthikeyan B. Detection, isolation and characterization of principle synthetic route indicative impurity in telmisartan. Arab J Chem. 2016;9:S1516–22.
10. Masada S, Tsuji G, Arai R, Uchiyama N, Demizu Y, Tsutsumi T, et al. Rapid and efficient high-performance liquid chromatography analysis of *N*-nitrosodimethylamine impurity in valsartan drug substance and its products. Sci Rep. 2019;9:11852.
11. Bharate SS. Critical analysis of drug product recalls due to nitrosamine impurities. J Med Chem. 2021;64:2923–36.
12. Beard JC, Swager TM. An organic chemist's guide to *N*-Nitrosamines: their structure, reactivity, and role as contaminants. J Org Chem. 2021;86:2037–57.
13. Boczar D, Wyszomirska E, Zabrzewska B, Chyła A, Michalska K. Development and validation of a method for the semi-quantitative determination of *N*-Nitrosamines in active pharmaceutical ingredient enalapril maleate by means of derivatisation and detection by HPLC with fluorimetric detector. Appl Sci. 2021;11:7590.
14. González R, Torrado G, Arribas JM, Peña MA Development of an analytical method for the determination and quantification of n-nitrosodimethylamine in olmesartan by HPLC-MS/MS. Microchem J. 2022;179:107402.
15. Vogel M, Norwig J. Analysis of genotoxic *N*-nitrosamines in active pharmaceutical ingredients and market authorized

products in low abundance by means of liquid chromatography – tandem mass spectrometry. J Pharm Biomed Anal. 2022;219:114910.
16. Ngongang AD, Duy SV, Sauvé S. Analysis of nine *N*-nitrosamines using liquid chromatography-accurate mass high resolution-mass spectrometry on a Q-Exactive instrument. Anal Methods. 2015;7:5748–59.
17. Lim H-H, Oh Y-S, Shin H-S. Determination of *N*-nitrosodimethylamine and *N*-nitrosomethylethylamine in drug substances and products of sartans, metformin and ranitidine by precipitation and solid phase extraction and gas chromatography–tandem mass spectrometry. J Pharm Biomed Anal. 2020;189:113460.
18. Schmidtsdorff S, Schmidt AH. Simultaneous detection of nitrosamines and other sartan-related impurities in active pharmaceutical ingredients by supercritical fluid chromatography. J Pharm Biomed Anal. 2019;174:151–60.
19. Yin M, Hu Y, Fan H, Wang Q, Wang M, Wang W, et al. Method for trace determination of *N*-nitrosamines impurities in metronidazole benzoate using high-performance liquid chromatography coupled with atmospheric-pressure chemical ionization tandem mass spectrometry. J Sep Sci. 2023;46:e2200225.
20. Mallavarapu R, Katari NK, Siddhani VK, Marisetti VM, Rekulapally VK, Vyas G, et al. Development and validation of rapid ultra high performance liquid chromatography with tandem mass spectroscopic method for the quantification of *N*-nitrosodimethyl amine and *N*-nitrosodiethyl amine in sitagliptin and metformin hydrochloride immediate and extended-release formulations. J Sep Sci. 2022;45:3067–81.
21. Miralles P, Chisvert A, Salvador A. Determination of *N*-nitrosamines in cosmetic products by vortex-assisted reversed-phase dispersive liquid–liquid microextraction and liquid chromatography with mass spectrometry. J Sep Sci. 2018;41:3143–51.
22. Wang L, Yang C, Zhang Q, Wang S, Lang H, Zhang S, et al. SPE-HPLC-MS/MS method for the trace analysis of tobacco-specific *N*-nitrosamines and 4-(methylnitrosamino)-1-(3-pyridyl)-1-butanol in rabbit plasma using tetraazacalix[2]arene[2]-triazine-modified silica as a sorbent. J Sep Sci. 2013;36:2664–71.
23. Talebpour Z, Rostami S, Rezadoost H. Evaluation of a method for the simultaneous quantification of *N*-nitrosamines in water samples based on stir bar sorptive extraction combined with high-performance liquid chromatography and diode array detection. J Sep Sci. 2015;38:1601–09.
24. Mejía-Carmona K, Lanças FM. Modified graphene-silica as a sorbent for in-tube solid-phase microextraction coupled to liquid chromatography-tandem mass spectrometry. Determination of xanthines in coffee beverages. J Chromatogr A. 2020;1621:461089.
25. Bian Y, Zhang Y, Zhou Y, Li GH, Feng XS. Progress in the pretreatment and analysis of *N*-nitrosamines: an update since 2010. Crit Rev Food Sci Nutr. 2021;61:3626–60.
26. Yamamoto E, Kan-no H, Tomita N, Ando D, Miyazaki T, Izutsu KI. Isolation of *N*-nitrosodimethylamine from drug substances using solid-phase extraction-liquid chromatography–tandem mass spectrometry. J Pharm Biomed Anal. 2022;210:114561.
27. Ramtoola Z. Investigation of the physical, chemical and microbiological liquid suspension. 2021.
28. Giménez-Campillo C, Pastor-Belda M, Campillo N, Hernández-Córdoba M, Viñas P Development of a new methodology for the determination of *N*-nitrosamines impurities in ranitidine pharmaceuticals using microextraction and gas chromatography-mass spectrometry. Talanta. 2021;223:121659. https://doi.org/10.1016/j.talanta.2020.121659
29. Harron DWG. The textbook of pharmaceutical medicine. Oxford, UK: Blackwell Publishing Ltd.; 2013.
30. BRASIL. Agência de Vigilancia Sanitária, Guia sobre o Controle de Nitrosaminas em Insumos Farmacêuticos Ativos e Medicamentos. Guia no 50/2021 - versão 2. 2022;1–28.
31. Khorolskiy M, Ramenskaya G, Vlasov A, Perederyaev O, Maslennikova N. Development and validation of four nitrosamine impurities determination method in medicines of valsartan, losartan, and irbesartan with HPLC-MS/MS (APCI). Iran J Pharm Res IJPR. 2021;20:541.
32. Greer B, Chevallier O, Quinn B, Botana LM, Elliott CT. Redefining dilute and shoot: the evolution of the technique and its application in the analysis of foods and biological matrices by liquid chromatography mass spectrometry. TrAC Trends Anal Chem. 2021;141:116284.

SUPPORTING INFORMATION

Additional supporting information can be found online in the Supporting Information section at the end of this article.

How to cite this article: Pereira dos Santos NG, Medina DAV, Lanças FM. Microextraction by packed sorbent of *N*-nitrosamines from Losartan tablets using a high-throughput robot platform followed by liquid chromatography-tandem mass spectrometry. J Sep Sci. 2023;2300214. https://doi.org/10.1002/jssc.202300214

Supplementary information

Microextraction by packed sorbent of N-nitrosamines from Losartan tablets using a high-throughput robot-assisted platform followed by liquid chromatography-tandem mass spectrometry

*Natalia Gabrielly Pereira dos Santos, Deyber Arley Vargas Medina, Fernando Mauro Lanças**

University of São Paulo, São Carlos Institute of Chemistry, São Carlos - SP, Brazil

**Corresponding author: Tel: +55 (16) 3373-8657.*

1. Supplementary information of the Introduction

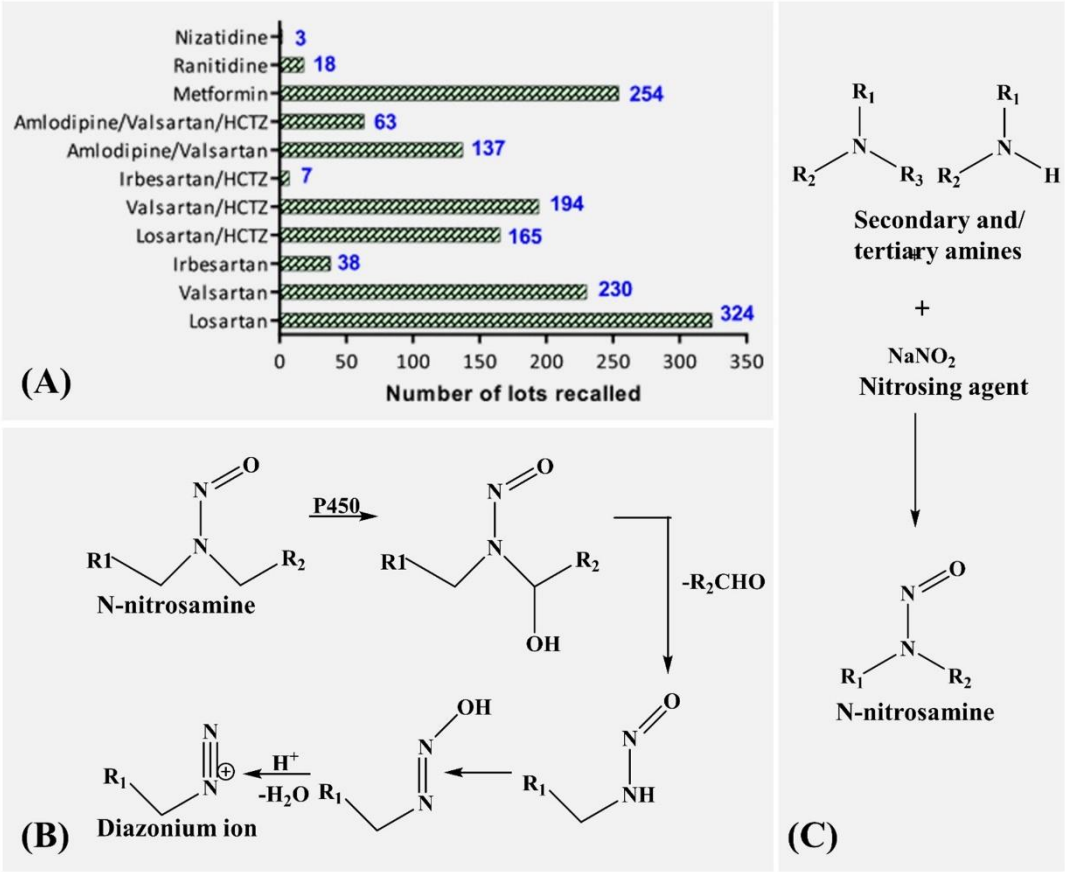

Figure S1. Information on the case of N-nitrosamines in sartans tablets. (A) Overview of the number of drug recalls for contamination with N-nitrosamines. Reprinted with permission from [11]. Copyright (2021) American Chemical Society. (B) Proposed mechanism for diazonium ion formation from N-nitrosamines, which may prove DNA mutation and perhaps cancer. (C) Main route of formation of N-nitrosamines.

2. Supplementary information in the materials and methods section

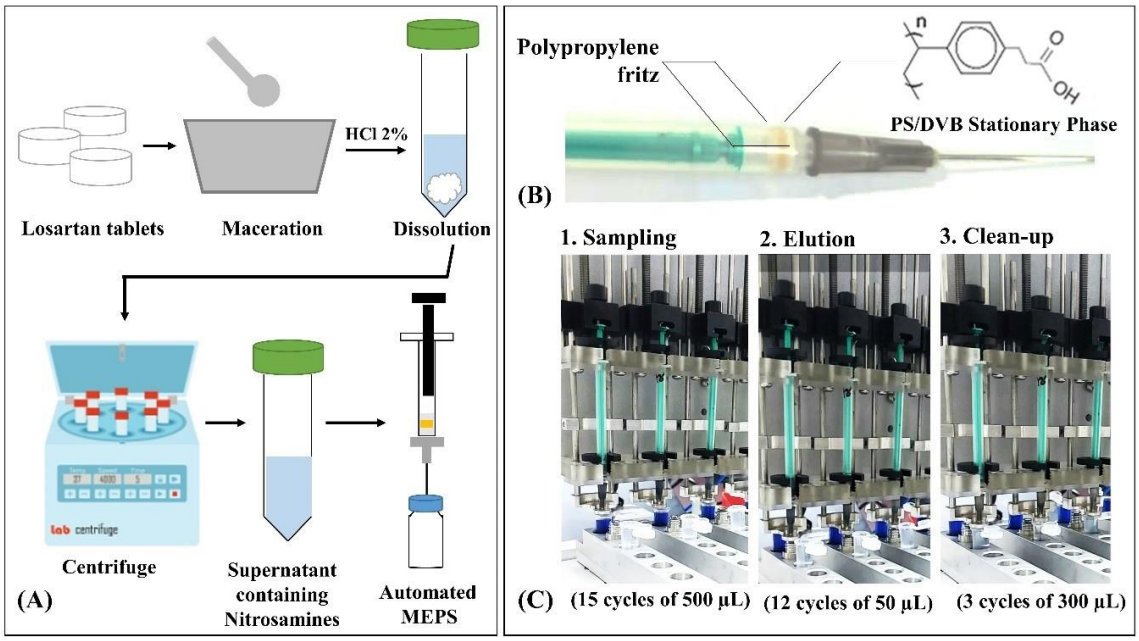

Figure S2. Instrumentation for sample preparation of Losartan tablets and extraction of N-nitrosamines. (A) Pretreatment of drug tablets. (B) picture of the syringe containing the packed extraction phase used in MEPS. C) pictures of the Automated MEPS optimized steps (a blue corant replaced sample for illustrative purposes).

Table S1. Experiments were carried out in the star experimental design to optimize the sampling and elution steps in MEPS.

	Sampling step		Elution step	
Experiment	**Number of Cycles**	**Volume (µl)**	**Number of cycles**	**Volume (µl)**
1	19	300	6	93
2	14	360	14	93
3	10	500	6	107
4	6	360	14	107
5	1	300	10	100
6	6	240	10	100

7	10	100	10	100
8	14	240	1	100
9	10	300	10	50
10	10	300	19	100
11	10	300	10	150

Table S2. Liquid chromatography-tandem mass spectrometry parameters for the N-nitrosamines detection

					Quantification transition			Qualification transition		
Analytes	t_R	log P	pk_a	Precursor Ion (m/z)	Product Ion (m/z)	CE (V)	Cone Voltage (V)	Product Ion (m/z)	CE (V)	Cone Voltage (V)
NDMA	1.12	0.039	3.52	75.00	58.08	15	20	43.06	15	20
NDEA	2.96	0.752	3.32	103.00	75.00	10	20	47.00	10	20
NEIPA	5.52	1.169	3.22	117.04	75.00	10	20	43.00	10	20
NDIPA	8.03	1.585	3.12	131.00	89.00	10	20	43.00	10	20

t_R: retention time, CE: collision energy

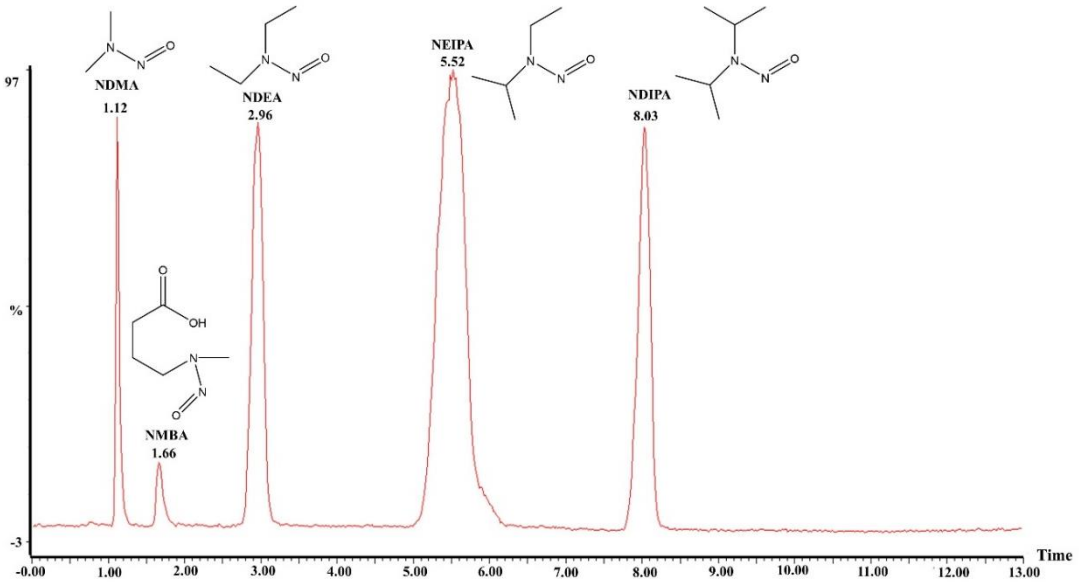

Figure S3. Chromatographic separation of N-nitrosamines obtained in MEPS-HPLC-APCI-MS/MS system.

3. Supplementary information of the results and discussion section

Response surface	$\frac{\partial_{Response}}{\partial_{aspiring-dispensingcycles}}$	$\frac{\partial_{Response}}{\partial_{Sample\ volume}}$

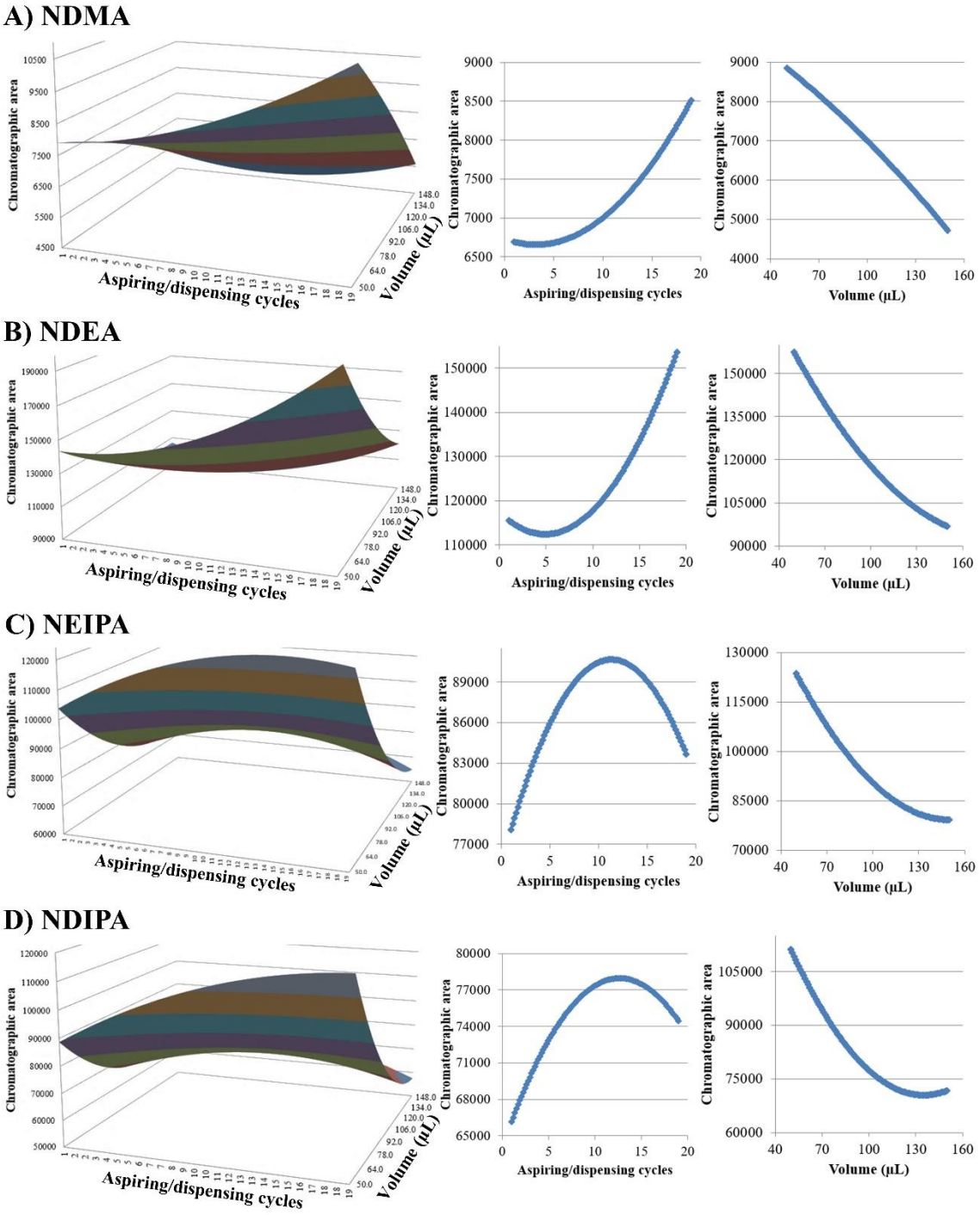

Figure S4. Surface response for the elution step as a function of the aspiring/dispensing cycles and volume of the sample for **A)** NDMA; **B)** NDEA; **C)** NEIPA; and **D)** NDIPA.

Table S3. AI limits and respective concentrations for N-nitrosamines in the drug Losartan tablets.

N-nitrosamines	Losartan dose	50 mg	100 mg
	AI limits (ng/day)	mg mL^{-1}	mg mL^{-1}
NDMA	96.0	1.920	0.960
NDEA	26.5	0.530	0.265
NEIPA	26.5	0.530	0.265
NDIPA	26.5	0.530	0.265

Table S4. Comparison of the developed MEPS-HPLC-MS/MS method similar to previous reports describing sample approach for determination of N-nitrosamines from Sartan formulations

Analytes	Sample	Sample preparation	Sample throughput	LOD	Instrumentation	Ref.
NDEA, NDMA, NDPA, NEIPA, NDIPA, NDELA, NMor, NPyr, Npip, NDiPLA, NMBA, NMEA	Sartan product	Dilute and Shoot	--	20 ng g^{-1}	LC-MS/MS	[7]
NDMA, NDEA, NMEA, NDPA, NDBA, NDPhA, NPyr, Npip, Nmor	API valsartan and losartan	Dilute and Shoot	--	10 - 140 ng g^{-1} (valsartan) and 20 - 460 ng g^{-1} (losartan)	SFC-MS	[19]
NDBA, NDPhA, NDEA, NDMA, NDIPA, NMEA, Nmor, Npip, NPyr, NMBA, NMPA, NDPA, EIPNA	Sartan product and API	SPE	--	0.025 - 1 ng g^{-1}	LC-MS/MS	[16]
NDMA	Ranitidine	Dilute and Shoot	--	1 ng g^{-1}	LC-MS	[20]
NDMA and NDEA	API	Derivatisation with dansyl chloride and Fmoc-Cl	--	0.013 - 0.017 ng g^{-1}	LC-FLD	[13]
NDMA, NDEA, NMBA, NEIPA	Sartan product	Dilute and Shoot	--	0.2 ng g^{-1}	LC-MS/MS	[21]
NDMA	Sartan product	Dilute and Shoot		0.04 ng g^{-1}	LC-MS/MS	[14]
NDMA, NDEA, NMBA, NEIPA	Sartan product	Automated MEPS	18 samples/hour	50 ng g^{-1}	LC-MS/MS	This study

Capítulo 8

Considerações finais

1 Considerações Finais

O desenvolvimento de colunas tubulares abertas do tipo WCOT a qual foi foco desse projeto de doutorado teve por objetivo demonstrar o potencial desse tipo de coluna para a aplicação em cromatografia líquida. No entanto, apesar de todos os esforços, ainda são necessárias diversas investigações para superar as limitações da WCOT para que, futuramente, esta possa alcançar o mesmo nível de eficiência e aplicação das colunas convencionais empacotadas.

Mediante os dados obtidos com as colunas WCOT, confirmamos que elas apresentam maior número de pratos teóricos (N) em relação a uma coluna empacotada, sob as condições isocráticas testadas, o que garantem picos extremamente estreitos, assim como observado em cromatografia gasosa. No entanto, sob condições de gradiente, nota-se um alargamento das bandas cromatográficas, ou seja, uma perda de eficiência (N) da coluna. Para essa dificuldade, foram averiguados dois tipos de gradientes: gradientes lentos, ou seja, que requerem um tempo mais demasiado para subir a proporção de solvente orgânico e, gradientes rápidos, que sobem mais rapidamente a proporção de orgânico. O que foi observado é que sob condições rápidas não havia separação entre os picos (atrazina, clomazone e metalocloro, usados como padrões), porém os picos eram mais estreitos. Já, sob condições de gradiente lento, havia separação cromatográfica, porém com alargamento de banda. Esse tipo de resultado pode ser explicado pelos gráficos de Poppe que correlaciona a performance e velocidade de uma coluna capilar. E, segundo o autor, para obter a melhor performance (separação), precisamos sacrificar a velocidade (análises mais lentas), e o inverso também é válido. Assim sendo, para as próximas investigações dentro dessa área ainda precisamos entender a razão do qual ocorre esse alargamento de banda sob condições de gradiente, e qual seria a melhor condição entre performance e velocidade.

A partir dessa reflexão, outros apontamentos podem ser feitos com respeito a dimensão da coluna WCOT que seja adequado para um sistema de cromatografia líquida. Como observado nos resultados apresentados, foram estudados os efeitos de fatores como comprimento da coluna, diâmetro interno e massa de fase estacionária. Dentro das condições experimentais às quais tínhamos, seja de preparo de colunas quanto de sistema nanoLC, conseguimos produzir colunas com até 25 µm de d.i, e comprimentos na faixa de 5-8 m. No entanto, estudos teóricos voltados para aplicação de colunas WCOT-LC propõem que para atingirmos o mesmo nível de eficiência que em cromatografia gasosa, estas colunas precisam atingir d.i. na faixa de 2 µm. Portanto, as colunas aqui preparadas, ainda não atingiram a

condição teórica, o que justifica as dificuldades em atingir o seu máximo de eficiência cromatográfica. Por conseguinte, para os próximos trabalhos ainda é necessário repensar outras alternativas para preparo dessas colunas, visando reduzir seu diâmetro, mas sem correr o risco de entupimento de coluna. Além disso, ainda são necessários equipamentos de nanoLC redimensionados para esse tipo de coluna, como bombas que suportem fluxos na faixa de nL/min e conexões adequadas para conectar capilares de sílica fundida, dentre outros aspectos.

Em suma, nosso trabalho demostrou experimentalmente que é possível fazer esse acoplamento entre colunas WCOT e LC, mas ainda há muito a investigar para obter o máximo de eficiência. Fatores como entupimento de coluna durante o preparo; desprendimento de fase estacionária durante a análise cromatográfica devido ao fluxo da fase móvel líquida, ainda precisam ser entendidos e superados, se visarmos tornar esse tipo de coluna uma opção comercial para cromatografia líquida.

2 PERSPECTIVAS FUTURAS

- A utilização de fases estacionárias baseadas em dimetil polisiloxano (DMPS) pode levar ao entupimento da coluna, uma vez que, tais fases são muito viscosas e dificulta a preparação robusta de colunas WCOT. Assim, talvez uma alternativa para minimizar as chances de entupimento seria testar outras fases estacionárias menos viscosas.

- A utilização de colunas *trapping* juntamente com colunas WCOT pode melhorar a separação analítica e garantir melhores resultados de resolução cromatográfica. Isso ocorre pois já temos uma pré-separação na coluna *trapping* que depois é otimizada com a utilização da coluna analítica.

- Ainda é necessário estudar metodologias para imobilizar o filme na parede do tubo e evitar o desprendimento da fase estacionária líquida durante a análise cromarográfica, na qual se faz uso de uma fase móvel líquida.

- A redução do diâmetro interno das colunas WCOT deve acompanhar o desenvolvimento da miniaturização da cromatografia líquida, mais especificamente, o desenvolvimento de bombas capazes de suportar fluxos mais baixos que 100 nL/min.

Capítulo 9

Lista de publicações científicas

1 Publicações Científicas

1. Multidimensional Capillary Liquid Chromatography-Tandem Mass Spectrometry for the Determination of Multiclass Pesticides in Surgarcane Spirits (cachaças).

Natalia Gabrielly Pereira dos Santos, Edvaldo Vasconcelos Soares Maciel, Karen Mejía-Carmona e Fernando Mauro Lanças.

Analytical and Bioanalytical Chemistry, v.412, pág. 7789-7797. DOI: 10.1007/s00216-020-02907-y

2. Enantioseparation of Underivatized Amino Acids by Capillary Liquid Chromatography. 2. (N, S-dioctyl-(D)-penicillamine) Ligand Exchange Chiral Stationary Phase.

Fernanda Augusto Daher, **Natalia Gabrielly Pereira dos Santos**, Edvaldo Vasconcelos Soares Maciel e Fernando Mauro Lanças.

Scientia Chromatographica, v.11, pág. 64-70, DOI: 10.5935/sc.2019.008

3. Robot-Assisted Single Drop Microextraction Coupled to High Performance Liquid Chromatography.

Natalia Gabrielly Pereira dos Santos, Deyber Arley Vargas Medina e Fernando Mauro Lanças.

Revisão

4. Microextraction by Packed Sorbent of N-nitrosamines from Losartan Tablets Using a High-Throughput Robot-Platform Followed by Liquid Chromatography-Tandem Mass Spectrometry.

Natalia Gabrielly Pereira dos Santos, Deyber Arley Medina e Fernando Mauro Lanças.

Journal of Separation Science, pág. 1- 12, DOI: 10.1002/jssc.202300214

5. Development of Wall Coated Open Tubular Column and their Application to Nano Liquid Chromatography Coupled to Tandem Mass Spectrometry.

Natalia Gabrielly Pereira dos Santos, Deyber Arley Vargas Medina, Fernando Mauro Lanças.

Molecules, v. 28, n. 13, pág. 1 – 17, DOI: 10.3390/molecules28135103

6. An Overview of Open Tubular Liquid Chromatography with Focus on the Coupling with Mass Spectrometry for the Analysis of Small Molecules.
Deyber Arley Vargas Medina, **Natalia Gabrielly Pereira dos Santos**, Juliana Soares Burato da Silva, João Victor Baolli Borsatto e Fernando Mauro Lanças.
Journal of Chromatography A, v. 1641, n. 461989, pág. 1-14. DOI: 10.1016/j.chroma.2021.461989

7. Enantioseparation of Underivatized Amino Acids by Capillary Liquid Chromatography.1. Background on Chiral Separation.
Natalia Gabrielly Pereira dos Santos, Edvaldo Vasconcelos Soares Maciel e Fernando Mauro Lanças.
Scientia Chromatographica, v. 11, n. 2, pág. 53-63. DOI: 10.5935/sc.2019.007

8. Electron Ionization Mass Spectrometry: Quo Vadis?
Edvaldo Vasconcelos Soares Maciel, **Natalia Gabrielly Pereira dos Santos**, Deyber Arley Vargas Medina, e Fernando Mauro Lanças.
Electrophoresis, v.43, pág. 1587-1600. DOI: 10.1002/elps.202100392.

9. Current Prospects on Nano Liquid Chromatography Coupled to Electron Ionization Mass Spectrometry (nanoLC-EI-MS).
Deyber Arley Vargas Medina**, Natalia Gabrielly Pereira dos Santos**, Edvaldo Vasconcelos Soares Maciel e Fernando Mauro Lanças.
Journal of Liquid Chromatography & Related Technologies, v.1, DOI: 10.1080/10826076.2022.2110114.

10. The Overshadowed of Electron Impact Mass Spectrometry in Analytical Biotechnology.
Deyber Arley Vargas Medina, Edvaldo Vasconcelos Soares Maciel, Natalia Gabrielly Pereira dos Santos, Fernando Mauro Lanças.
Current Opinion in Biotechnology, v.82, DOI: 10.1016/j.copbio.2023.102965

11. Cyclodextrins-Based Sorbents for Sustainable Sample Preparation Focusing on Food Analysis.
Edvaldo Vasconcelos Soares Macial, Natalia Gabrielly Pereira dos Santos, Deyber Arley Vargas Medina, Fernando Mauro Lanças.

Green Analytical Chemistry, submetido.

12. Graphene-Based Sorbents for Modern Magnetic Solid-Phase Extraction Techniques.
Fernando M. Lanças, Deyber Arley Vargas Medina, **Natalia Gabrielly Pereira dos Santos** e Marcela Jordan Sinisterra.
Analytical Applications of Functionalized Magnetic Nanoparticles/ Royal Society of Chemistry, v.1, pág. 174-199. DOI: 10.1039/9781839162756-00174.

13. NanoLC-EI-MS: Perspectives in Biochemical Analysis.
Natalia Gabrielly Pereira dos Santos, Edvaldo Vasconcelos Soares Maciel, Deyber Arley Vargas Medina e Fernando Mauro Lanças.
International Journal of Molecular Sciences, v.24, n.14, pág. 1-14. DOI: 10.3390/ijms241411746